MONTHLY NOTICES

OF THE

ROYAL ASTRONOMICAL SOCIETY

Vol. 106 No. 4

MEETING OF 1946 MAY 10

Professor H. H. Plaskett, President, in the Chair

The election by the Council of the following Fellows was duly confirmed:—

Hermann Bondi, Fellow of Trinity College, Cambridge;

Norman Frank Henry Knight, 72 Chadacre Road, Stoneleigh, Epsom, Surrey; and

Charles Arthur Padgham, 6 Manor Cottages, Lamberhurst, Tunbridge Wells, Kent.

The following candidates were proposed for election as Fellows of the Society, the names of the proposers from personal knowledge being appended:—

William Alexander Calder, M.A., Ph.D., Howard University, Washington, D.C., U.S.A. (proposed by E. M. Lindsay);

Adolph Hermann Friedmann, LL.D., 15 Frognal Court, London, N.W.3 (proposed by E. A. Milne);

Thomas Alfred Grocock, M.A., B.Sc., The Grammar School, Ripon, Yorkshire (proposed by S. Chapman);

Carl Keenan Seyfert, M.A., Ph.D., Warner and Swasey Observatory, Cleveland, Ohio, U.S.A. (proposed by E. M. Lindsay); and

T. V. Viswanathan, M.A., B.Sc., Presidency College, Madras, India (proposed by V. M. Sundara Rajan).

Forty-seven presents were announced as having been received since the last meeting, including:—

Hydrographic Office of the U.S. Navy Department, *Tables of Computed Altitude and Azimuth* (presented by H.M. Nautical Almanac Office); and

Manuscript letter concerning the Comet of 1811, written by Mr. S. Pierce (presented by Miss Eddington).

The President announced that the Council had elected the following as Associates of the Society:—

Professor Thaddäus Banachiewicz, Director of the University Observatory of Cracow, Poland;

Professor Ira Sprague Bowen, Director of the Mount Wilson Observatory, Pasadena, Cal., U.S.A.;
Dr André Joseph Alexandre Couder, Astronomer at the Observatory, Paris, France;
Professor André Danjon, Director of the Paris Observatory, France; and
Dr Eugène Delporte, Director of the Royal Observatory, Uccle, Belgium.

The President further announced that there would be a Special Meeting of Fellows on 1946 June 14, when a discussion would take place on the proposed large telescope for Britain.

Professor J. H. Oort delivered the George Darwin Lecture (see p. 159), taking as his subject "Some Phenomena connected with Interstellar Matter".

After the Lecture, the President presented Professor Oort with the Gold Medal of the Society, which had been awarded to him for his investigation on the dynamics and rotation of the galactic system. The President said:—

"It is now my pleasant duty to present the Gold Medal. After the brilliant George Darwin Lecture which we have just heard Fellows will neither expect nor wish a stumbling account from a non-expert of Professor Oort's contributions to our knowledge of galactic structure and dynamics. In paying him this, the highest honour in its power, the Council has undoubtedly had in mind not only all the detailed investigations which Professor Oort has carried out, but also two characteristics which distinguish his work.

"The first of these is the unerring insight which seems throughout to have governed his choice of problems. It was, it seems to me, no accident that in *B.A.N.*, 23 (1922) Professor Oort was among the first to recognize the importance of the zone of avoidance in the motions of the high velocity stars, first discovered independently by B. Boss and by Adams and Joy. How Professor Oort pursued these high velocity stars through *Groningen Publications*, 40 (1926) to the triumphant explanation in *B.A.N.*, 159 (1928) of the zone of avoidance as that region in which high velocity stars, moving with the general stream of galactic rotation, would have a velocity in excess of the velocity of escape from the galactic system, is one of the more dramatic stories of astronomical research. Nor can there be much doubt that it was just these studies of the high velocity stars which enabled him to be the first to see the underlying significance of Lindblad's hypothesis of galactic rotation, and to re-formulate that hypothesis in the physically clear and simple form which it takes in *B.A.N.*, 120 (1927). As a result of this contribution, and almost over-night, the determination of radial velocities ceased to be one of the less interesting of astronomical pursuits, and became an accurate indicator of stellar distances and a most sensitive probe for finding the distribution of mass in the galactic system.

"Another example of this insight is to be found in *B.A.N.*, 308 (1938). Absorption of light in interstellar space has always been the greatest obstacle to the determination of the spatial distribution of stars, but in this paper, if it has not become a positive help, it has at least ceased to be a hindrance. From Hubble's determination of the optical thickness of the absorbing layer normal to the galactic plane, and from an examination of colour excesses of stars lying in medium galactic latitudes, Professor Oort is able to show that the greater part of this absorbing layer lies within 200 parsecs on either side of the galactic plane. Now if the absorption

all takes place in front of the stars considered, and if these stars lie in equi-density surfaces which are parallel to the galactic plane, then it may be shown, irrespective of the luminosity function and the distribution with distance, that the number of stars between m and $m+\delta m$, counted at a given galactic latitude, bears to the number counted at the galactic pole, within another appropriate magnitude interval, the ratio of the cube of the cosecant of the latitude. Any excess or defect in the number of stars from the predicted number may therefore be attributed to a departure of the equi-density surfaces from parallelism to the galactic plane, and Professor Oort is thus able to show, both above and below the galactic plane, a rise in star density towards the galactic centre and some evidence otherwise of a deficiency of stars in the immediate neighbourhood of the Sun. The method of attack is clearly a most powerful one, and the results, though admittedly and necessarily provisional, are startling in that they suggest that the Sun lies in a 'local void' rather than a 'local cluster'.

"Other examples, no less striking, of our Medallist's insight might be mentioned, but I must now pass to consider very briefly the other dominating characteristic of his work. This is its thoroughness. Every relevant observation appears to be known, the systematic errors are fully allowed for, and above all the observations which do not fall in line with any proposed hypothesis are set out without ambiguity. To read any one of Professor Oort's papers is to be reminded time after time of this scrupulous attention to detail, so essential to and so characteristic of the best scientific work. It was Michelson, I believe, who once compared experimental investigation to a game with a fair but redoubtable opponent who penalized every mistake and took advantage of every weakness. Of the various opponents encountered by men of science none is more redoubtable than the Galactic System; slipshod work meets its deserved fate more quickly in this field than in any other, while inadequate consideration of even the smallest detail is penalized with almost equal severity. In spite of the clouds of smoke, both literal and metaphorical, which obscure its form, the Galactic System seems at length to have met its master in the thoroughness of our Medallist, working quietly and thoughtfully in his room at Leiden.

"These and other astronomical considerations were no doubt present in the minds of the Council when it awarded the Gold Medal this year to Professor Oort, and certainly it is these contributions which excite our greatest admiration. Yet I venture to think that we admire Professor Oort for quite another reason. For five long years he and his fellow-countrymen have lived under Nazi domination, deprived of liberty, of justice and even of hope. What else can there have been to live for but to make some final contribution to knowledge, and how fatally easy it must have been to give at least lip-service to the Nazi conqueror if this would forward this last human ambition! It was a supreme act of courage, almost daily renewed, which refused this temptation, and which saw the University of Leiden and the Observatory close rather than surrender to evil things. To such courage none can fail to pay tribute.

"Professor Oort, in presenting you with this Medal, I hand with it the very best wishes of the Council and of Fellows for future astronomical achievements to match those in the past, and at the same time greetings from all British astronomers to their colleagues in Holland."

ADDITIONAL ORDINARY MEETING OF 1946 JUNE 14

Professor H. H. Plaskett, President, in the Chair

The election by the Council of the following Fellows was duly confirmed after a ballot which was held at the end of the meeting:—

Ira Sprague Bowen, Director, Mount Wilson Observatory, Pasadena, Cal., U.S.A.;

Michael Edwin Chivers, c/o the Authors' Club, 2 Whitehall Court, London, S.W.1;

Ernest William Mason, Beechwood, 1 Osborne Road, Southampton, Hampshire;

Isaac Eyton Roberts, Eyton House, Bagillt, Flintshire;

Hugh Simmons, Solaris, Edlesborough, near Dunstable, Bedfordshire;

Horace Geoffrey Spalton, Castle Fields, Willington, Derbyshire; and

Wladyslaw Jerzy Swiatecki, 170 Victoria Road, Ruislip, Middlesex.

The following candidates were proposed for election as Fellows of the Society, the names of the proposers from personal knowledge being appended:—

Robert Malcolm Coates, A.I.N.A., c/o National Provincial Bank Ltd., Cornmarket Street, Oxford (proposed by O. M. Watts);

Ralph William Nicholls, A.R.C.S., Imperial College of Science and Technology, S. Kensington, London, S.W.7 (proposed by R. W. B. Pearse);

Merle Tuberg, National Research Fellow in Theoretical Astrophysics, Girton College, Cambridge (proposed by S. Chandrasekhar); and

George Alfred Tunnell, B.Sc., 75 St. Joseph's Drive, Southall, Middlesex (proposed by A. Burnet).

Fifty-eight presents were announced as having been received since the last meeting.

The meeting was specially arranged for a discussion on "The Use of a Large Telescope in Britain". The President, in opening the discussion, informed the meeting of the suggested plans and called on the speakers as follows:—

Dr R. d'E. Atkinson, read the contribution of the Astronomer Royal on "Conditions of observation in Great Britain";

Professor W. M. H. Greaves on "Programmes of observations made possible by a large instrument";

Mr F. J. Hargreaves on "Telescope construction";

Dr E. H. Linfoot on "Telescope design";

Dr C. R. Burch on "Telescope design";

Mr W. J. Bates described a new device for testing mirrors; and

Dr W. M. Hampton spoke on the construction of a mirror, with special reference to the production of the glass.

Many members of the audience took part in the informal discussion which followed.

THE PROPER MOTIONS OF M TYPE STARS

J. Jackson, F.R.S., H.M. Astronomer at the Cape

(Received 1946 February 11)

Summary

The proper motions of over 1200 M type stars in the Yale Catalogues and 440 M type stars in Cape Astrographic Catalogues are analysed. The probable error of the Yale motions is $\pm 0''.0112$ and of the Cape motions $\pm 0''.0055$. In the Yale Catalogues about 2 per cent. of the proper motions are greater than $0''.070$ and another 2 per cent. between $0''.050$ and $0''.070$. The Cape Catalogues also give about 2 per cent. greater than $0''.070$ but a smaller number between $0''.050$ and $0''.070$. It is concluded that at least half of the Yale motions between $0''.050$ and $0''.070$ are spurious or exaggerated—the selection of stars with these motions including stars for which the actual errors are three or four times the probable error.

There may be considerable numbers of stars intermediate in brightness between the giants and the dwarfs but they cannot easily be separated from the great number of giant stars of the same apparent brightness. Well over 95 per cent. of M type stars to apparent visual magnitude 8·5 must be giants. The best hopes of narrowing the gap between giants and dwarfs appear to be amongst stars of apparent magnitude 8·0–10·0 and annual proper motion of the order of a tenth of a second, where we may find stars somewhat brighter than the dwarfs we already know and with measurable parallax.

Introduction.—Determinations of stellar parallax have shown two groups of stars of late types—giants and dwarfs. We here confine our attention to M type stars. Most of those about which we have definite knowledge are giants with absolute (visual) magnitudes not very different from 0·5, but a considerable number of faint M type stars with large proper motion have been found to have absolute magnitudes of the order of 10·0, and in recent years when observations have been extended to very faint stars a number considerably fainter still in absolute magnitude have been found. The question of stars of intermediate absolute brightness has often been raised but not solved. For the sake of simplicity in numerical statement let us consider stars of absolute magnitude 0·0 (giants) 10·0 (dwarfs) with an intermediate set at magnitude 5·0. Working to the same apparent magnitude the volume of space we can observe for the three classes are in the ratios of a million (giants), a thousand (intermediates), one (dwarfs).

The fact that we know so many dwarfs as we do is a tribute to the skill and labour which have been applied in detecting large proper motion among the faint stars. (Determinations of spectral type and parallax have followed that of proper motion.) The results also indicate that dwarfs are really numerous in space compared with giants. If large numbers of intermediate stars exist are we in a

position to pick them out? Let us consider stars down to apparent magnitude 9·0. This will include for the whole sky perhaps 10,000 stars of M type. Only a few are dwarfs, mostly known already. If giants and intermediates are equally numerous in space about 10 will be intermediates: only if intermediates are 100 times more numerous in space than giants, will one in ten of the M type stars prove to be an intermediate. Large proper motion has helped us to pick out the dwarfs but as we cannot expect proper motion for the intermediates to be more than a tenth of those for the dwarfs the inevitable errors of observation in the determination of proper motion rise in importance.

In *Astronomical News Letter* No. 35 (1945 August) Bok has suggested that the Yale Catalogues contain a considerable number of stars of M type with a proper motion between 0″·040 and 0″·080 which might be worth observation for parallax. Stars of such proper motion (without consideration of type) would not be expected to have a parallax greater than 0″·010. For apparent magnitude 8·5 this parallax corresponds to an absolute magnitude of 3·5. Stars of such probable parallax are no great attraction to parallax observers and moreover the parallax would not be easily confirmed. On the other hand, if the absolute magnitude were 5·0 then the parallax would be 0″·020, a somewhat better proposition but still not easily confirmed. Certainly a number of stars of M type with magnitudes as bright as 8·5 and proper motions of the order of 0″·040 to 0″·080 (or better 0″·200) should be observed for possible absolute magnitudes between 5·0 and 8·5 (parallax between 0″·020 and 0″·100). In fact such stars are already under observation at a number of observatories.

A simple consideration of the small percentage of M type stars with proper motion of the order of 0″·050 in the Yale Catalogues indicates that many of them will be spurious or greatly exaggerated. The analysis given in this paper was undertaken to find out more accurately the reliability of the larger proper motions of M type stars in the Yale Catalogues and Cape Astrographic Zone Catalogues.

The Yale Catalogues.—The Yale Volumes 11–14 contain the result of the repetition of the A.G. zones by photography from $-10°$ to $-30°$. On account of the overlaps of the A.G. zones a small number of stars appear in two catalogues and no attempt has been made to separate them; such stars are counted twice. This however will not influence the conclusions drawn in this paper. Of the 50,000 stars in these volumes 1,266 are given as of M type. For a few stars proper motions are not given for one reason or another—bright stars or unsatisfactory early observations. The number of stars for which no proper motion is given in R.A. is 52, in Dec. 49, in general the same stars.

We thus have 1,214 proper motions in R.A. and 1,217 in Dec. Means were taken for each $1^h\ 30^m$ of R.A., i.e. over an area approximately 20° square. In taking the means all proper motions over 0″·050 were rejected. These were frequently all of one sign and to balance them an equal number of the largest of the opposite sign were also rejected. Table I gives the mean motion for each area, the number of stars retained in R.A. and the approximate mean magnitude.

From the mean proper motion we derive on giving equal weight to each region (unit 0″·0001 a year)

$$\text{Mean Proper Motion in R.A.} = \quad -26\sin\alpha + 130\cos\alpha$$

$$\text{Mean Proper Motion in Dec.} = -29 + 29\sin\alpha - \ 46\cos\alpha.$$

As Struve-Peters's value of the precession was used in the Yale Catalogues we have to apply corrections of $-53 \sin\alpha \tan 20°$ in R.A. and $+53 \cos\alpha$ in Dec. to reduce to Newcomb's precession. We then have

$$\text{Mean Proper Motion in R.A.} = \quad -45 \sin\alpha + 130 \cos\alpha$$
$$\text{Mean Proper Motion in Dec.} = -29 + 29 \sin\alpha + \quad 7 \cos\alpha.$$

From these we derive as the components of the solar motion.

$$X = -45, \qquad Y = -130, \qquad Z = +31.$$

TABLE I

Yale Mean Proper Motions. Unit 0″·0001 a year

	R.A.	Dec.	No.	Mean Mag.
h m h m				
0 0 – 1 30	+ 93	− 62	33	8·1
1 30 – 3 0	97	84	42	8·2
3 0 – 4 30	88	− 27	49	8·4
4 30 – 6 0	+ 29	+ 9	74	8·6
6 0 – 7 30	−101	+ 27	132	8·7
7 30 – 9 0	59	− 3	149	8·6
9 0 – 10 30	46	+ 34	91	8·6
10 30 – 12 0	103	+ 3	72	8·5
12 0 – 13 30	115	+ 12	57	8·5
13 30 – 15 0	105	0	63	8·5
15 0 – 16 30	48	+ 4	52	8·5
16 30 – 18 0	− 14	− 83	64	8·7
18 0 – 19 30	+ 99	− 65	118	8·7
19 30 – 21 0	128	− 60	73	8·7
21 0 – 22 30	146	−104	41	8·4
22 30 – 0 0	+186	− 64	28	8·3

The solar apex is at R.A. 251° Dec. +13°. The mean parallactic motion is found to be 0″·0141 corresponding to a mean parallax of 0″·0034. This would correspond to a reduction from apparent magnitude to absolute magnitude of −7·3. The mean visual magnitude of the stars is about 8·5 so that the absolute magnitude is 1·2, but this is subject to considerable uncertainty as a result of the uncertainty in the systematic corrections to the rather small proper motions.

In this paper however we are not concerned with mean proper motions but with the individual proper motions. From each proper motion we have subtracted the mean proper motion of the region in which it is situated so as to obtain residual proper motions. Table II gives the number of stars for each value of the residual proper motion from −0″·050 to +0″·050. As there are no great differences for positive and negative values or for right ascension and declination all the four sets of frequencies have been summed as shown in the sixth column of the table.

The actual distribution of residuals is fairly like an error curve. If we compare the number of residuals up to about 10 with the number up to about 40 we find that they correspond to the error curve for a probable error about ±0″·0132 but there is a definite excess of residuals in the region 11 to 15. If we try to fit the number of residuals up to 13 with those up to 40 we find the error curve corresponds to a probable error of ±0″·0126. In either case we get more than the estimated

TABLE II

Frequency of Residual Proper Motions for M type Stars in the Yale and Cape Catalogues

P.M.	YALE R.A. Pos.	YALE R.A. Neg.	YALE Dec. Pos.	YALE Dec. Neg.	Total	CAPE R.A. Pos.	CAPE R.A. Neg.	CAPE Dec. Pos.	CAPE Dec. Neg.	Total
0	20	...	35	...	55	15	...	13	...	28
1	27	22	25	22	96	11	18	28	12	69
2	19	28	24	22	93	16	9	10	19	54
3	28	15	31	24	98	15	17	13	14	59
4	25	22	24	17	88	14	13	17	15	59
5	18	28	20	22	88	10	15	11	10	46
6	25	26	18	30	99	12	15	12	10	49
7	15	14	28	18	75	18	19	21	6	64
8	30	25	14	20	89	9	9	11	5	34
9	19	23	30	19	91	9	6	10	10	35
10	22	22	25	19	88	7	10	7	12	36
11	28	22	15	16	81	11	8	6	7	32
12	24	22	18	24	88	8	6	6	4	24
13	24	22	23	25	94	5	4	10	6	25
14	22	19	22	16	79	4	3	6	3	16
15	18	20	20	22	80	9	3	4	4	20
16	17	14	20	14	65	7	8	2	4	21
17	8	17	17	18	60	2	1	9	5	17
18	9	8	24	9	50	1	4	9	7	21
19	12	13	21	7	53	6	5	4	3	18
20	7	6	13	9	35	2	5	4	4	15
21	9	9	12	8	38	3	3	3	4	13
22	19	19	10	13	61	2	3	1	4	10
23	12	15	12	8	47	0	0	1	4	5
24	14	13	10	9	46	1	2	2	3	8
25	11	9	6	11	37	0	1	3	1	5
26	10	10	8	8	36	1	2	2	1	6
27	12	10	6	8	36	4	1	0	0	5
28	9	9	10	7	35	3	3	1	2	9
29	6	11	12	9	38	1	0	0	0	1
30	8	7	4	10	29	1	2	0	0	3
31	4	4	9	8	25	2	1	1	2	6
32	6	7	7	8	28	0	0	0	0	0
33	7	6	8	9	30	0	1	2	3	6
34	1	1	6	3	11	1	1	1	0	3
35	4	4	3	7	18	2	0	0	2	4
36	4	5	4	8	21	1	1	1	0	3
37	2	6	4	5	17	1	0	0	3	4
38	9	4	3	6	22	0	0	1	1	3
39	5	4	0	6	15	0	1	0	2	2
40	2	4	2	3	11	3	0	1	0	4

TABLE II—*continued*

P.M.	YALE R.A. Pos.	YALE R.A. Neg.	YALE Dec. Pos.	YALE Dec. Neg.	Total	YALE R.A. Pos.	YALE R.A. Neg.	YALE Dec. Pos.	YALE Dec. Neg.	Total
41	5	5	2	2	14	0	1	2	0	3
42	3	1	4	2	10	0	2	0	0	2
43	1	4	1	2	8	1	0	0	0	1
44	1	0	0	2	3	1	0	0	0	1
45	4	4	3	2	13	2	0	0	1	3
46	3	3	0	1	7	0	2	1	0	3
47	2	4	1	2	9	0	0	0	0	0
48	1	5	8	1	15	1	0	0	0	1
49	2	1	0	2	5	0	1	0	1	2
50	0	1	2	1	4	0	0	0	0	0

number of residuals over 50 which of course is to be explained partly by actual large proper motions and partly by the known fact that large errors occur more frequently than is calculated from the normal error law.

In the Yale Volumes a probable error is given for each proper motion. The largest probable errors $\pm 0''\cdot014$ occur in the R.A.s of zone $-14°$ to $-18°$, the smallest about $\pm 0''\cdot009$ in the declinations for $-18°$ to $-20°$. From a sampling of the observations I find the average probable error for the whole material to be $\pm 0''\cdot0117$ in R.A. and $\pm 0''\cdot0106$ in Dec., say $\pm 0''\cdot0112$ for the combined residuals. We have seen that residuals up to at least $\pm 0''\cdot040$ follow approximately an error law with a probable error of $\pm 0''\cdot013$ so that the scattering in the observed motions of these stars is due more to the errors of observation than to the actual motion of the stars. Now from a well determined frequency curve it is possible to compute corrections to the observed motions.* On account of the excess of motions in the neighbourhood of $0''\cdot010$ to $0''\cdot015$ there is some difficulty in deriving reliable corrections for values in that region. But for motions from $0''\cdot020$ to $0''\cdot060$ the statistical correction† indicates that the actual motions should be approximately halved: for larger motions the correction must fall off both relatively and actually. These corrections are based on the mean value of the probable errors given in the Yale Volumes, viz. $\pm 0''\cdot0112$.

Another way of considering the reality of the large proper motions is by computing the number of spurious ones which would arise from different values

* Eddington, *M.N.*, **100**, 354, 1940.

† This was originally derived from Eddington's formula, care being taken not to overestimate the correction. As this paper is primarily concerned with individual stars the application of the formula appears to be justified although this treatment may not give statistically correct results. However, if we consider that the observed frequencies conform to a probable error of $\pm 0''\cdot013$, and the observational probable error is about $\pm 0''\cdot011$ the true distribution should correspond to a probable error of $\pm\sqrt{(0''\cdot013)^2-(0''\cdot011)^2}$ or $\pm 0''\cdot007$. This shows that statistically all the main bulk of the observed proper motions should be reduced to little more than half.

of the probable error according to the normal law. The results are shown below.

P.M. greater than	Observed No.	Observed minus Computed for P.E.			
		±0″·0112	±0″·013	±0″·014	±0″·015
0″·050	97	92	76	61	41
0″·055	75	72	65	57	44
0″·060	60	60	56	51	44
0″·065	50	50	50	47	42
0″·070	44	44	44	44	40

From this table it is clear that the 44 proper motions exceeding 0″·070 cannot be explained by the normal law of errors. Some of them may result from large accidental errors which as is well known are generally more numerous than expected. But still the majority of them are probably substantially correct even if somewhat exaggerated. It is probable however from previous considerations that of the 53 between 0″·051 and 0″·070, a considerable fraction, at least half, are spurious or require to be reduced. Eighteen of the stars with motions over 0″·050 are in the G.C. and for all but five, the proper motion of the G.C. is substantially less than, although generally bearing some resemblance to, the Yale motion. Twenty-four proper motions exceed 0″·100. The 97 motions over 0″·050 refer to 85 stars, as a number of stars have large motion in both coordinates, and one star was counted twice because it occurs in an overlap. It may be of interest to give the determinations of proper motion for this star BD −14° 6274, magnitude 9·4, viz.,

R.A. +0″·175 ± 0″·010 and +0″·126 ± 0″·014
Dec. −0″·034 ± 0″·010 and −0″·092 ± 0″·010.

For both coordinates the difference is greater than we would expect, especially when we consider that the same recent observation was used for both determinations.

Cape Astrographic Catalogues.—For the zone −40° to −52° proper motions have been determined from plates taken with the Cape Astrographic Telescope for all stars down to magnitude 9·5 of the CPD. Although the interval is somewhat less than for the Yale Catalogues the probable errors are much smaller. The Cape proper motions have the great advantage that the observations at both ends of the time interval were made photographically with the same telescope and so should be free from errors due to colour which might easily arise for such late type stars when the early observations are visual and the recent ones photographic. For the Cape proper motions there are usually two quite independent determinations although generally only one in the two end degrees of the zone, while for a certain number of stars the number of determinations is three. We may, however, for this discussion take the mean as two separate determinations and the probable error of the proper motions as ±0″·0055 or just half that of the Yale proper motions.

The two volumes giving the Cape proper motions include more than 40,000 stars; of that total 465 have been classified as of M type. It is, however, necessary to reject from our discussion 23 which are fainter than 9·5 CPD and were included

merely because of their considerable proper motions. Two other stars, too bright to be satisfactorily observed were also excluded, leaving 440 stars for consideration. This is about a hundred less than we would expect from the relative areas of the Yale and Cape zones and is probably due to the fact that for red stars magnitude 9·5 of the CPD scale is brighter than the limit of the visual meridian catalogues.

The proper motions of the 440 M type stars have been analysed in a similar way to that of the Yale Zones. Hourly means were taken in the same way. (Table III.) These on analysis gave (unit 0″·0001 a year)

$$\text{Mean Proper Motion in R.A.} = -32 - 4\sin\alpha + 89\cos\alpha$$
$$\text{Mean Proper Motion in Dec.} = -37 + 89\sin\alpha + 2\cos\alpha.$$

TABLE III

Cape Mean Proper Motions. Unit 0″·0001 a year

	R.A.	Dec.	No.	Mean Phot. Mag.
h h				
0 – 1	– 6	+ 83	5	9·1
1 – 2	+ 55	– 39	11	9·4
2 – 3	29	– 19	7	10·2
3 – 4	61	+ 71	22	10·1
4 – 5	+ 75	+ 87	13	9·7
5 – 6	– 39	– 17	19	10·0
6 – 7	61	+ 24	15	9·5
7 – 8	36	38	11	9·1
8 – 9	46	68	22	9·7
9 – 10	119	+ 30	22	10·0
10 – 11	102	– 17	29	10·2
11 – 12	202	19	9	9·9
12 – 13	164	13	20	9·7
13 – 14	113	68	24	9·9
14 – 15	87	136	20	9·6
15 – 16	56	127	23	9·8
16 – 17	49	115	26	10·1
17 – 18	– 49	138	26	9·9
18 – 19	+ 11	121	12	9·4
19 – 20	+ 16	103	16	9·3
20 – 21	+ 99	116	13	9·3
21 – 22	– 31	49	13	10·0
22 – 23	+132	113	13	9·7
23 – 24	– 61	– 82	12	9·8

As the effect of galactic rotation had been introduced into these motions it should be removed in analysing for the solar motion. When this is done we get from the above

$$\text{Mean Proper Motion in R.A.} = -21 - 3\sin\alpha + 61\cos\alpha$$
$$\text{Mean Proper Motion in Dec.} = -50 + 59\sin\alpha + 8\cos\alpha.$$

From the R.A. we get $X = -3$, $Y = -61$ and from the declinations $X = -11$, $Y = -82$, $Z = +72$. Giving double weight to the X, Y from the right ascensions we have:

$$X = -6, \qquad Y = -68, \qquad Z = +72.$$

The apex of the solar motion is found to be at R.A. 265°, Dec. +47° and the parallactic motion 0″·0099. The corresponding parallax is 0″·0024 and if we take the mean photographic magnitude of the stars as 9·7, the corresponding absolute (photographic) magnitude is 1·6.

On account of the weakness of the material in some right ascensions the mean proper motions subtracted from the actual ones were the computed and not the

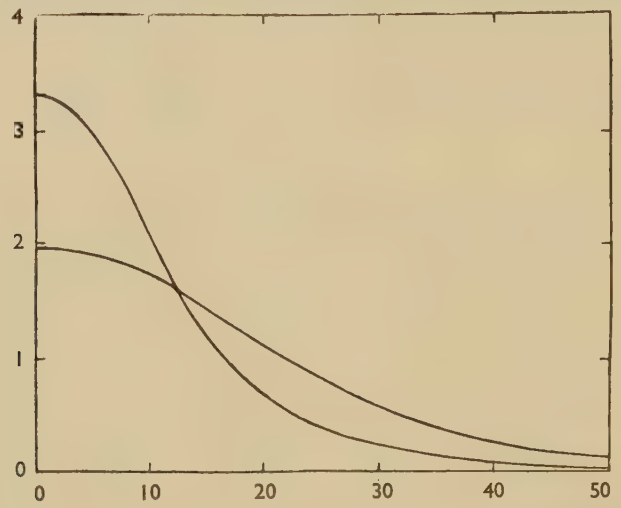

Frequency curves for residual proper motions of M type stars. Steeper curve from the Cape observations, flatter from Yale observations. Unit of proper motion 0″·001 *per annum. Ordinates in percentage for each* 0″·001, *positive or negative.*

observed values. The frequency of the residual motions are given in Table II with the Yale motions. The smoothed results are also shown in the figure. A summary of the motions is given in Table IV.

TABLE IV

Summary of Frequencies

P.M. Unit 0″·001	Number		Percentage	
	Yale	Cape	Yale	Cape
0 – 5	518	315	21·3	35·8
6 – 10	442	218	18·2	24·8
11 – 15	422	117	17·4	13·3
16 – 20	263	92	10·8	10·5
21 – 25	229	41	9·4	4·7
26 – 30	174	24	7·2	2·7
31 – 35	112	19	4·6	2·2
36 – 40	86	16	3·5	1·8
41 – 45	48	10	2·0	1·1
46 – 50	40	6	1·6	0·7
51 – 60	37	2	1·5	0·2
61 – 70	16	3	0·7	0·3
71 – 80	11	3	0·5	0·3
81 – 90	5	2	0·2	0·2
91 – 100	4	0	0·2	0·0
101 – 150	10	3	0·4	0·3
151 – 200	6	2	0·2	0·2
>200	8	7	0·3	0·8

During the process of making the counts it was most obvious that the number of large motions was much smaller in the Cape than in the Yale results. Actually about half of the Cape residual motions are in the interval $+0''\cdot007$ to $-0''\cdot007$ while for the Yale residuals the corresponding interval was $+0''\cdot013$ to $-0''\cdot013$. With so small a probable error as $\pm0''\cdot0055$ the statistical corrections to the Cape motions are comparatively small not exceeding $0''\cdot007$ at $0''\cdot020$ and falling off in both directions. It does not exceed $0''\cdot003$ at $0''\cdot030$ so that motions exceeding $0''\cdot040$ in the Cape Catalogues do not need any reduction on the average. The following table shows the percentage of M type stars exceeding certain values of the residual proper motion in the Yale and Cape Catalogues.

	Percentage	
P.M. greater than	Yale	Cape
$0''\cdot030$	15·8	8·3
$0''\cdot035$	11·2	6·1
$0''\cdot040$	7·6	4·3
$0''\cdot045$	5·6	3·2
$0''\cdot050$	4·0	2·5
$0''\cdot055$	3·1	2·4
$0''\cdot060$	2·5	2·3
$0''\cdot065$	2·1	2·1
$0''\cdot070$	1·8	1·9

Accepting the Cape proper motions as essentially correct we find that the Yale motions greater than $0''\cdot070$ are essentially correct in number but those between $0''\cdot030$ and $0''\cdot070$ are twice too numerous.

It is very doubtful if any definite conclusions can be drawn from the proper motions regarding the existence of stars intermediate between the giants and dwarfs. The great majority of the stars considered are giants while the dwarfs monopolize the very large proper motions. It was noted that there appeared to be an excess of Yale stars with residual proper motions between $0''\cdot011$ and $0''\cdot015$. The Cape results show a similar excess between $0''\cdot016$ and $0''\cdot018$ but the significance seems doubtful. Conclusions must await further observations especially of parallax. All the M type stars for which we have definite knowledge appear to be giants (absolute magnitude brighter than $+2\cdot0$) or dwarfs (absolute magnitudes fainter than $8\cdot0$).* What hopes have we of reducing the gap? At the brighter end the stars must appear bright if the parallax is to fall in a range which can be confirmed by trigonometric methods. Such stars if they existed would have been found already. Our best hopes appear to be at the intrinsically fainter end of the gap, say at absolute magnitude $8\cdot0$. It is hardly likely that we will find any apparently brighter than $8\cdot0$ as they would have a parallax greater than $0''\cdot100$ and would surely have been detected before this. But it is conceivable that amongst stars of apparent magnitude $9\cdot0$ there may be some still unknown with a parallax of $0''\cdot064$ (and perhaps an annual proper motion two or three times larger than this). We are however more likely to find the stars we seek amongst those of apparent magnitude $10\cdot0$ and a parallax of $0''\cdot040$. With a smaller parallax it is true the star would lie further in the gap but the parallax would be more difficult to confirm and the star more difficult to distinguish from a giant. A careful examination

* *Observatory* **66**, 374, 1946.

of M type stars of apparent visual magnitude 8·0–10·0 and annual proper motion of the order of 0″·100 appears to give us greatest hopes of success. A star in that magnitude range is not a normal giant if its parallax exceeds 0″·020.

The author will be pleased to communicate to any one interested a list of M type stars from the Cape and Yale Catalogues with proper motions exceeding 0″·050 although it must be admitted that a number of the Yale motions will prove to be spurious.

Note on the Cape Parallaxes of M type stars.—Since the 1935 edition of the Yale General Catalogue of Parallaxes a fairly large number of parallaxes have been published. The lists from the Cape Observatory have included 28 M type stars and 13 stars of colour class m. All the latter can be considered dwarfs. Of the M type stars six are giants or probable giants having no appreciable proper motion, nine can be taken as definitely dwarfs, leaving the following 13.

R.A.S. No.	Spectrum	Phot. Mag.	Parallax Unit 0″·001	Abs. Phot. Mag.
891	Mo	10·5	+37± 8	8·5
935	M	10·8	+16± 8	7·2
1108	Mo	11·6	+ 7±10	(6·6)
1128	Mo	10·8	+ 6±11	(5·6)
1178	M1	11·4	+34± 8	9·2
1265	Map	10·1	+78± 8	9·6
1294	Mo	12·2	+18± 7	8·8
1362	Mo	11·9	+31± 7	9·6
1364	Mo	11·1	+11± 7	6·8
1372	M	12·4	+19± 7	9·1
1379	Mo	12·3	+ 8± 4	(7·5)
1390	Mo	11·2	+30± 7	8·8
1392	Mo	12·1	+ 5± 6	(6·6)

In computing the absolute photographic magnitude 0″·003 has been added to the relative parallax given in the 4th column. The less certain magnitudes are in brackets; they are naturally furthest removed from the normal dwarfs. These stars except perhaps No. 1128 seem to have sufficiently large motions to make it very unlikely that the parallax is of the order of 0″·002 required to make them normal giants. The two largest parallaxes, those of Nos. 891 and 1265 have been confirmed at other observatories. As it is necessary to apply a correction of about −1·6 to the photographic magnitudes to reduce them to the visual standard these results seem to indicate the existence of M type stars with absolute visual magnitudes intermediate between giants and dwarfs. They are to be found amongst stars of about visual magnitude 10·0 and with proper motions of 5″ to 10″ a century.

Royal Observatory,
Cape of Good Hope :
1946 *January* 15.

THE CHEMICAL COMPOSITION OF THE STARS

F. Hoyle

(Received 1947 January 6)

Summary

The usual view that the stars contain at least ten per cent. by mass in the form of heavy elements is inconsistent with data concerning both the composition of interstellar material and the composition of stellar atmospheres. The data suggest that at the time of condensation of the stars at least 99 per cent. by mass must be in the form of hydrogen. On this view the mean molecular weight μ at the time of condensation is close to 0·5, and a subsequent increase in μ can only arise from the conversion of hydrogen to helium by thermonuclear reactions. The effect of this on the luminosities of stars is examined, and it is shown that the resulting theory is at least in as good agreement with the observed luminosities as the old theory.

It is emphasized that the possibility of a very high hydrogen content has been generally recognized for many years. The new feature of the present work is the argument given in favour of a hitherto neglected alternative.

1. On the basis that the stars contain an appreciable fraction by mass in the form of heavy elements, curves are given in Fig. 1 corresponding to the three values 1/1·85, 1, 2 of μ. These curves, which represent the luminosity of a star as a function of the mass over the range 0·1⊙ to 100⊙, were obtained by the theoretical methods given in a previous paper.*

The mean molecular weight is given in terms of X, Y, which are the fractions by mass in the form of hydrogen and helium respectively, by the relation

$$\mu = 4/(2+6X+Y).$$

The values adopted in calculating the curves of Fig. 1 were $X=0{\cdot}9$, $Y=0$ for $\mu=1/1{\cdot}85$; $X=1/3$, $Y=0$ for $\mu=1$; and $X=Y=0$ for $\mu=2$. The values for

* F. Hoyle and R. A. Lyttleton, *M.N.*, **102**, 177, 1942.

The opportunity has been taken to correct an error in the values previously adopted for the photo-electric opacity coefficient. The main effect of the new values is that electron scattering becomes important for smaller masses. Thus the points B on the curves mark the transition from opacity by electron scattering on the upper side to photo-electric absorption on the lower side of B. That is, the approximation is made of using electron scattering alone for masses above B and photo-electric opacity alone for masses below B. The transition values are

μ	1/1·85	1	2
Mass	7·6⊙	6·8⊙	5·5⊙

which may be compared with the values

μ	1/1·85	1	2
Mass	11⊙	25⊙	24⊙

given in the earlier paper. This change is due to a former overestimate by a factor of about three in the photoelectric opacity for stars of masses greater than 5⊙. Quantitatively the luminosity is increased by about one magnitude for masses of order 5⊙, but is unaffected for masses of order ⊙ on the lower side and 20⊙ on the upper side.

$\mu = 2$ are unique, but other combinations of X, Y can be found for $\mu = 1/1{\cdot}85$ and $\mu = 1$. However, the alternative combinations only lead to a slight correction in the luminosity. This correction in any case can easily be found from the previous analysis.*

The earlier work also enables the radius of a star to be determined as a function of μ and the mass. But there is an important difference between the calculation of the luminosity and that of the radius. For the luminosity is rather insensitive to variations of μ from one part of the star to another, whereas the radius is very sensitive to variations of μ of a certain type.† Thus while the exact distribution of μ must be specified in a calculation of the radius, the luminosity on the other hand can be satisfactorily estimated from the average value of μ for the star as a whole. The values of μ in Fig. 1 may be regarded as such average values.

2. The points marked in Fig. 1 represent the observed luminosities of a number of selected stars used by Kuiper in his discussion of the empirical mass-luminosity relation.‡ These points bring out the well-known result that in order to explain the observed luminosities of stars with masses less than $2\odot$ it is necessary to assume that μ is close to, or greater than, unity. This requires X to be close to, or less than, $\frac{1}{3}$. The question arises as to what sequence of stellar evolution can lead to such low values of X.

In the first place we can dismiss the suggestion (for stars of mass less than $\odot$) that the conversion of hydrogen to helium by thermonuclear reactions is responsible for producing important changes in the value of X, because the generally accepted time-scale of about 10^{10} years is far too short for this process to be applicable to small stars. This means that if we accept the usual theory in which the stars are regarded as containing an appreciable fraction by mass in the form of heavy elements then we must also accept the corollary that X is close to, or less than, $\frac{1}{3}$ at the time of condensation from the interstellar material. Now the composition of the interstellar material according to Dunham is such that hydrogen is about 10,000 times as abundant as the commonest metals.§ This evidently differs by a very large margin from the composition required by the above discussion. Thus we are faced || with a situation in which either the usual view of the internal composition of the stars must be abandoned or Dunham's estimates must be regarded as entirely atypical. The work of Russell and B. Strömgren leaves little doubt as to the choice to be made between these two alternatives.¶ Thus Russell in a general study of stellar atmospheres has obtained a hydrogen abundance that exceeds the combined abundance of the metals by a factor of at least 1000, while Strömgren finds a factor of about 5000 for the solar atmosphere. These results fit so well with Dunham's work that the usual view of the chemical composition of the stars, on which the curves of Fig. 1 are based, is called into serious question.

* *Loc. cit.*

† F. Hoyle and R. A. Lyttleton, *M.N.*, **102,** 218, 1942.

‡ G. P. Kuiper, *Ap. J.*, **88,** 472, 1938.

§ T. Dunham Jr., *Proc. Amer. Phil. Soc.*, **81,** 277, 1939.

|| We reject the unsatisfactory idea that the average composition of the stars at the time of their condensation can differ by an extremely wide margin from the average composition of the interstellar material.

¶ H. N. Russell, *Ap. J.*, **78,** 239, 1933; B. Strömgren, *Festschrift für Elis Strömgren*, p. 218, Copenhagen, 1940.

3. In this section it will be accepted that the composition of the stars at the time of condensation is close to the estimate given by Dunham. That is, the fraction by mass in the form of heavy elements will be taken as less than one per cent. This means that μ is initially close to 0·5 for all stars. The thermonuclear processes taking place within the interiors of normal stars do not affect the proportion of heavy elements, so that an analysis of the composition of stellar atmospheres must in general show a ratio of hydrogen to heavy elements of the same order as the interstellar material. This provides the connection between Dunham's values and the results obtained by Russell and Strömgren.

It was shown in previous work * that the luminosity of a star is extremely insensitive to the carbon content. Thus the change in luminosity due to a reduction in the carbon content by a factor of 100 is quite negligible.

The main change arises from the reduction of the opacity due to photo-electric absorption to about one per cent. of the usual estimates. This means that opacity by electron scattering exceeds photo-electric absorption in stars with masses much less than $5\odot$. Thus the tables given by Morse † show that the change over between the two forms of opacity must now occur near $0{\cdot}5\odot$ instead of above $5\odot$ as in Fig. 1. The curves in Fig. 2 were obtained by methods similar to those used in calculating the curves of Fig. 1, except that allowance is made in Fig. 2 for the greater importance of electron scattering.‡ The opacity is again by electron scattering for masses above B and by photo-electric absorption below B. The observational points are the same as in Fig. 1.

On the present theory μ must be close to 0·5 at the time of condensation of the stars. The time-scale is too short for the conversion of hydrogen to helium to increase μ appreciably above 0·5 in small stars. On the other hand the rate of conversion of hydrogen is extremely rapid in a highly luminous star of large mass, and μ in such a star can lie anywhere between 0·5 and 4/3 according to the history of the star.

It is seen from Fig. 2 that the observed points are in satisfactory agreement with these requirements. In particular the fit of stars of moderate mass to the $\mu = 0{\cdot}5$ curve is regarded as very good. The fit may well become better still when accurate numerical integrations are available to replace the approximations that are at present necessary for calculating the curves. It will be noted that the Sun turns out to be a star that is largely composed of hydrogen. In the writer's opinion the theory leading to the curves of Fig. 2 not only gives agreement with the data of Dunham, Russell and Strömgren, but also gives better agreement with the observational points than the curves of Fig. 1.

In the past, attempts have sometimes been made to use the radius as well as the luminosity of a star in a discussion of its composition. The sensitivity of the radius to variations of μ from one part of the star to another makes this an unsatisfactory procedure, except in cases where μ is close to 0·5 throughout the star.

4. The work of Section 3 has a bearing on a number of theories that have been proposed by the writer. Firstly, the attempt § to explain the form of the luminosity function now requires revision, because the time of condensation of small

* *Loc. cit.*

† P. M. Morse, *Ap. J.*, **92**, 27, 1940.

‡ The formula (35) of *M.N.*, **102**, 177, 1942 was used for stars with electron scattering opacity and the homology (37) for the photo-electric opacity.

§ F. Hoyle, *M.N.*, **105**, pages 306 to 311, 1945.

stars from the interstellar material is altered from the previous value of 10^{11} years to a value of order 10^{9} years.

Secondly, the process recently suggested * for the formation of heavy elements in supernova-type stars is seen to be sufficient to give the amount of heavy elements required by the present theory. The number of supernovae occurring within the average extra-galactic nebula is about $2 \cdot 10^{7}$ in 10^{10} years. Thus if the average

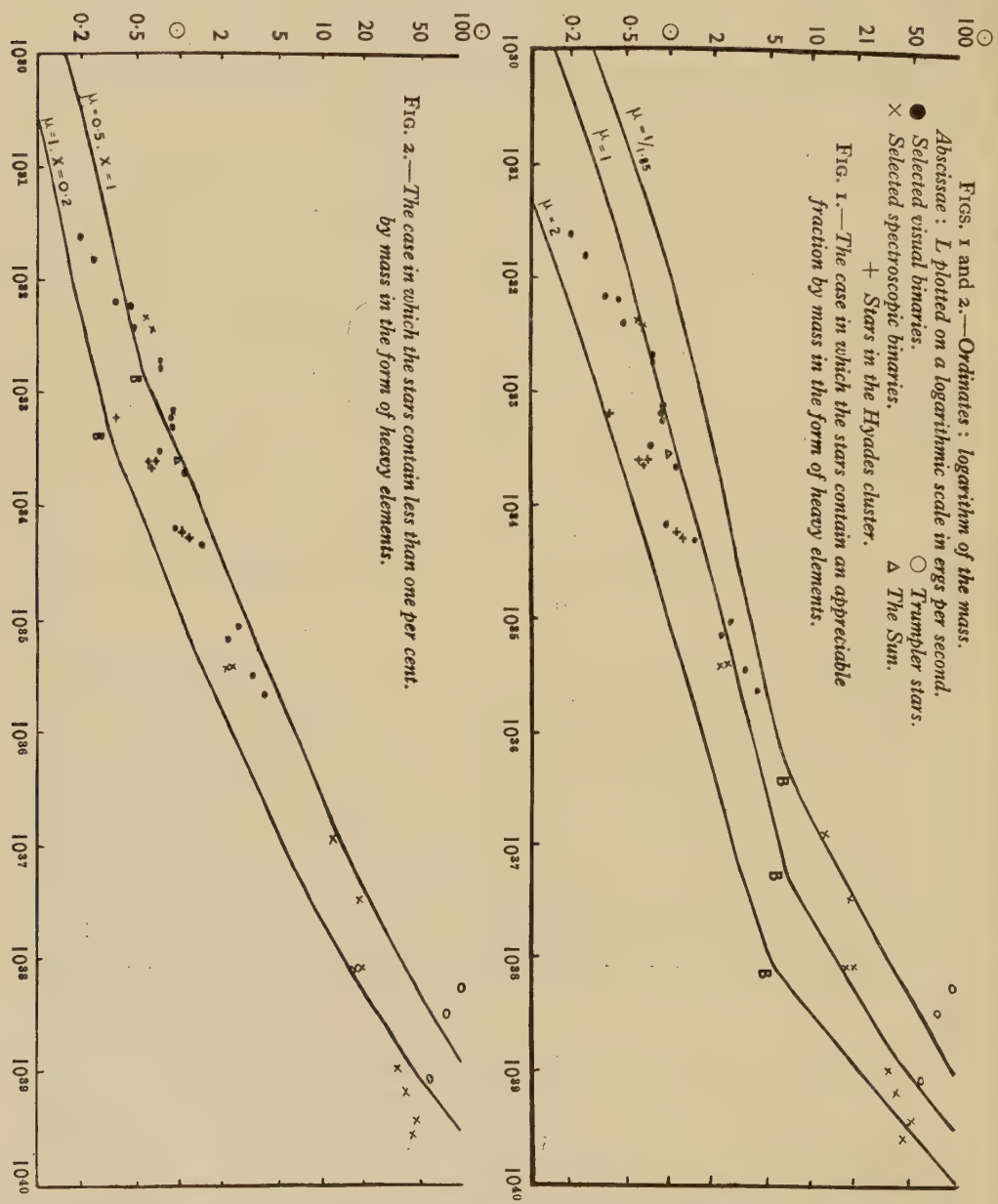

FIGS. 1 and 2.—*Ordinates: logarithm of the mass. Abscissae: L plotted on a logarithmic scale in ergs per second.*
● *Selected visual binaries.* ○ *Trumpler stars.*
× *Selected spectroscopic binaries.* △ *The Sun.*
\+ *Stars in the Hyades cluster.*

FIG. 1.—*The case in which the stars contain an appreciable fraction by mass in the form of heavy elements.*

FIG. 2.—*The case in which the stars contain less than one per cent. by mass in the form of heavy elements.*

* F. Hoyle, "On the Synthesis of the Elements from Hydrogen", *M.N.*, **106**, 1946 (in the press).

mass of heavy elements thrown off per supernova is taken as $5\odot$ this gives $10^8\odot$ for the mass of heavy elements distributed in interstellar space in 10^{10} years. This is of the required order of magnitude.

Finally, the high ratio of hydrogen to metals in the interstellar material is a powerful argument in favour of the supernova theory * of the origin of the solar system, for it almost certainly rules out all attempts to explain the formation of planetary systems either as a stage in stellar condensation or in terms of material removed from an ordinary star.

St. John's College,
Cambridge:
1946 *December* 29.

* *Proc. Camb. Phil. Soc.*, **40**, 256, 1944 and *M.N.*, **105**, 175, 1945.

STELLAR ENERGY GENERATION

R. v. d. R. Woolley

(Received 1946 August 2 *)

Summary

An explicit relation between calculated central temperature and M, L and R is developed for gaseous non-degenerate stars of small mass, assuming a definite law of energy generation. This relation is compared with observed data. It is shown that the observed data do not agree with the supposition that proportion of hydrogen to other elements is the only difference in composition between one star and another. It is suggested that differences in hydrogen concentration between centre and surface are important, and further that in some stars at least the observations indicate the existence of appreciable degenerate cores.

1. There is a well-known empirical relation between the observed mass M and the luminosity L of a star. A theoretical relation between M and L, agreeing reasonably well with the empirical relation, was deduced by Eddington, who made certain assumptions about the internal constitution of the stars. Later, similar theoretical relations were deduced by other writers who were able to remove some of Eddington's assumptions, and a relation holding good for non-degenerate gaseous stars of small mass can now be deduced from general considerations. Now the star exhibits a third observable characteristic, the radius R, and it was shown by Vogt and independently by Russell that if the rate of generation of energy ϵ is a function of the density, temperature and chemical constitution of the star only, then for stars of the same chemical constitution a relation must exist between M, L and R which together with the mass luminosity relation will determine R. Accordingly any explicit stellar model taken together with any explicit chemical composition and law of energy generation will lead to definite values of L and R for a given M.

The present paper develops an explicit relation for non-degenerate stars of small mass on the assumption that $\epsilon=\epsilon_0\rho T^\nu$ and that the chemical constitution does not vary inside a star. The relation developed does not represent the observed points with any reasonable value of ν. It is suggested that variation of hydrogen concentration from centre to surface of a star is an important factor in determining the relations between M, L and R. The observed quantities suggest further that in some stars there must be an appreciable degenerate core.

2. It is shown by Chandrasekhar †, following Strömgren, that for (non-degenerate) gaseous stars in radiative equilibrium in which the radiation pres-

* Originally submitted in different form, 1946 April 3 ; the author wishes to acknowledge his indebtedness to a referee for an extremely valuable suggestion concerning the presentation of this paper.

† *Study of Stellar Structure*, pp. 234–8, 1938.

sure is negligible throughout the configuration, and in which the rate of generation of energy ϵ and the opacity κ follow the laws

$$\epsilon = \epsilon_0 \rho^{\alpha} T^{\nu} \qquad \kappa = \kappa_0 \rho T^{-3-s}$$

the solutions of the equations of equilibrium are related to one another by homologous transformations. Under these circumstances the mass-luminosity relation is

$$L = \text{constant} \times \frac{1}{\kappa_0} \frac{M^{5+s}}{R^s} \mu^{7+s}. \tag{2.1}$$

It may be shown from the homology relations given by Chandrasekhar that

$$L = \text{constant} \times T_c^{\nu} M^{\alpha+1} R^{-3\alpha}, \tag{2.2}$$

$$T_c = \text{constant} \times \mu M R^{-1}. \tag{2.3}$$

Chandrasekhar shows that the same homology invariance is exhibited by stars (of small mass) having convective cores, and also that if β, the ratio of gas pressure to total pressure, is nearly unity (so that variations in β, but not in $1-\beta$ may be neglected) μ in the above relations is effectively replaced by $\mu\beta$ where β is a mean value for the star.

The relations (2.1), (2.2), (2.3) are identical with those derived from Eddington's standard model, if μ is replaced by $\mu\beta$. Equation (2.2) may be generalized, without serious error, to

$$L = \text{constant} \times f(T) M^{\alpha+1} R^{-3\alpha} \tag{2.21}$$

if $\epsilon = \epsilon_0 \rho^{\alpha} f(T)$ when $f(T)$ is a polynomial introducing high powers of T only.

3. The relations (2.2) or (2.21) may be compared with the observed values of M, L and R by making definite assumptions about s and α, namely $s = \frac{1}{2}$ and $\alpha = 1$ and by using (2.1) to determine μ and κ_0 which are linked by the approximate relations

$$\mu = \frac{2}{1+3X_0}, \qquad \kappa_0 = 3{\cdot}9 \times 10^{25}(1-X_0^2) \times \frac{1}{t},$$

where X_0 is the proportion of hydrogen by weight and t the guillotine factor. Since μ enters into (2.1) with a much higher power than κ_0 we shall neglect variations in κ_0 and use simply

$$15 \log \mu = 2 \log L + \log R - 11 \log M \tag{3.1}$$

which gives results sufficiently accurate for our purpose* except when μ approaches 0·5. The procedure has been retained for the few stars in which the indicated value of μ is nearly 0·5 for the sake of uniformity of treatment. An exception is however made for the two stars α Aurigae for which μ is taken equal to 1·0 following Strömgren.

Table I shows values of $\log M$, $\log L$ and $\log R$ according to Kuiper.† From these $\log \mu$ has been derived from (3.1) taking $\log \mu = 0$ for the Sun; $\log \mu M/R$ and $\log LM^{-2}R^3$ are also shown.

* The differences between $\log T_c$ found by this simple treatment and values quoted by Chandrasekhar are trifling (that is to say, the greatest difference in the logarithm is 0·04 : the mean (without regard to sign) for sixteen stars is 0·02).

† *Ap. J.*, **88**, 429, 472, 1938.

TABLE I

Star	log M	log L	log R	log μ	log μMR^{-1}	log $LM^{-2}R^3$
α Auri A	+0·62	+2·08	+1·20	0·00	−0·58	+4·44
B	+0·52	+1·90	+0·82	0·00	−0·30	+3·32
99 Herc	+0·48	+0·40	+0·09	−0·29	+0·10	−0·29
ζ U Maj	+0·41	+1·48	+0·28	−0·08	+0·05	+1·50
β Auri A	+0·38	+1·83	+0·43	0·00	−0·05	+2·37
B	+0·37	+1·83	+0·43	0·00	−0·06	+2·38
α C Maj A	+0·37	+1·59	+0·25	−0·04	+0·08	+1·60
τ Cygn	+0·36	+1·04	+0·28	−0·11	−0·03	+1·16
α C Min A	+0·17	+0·76	+0·23	−0·01	−0·07	+1·11
β 648	+0·15	+0·20	+0·06	−0·08	+0·01	+0·08
26 Drac	+0·14	+0·11	+0·04	−0·08	+0·02	−0·05
γ Virg B	+0·11	+0·49	+0·01	−0·02	+0·11	+0·30
A	+0·10	+0·50	+0·02	−0·01	+0·07	+0·36
δ Equl	+0·10	+0·21	+0·02	−0·04	+0·04	+0·07
α Cent A	+0·04	+0·10	+0·09	−0·01	−0·06	+0·29
p Erid	+0·04	−0·91	−0·35	−0·17	+0·22	−1·88
Sun	0·00	0·00	0·00	0·00	0·00	0·00
ζ Herc	−0·02	+0·59	+0·29	+0·11	−0·20	+1·50
70 Ophi A	−0·05	−0·38	−0·03	−0·02	−0·04	−0·37
α Cent B	−0·06	−0·43	−0·06	−0·02	−0·02	−0·49
ξ Boot A	−0·06	−0·32	−0·06	0·00	0·00	−0·38
B	−0·12	−0·83	−0·10	−0·03	−0·05	−0·89
70 Ophi B	−0·13	−0·86	−0·16	−0·03	0·00	−1·08
η Cass A	−0·14	−0·09	−0·09	+0·08	+0·03	−0·08
ADS 3135	−0·20	+0·07	−0·06	+0·14	+0·01	+0·28
ADS 3169	−0·21	+0·06	−0·03	+0·16	−0·02	+0·39
ADS 10075	−0·26	−0·66	−0·15	+0·09	−0·02	−0·59
85 Pegs A	−0·28	−0·37	−0·18	+0·14	+0·04	−0·35
η Cass B	−0·33	−1·16	−0·25	+0·07	−0·01	−1·25
μ Herc (M4)	−0·35	−1·37	−0·10	+0·07	−0·18	−0·97
ADS 3210	−0·44	−0·37	−0·13	+0·26	−0·05	−0·12
−8° 4352 (M4)	−0·45	−1·40	−0·12	+0·14	−0·19	−0·86
Kr 60A(M4+)	−0·60	−1·77	−0·29	+0·18	−0·13	−1·44

Table IIA shows the same quantities for certain double stars which were rejected by Kuiper since the parallax is smaller than 0″·045 in some cases and the orbits uncertain in others. The orbital quantities and trigonometrical parallaxes of these stars are shown in Table IIB. Since the uncertainties enter into the product μMR^{-1} with low weight, the stars yield valuable information in the present

TABLE IIA

Star	log M	log L	log R	log μ	log μMR^{-1}	log $LM^{-2}R^3$
δ 31	+0·43	−0·36	−0·12	−0·38	+0·17	−1·58
Brs O	+0·38	−0·50	+0·06	−0·22	+0·10	−1·08
Σ 2173	+0·35	+0·10	+0·12	−0·24	0·00	−0·27
A 2715	+0·31	+1·47	+0·28	−0·01	+0·02	+1·69
Σ 1785	+0·18	−0·78	−0·19	−0·25	+0·12	−1·71
Brs O 13	−0·21	−0·60	−0·17	+0·20	+0·16	−0·69
Mlb O 4	−0·22	−0·73	−0·05	+0·22	+0·05	−0·14

connection. In cases when the mass ratio has not been observed, it has been estimated from the magnitude difference. A binary star treated in this way is

TABLE IIB

Star	R.A. 1900·0 h m	Dec. 1900·0 ° ′	a ″	P y	Trig. Parallax ″	″
δ 31	1 30·4	−30 26	0·173	4·56	0·036	±0·009
Brs O 5	11 20·4	−61 06	4·047	233·5	0·067	13
Σ 2173	17 25·2	− 0 59	1·06	46·0	0·050	4
A 2715	5 56·9	+ 9 39	0·27	17·5	0·027	4
Σ 1785	13 44·5	+27 29	2·475	155·7	0·060	9
Brs O 13	17 11·5	−46 32	3·503	100·9	0·132	6
Mlb O 4	17 12·1	−34 53	1·83	42·2	0·147	6

considered to give one set of values of M, L and R only (the value for the brighter component). Kuiper's bolometric corrections and effective temperatures have been used. Values of $\log \mu MR^{-1}$ are plotted against values of $\log LM^{-2}R^3$ in Fig. 1. Stars of type M4 for which the bolometric correction and effective temperature are very uncertain are shown as crosses, and stars from Table II are shown as open circles. The remaining stars are shown as closed dots. No relation such as (2.2) with a high positive value of ν represents the points. The line for $\nu = 20$ is shown in the figure.

4. A possible explanation of the failure of the observed points to give any agreement with a law such as $\epsilon = \epsilon_0 \rho T^\nu$ or $\epsilon_0 \rho \sum_\nu T^\nu$ is that the stars differ in chemical constitution. Whether energy is generated by the carbon cycle or by some other reaction the chief source of energy is hydrogen, so that if x is the proportion of hydrogen by weight the law of generation is $\epsilon = \epsilon_0 \rho x f(T)$ or $\epsilon_0 \rho x^2 f(T)$. (But a change from carbon cycle at one temperature to proton–proton reaction to another is still of type $\epsilon = \epsilon_0 \rho f(T)$ if there is no change of hydrogen concentration.)

Consider first the case where x changes from star to star but remains constant within a given star. Then equations (2.1), (2.2) and (2.3) apply, and (2.2) may be written

$$L = \text{constant} \times \epsilon_0(x) T_c^\nu M^2 R^{-3}. \qquad (4.1)$$

If we eliminate T_c and R from (2.1), (2.3) and (4.1) we find

$$L \propto \epsilon_0(x)^{-\frac{s}{3+\nu-s}}$$

so that the dependence of L on $\epsilon_0(x)$ is small if ν is large and s small. The combination $LM^{-2}R^3$ is however proportional to $\epsilon_0(x) T_c^\nu$ and should therefore be small (for a given indicated T_c) where $\mu \to 2$, since this corresponds to small x. This is not borne out by the observations, under-luminous stars such as δ 31 having *small* values of μ, and over-luminous stars (α Auri, β Auri and α C Min) having average values.

We are led to the question whether stars with equal mean hydrogen concentrations can have different hydrogen concentrations in their energy generating centres. This is the reverse of the classical question whether diffusion can separate heavy materials from hydrogen during the life of a star, as the question here is whether diffusion or other mixing can maintain a sufficient supply of hydrogen at the centre to make good the deficiency caused by atom building. A convective core must be

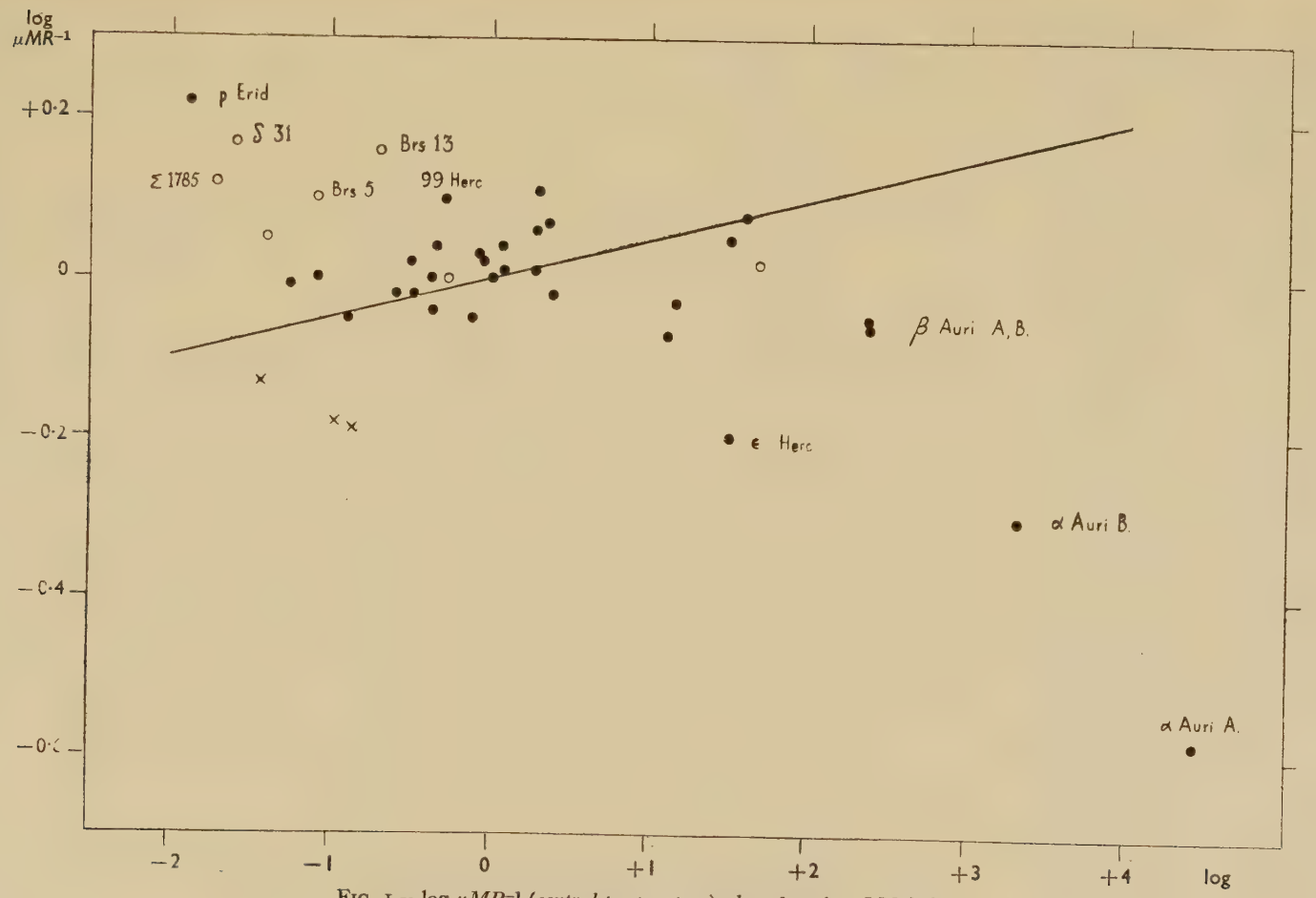

FIG. 1.—log μMR^{-1} (*central temperature*) *plotted against* $LM^{-2}R^{3}$.

well mixed, but it may not be able to exchange material freely with the middle and outer parts of the star. If x varies from point to point in the stars, they are not homologous with one another and the formulae (2.1), (2.2), (2.3) are invalid.

Any further discussion is bound to be very rough, until the question which combinations of L, M and R should correlate can be settled by numerical integration. It may however be pointed out that the mean energy output per gramme LM^{-1} shows a good correlation with MR^{-4}, which may be taken as a rough indication of the average density gradient. In Fig. 2, $\log LM^{-1}$ is plotted against $\log MR^{-4}$. While there is considerable scatter, the general tendency for high luminosity per gramme to be associated with low density gradient is well marked.

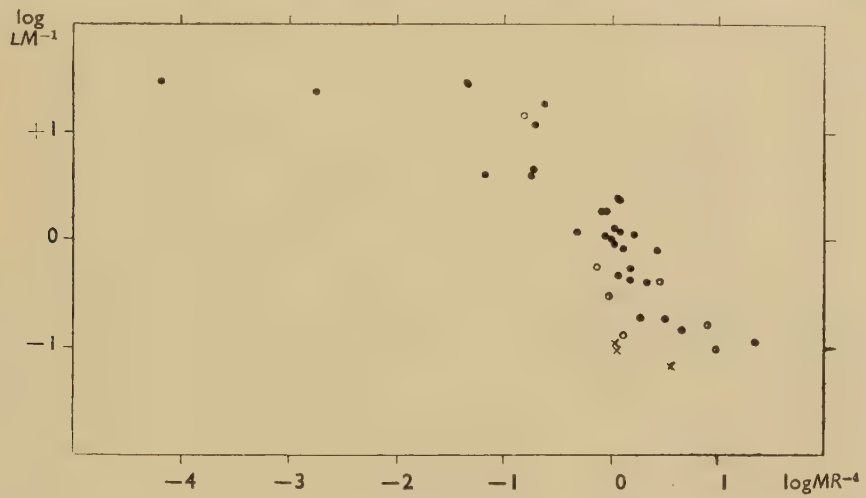

FIG. 2.—log LM^{-1} *plotted against* log MR^{-4}.

Differences in hydrogen concentration between centre and surface have been supposed possible by van Albada * who attributes central hydrogen starvation to *red giants*. As these stars are much *more* luminous per gramme than main sequence stars, the present argument reverses this suggestion and supposes that the red giants are rich in hydrogen at their centres, while stars like the Sun are deficient. It may be supposed that passage of hydrogen to the core from the middle zone is hindered by the density gradient and perhaps promoted by radiation pressure acting on heavy elements more than hydrogen. In this case central hydrogen deficiency would be greater in stars of high density gradient and low ratio of radiation to gas pressure than in giants. This is what is observed, if low energy per gramme is due to central hydrogen starvation.

5. White dwarfs are not homologous with main sequence stars, although their ratio of radiation pressure to total pressure is very low. This is a well-known theoretical result. It is abundantly confirmed by the observed quantities, since the white dwarfs show large positive values of $\log MR^{-1}$ and large negative values of $\log LM^{-2}R^{3}$. In other words, if we treat them as homologous with main sequence stars, white dwarfs show very high central temperatures yet are markedly under-luminous.

* *B.A.N.*, **10**, 63, 1945.

It is shown by Chandrasekhar (following Siedentopf and Strömgren) that a certain inequality is satisfied by ξ, the distance from the centre of a star of the point where degeneracy sets in, expressed in units equal to the radius of the star. Taking particular values of the molecular weight and guillotine factor, Chandrasekhar finds

$$8{\cdot}5 \times 10^{-3}\left(\frac{M^9}{L^2R^7}\right)^{1/4}\left(\frac{1}{\xi}-1\right)^{7/4} \gg 1.$$

Replacing the inequality by equality sets an upper limit to ξ, say $\xi_{\max.}$ Values of $\xi_{\max}$ for certain stars are shown in Table III.

TABLE III

The Upper Limit for Degeneracy

Star	$\xi_{\max}$	Star	$\xi_{\max}$
Sirius B	0·94	Sun	0·06
δ 31	0·28	ζ Herc	0·02
Σ 1785	0·22	β Auri A	0·02
p Erid	0·22	β Auri B	0·02
Brs O 5	0·20	α Auri B	0·013
99 Herc	0·14	α Auri A	0·007

Table III suggests that δ 31, p Erid, Brs O 5, Σ 1785 and possibly 99 Herc may have appreciable degenerate cores in the manner suggested by Milne, and their low luminosity may be connected with this. The degenerate cores may or may not be very deficient in hydrogen. The arguments developed for homologous non-degenerate gaseous stars do not lead to correct values of the central temperatures of stars with degenerate cores. The argument here put forward is that the *observed* very low luminosity of the white dwarfs is connected with the low luminosity of δ 31, etc. (as judged by their position towards the top left-hand corner of Fig. 1), and that the observations support the existence of degenerate cores in these stars.

Commonwealth Observatory,
Canberra, Australia :
1946 *July* 24.

THE PRESENT STATE OF INVESTIGATIONS INTO COMET WOLF I

M. Kamienski, Assoc.R.A.S.

(Received 1946 April 10)

Summary

1. This paper contains the main results of the author's investigations on the periodic Comet Wolf I for the period 1800–1942. The comet was discovered in 1884, and in 1875 as well as in 1922 approached Jupiter within 0·12 astronomical units.

2. All the 1888 observations of the comet during its 9 returns to the Sun in the period 1884–1942 are well represented by *one* system of elements for 1884 September 24·0, taking into consideration perturbations in its motion due to Venus, the Earth, Mars, Jupiter, Saturn and Uranus as well as the quasi-retardation of its motion.

3. The orbit of the comet was studied back to the year 1800, but the minimum distance of the comet from Jupiter was 0·12 astronomical units in 1875. Since this was not zero, the comet could not originate from Jupiter.

4. Schulhoff's and Coniel's statement concerning the division of a combined comet into Comet Wolf I and that of Barnard 1892 V, near Jupiter at the end of 1815, is erroneous as to Comet Wolf I and remains quite unfounded as to Comet Barnard.

---

1. Comet Wolf I was discovered by M. Wolf in 1884; it was then bright enough, 6^m, but in the course of time it has been constantly losing its brightness. When last it appeared in 1942, its photographic magnitude was scarcely $19^m{\cdot}3$. It was observed at its every return to the Sun, except in 1904/1905, namely in:

1. 1884/1885	4. (1904/1905)	7. 1925
2. 1891/1892	5. 1911/1912	8. 1933/1934
3. 1898/1899	6. 1918/1919	9. 1942

All these apparitions have already been exactly worked out, taking into consideration perturbations in its motion due to Venus, the Earth, Mars, Jupiter, Saturn and Uranus.

The *Memoirs*, containing the theory of the motion of this comet during 1884–1942, were published by the author in several scientific periodicals, mainly in *Acta Astronomica* and in the *Publications of the Astronomical Observatory of the Warsaw University* (1925–1939). The work done during the last war has not yet been published in general. Further, a part of the manuscripts, as well as all the original computations, was destroyed by fire in August 1944, when the Warsaw Observatory was burned by the Germans.*

2. On the other hand, with a view to explaining the origin of this comet as well as its relation to other short period comets, the author examined its orbit as far back as the year 1800, and drew some important conclusions (see below,

* *Circ. astr. Obs. Univ. Warsaw*, No. 21, 1945.

Section 10, *A* and *B*). In that way, the researches on the motion of this comet extend to the comparatively long period of time of 142 years. There is no other comet, with the exception of the famous Comet Halley, which has been investigated in detail over such a long space of time.

3. All the apparitions of this comet during 1884–1919, containing in sum 1888 observations, were grouped in 50 normal places. Then they were joined with *one* system of elements.* It appeared that in the motion of the Comet Wolf I a phenomenon of quasi-retardation was quite clearly demonstrated, which does not exist in any other comet.

The main fundamental system P_1 of elements, connecting all the observations of the comet during 1884–1919, is the following:

Epoch and osculation: 1884 September 24·0 M.B.T.

$$P_1 \quad \left.\begin{array}{ll} M = 352^\circ\,01'\,26''\cdot49 & \Omega = 206^\circ\,18'\,31''\cdot35 \\ \phi = 34^\circ\,07'\,11''\cdot83 & \pi = 19^\circ\,00'\,55''\cdot44 \\ \mu = 523''\cdot77484 & i = 25^\circ\,15'\,40''\cdot05 \end{array}\right\} 1880\cdot0$$

$$\Delta M = -0''\cdot00000\,021\,(t-t_0)^2$$

$$\Delta\mu = -0''\cdot00000\,042\,(t-t_0).$$

Here $(t-t_0)$ must be expressed in days and counted from 1884 September 24·0.

The system P_1 represents very well all the 50 normal places in the above period 1884–1919. The mean error ϵ of such a representation is very small:

$$\epsilon = \pm 1''\cdot77.$$

In the table below a comparison is given of the goodness of fit of the author's researches on Comet Wolf I with similar values of other authors for the best studied comets of short period.

Comet	Computer	Number of returns	Number of normal places	Number of unknowns	ϵ
Faye	A. Möller	4	23	7	$\pm 4''\cdot1$
Winnecke	A. Haerdtl	6 (4)	12	7	$\pm 4\cdot6$
Encke	O. Backlund	5	22	8	$\pm 3\cdot8$
Wolf I	M. Kamienski	6 (5)	50	6 (7)	$\pm 1\cdot8$

4. During the period 1884–1919 the comet did not make a close approach to Jupiter. However, in 1922 its approach to this planet was so close that it passed through the system of its satellites. The mutual distance, Δ, of these bodies was then:

$$1922 \text{ September } 27^d\cdot10, \quad \Delta = 0\cdot1247\,\text{A}.$$

In consequence, the perturbations in its motion attained very great values, namely:

1922 June 8·0–1922 Dec. 15·0

Perturbation in the mean anomaly $\Delta M = +20^\circ\,05'\,55''\cdot6$

Perturbation in the mean daily motion $\Delta\mu = -\ 96''\cdot3737$

The perihelion distance increased from 1·54 to 2·37 and the period of revolution from $6^y\cdot71$ to $8^y\cdot21$. Nevertheless, the comet was found at its next return in 1925

* *Publ. astr. Obs. Univ. Warsaw*, **7**, 1933.

near enough to the computed place. The system P_1 represents its normal places in 1925 with the maximum residual of

$$\Delta\alpha\cos\delta = -5^s\cdot16, \qquad \Delta\delta = +4''\cdot8.$$

When we take into consideration the enormous perturbations of the comet's motion in 1922 as well as the circumstance that in 1925 it was travelling in quite a different part of interplanetary space we must come to the conclusion that these residuals are not too great.* The cause of them will be probably explained after some supplementary researches (see below, Section 10 *D*).

5. The next apparition of this comet in 1933/1934 is however represented by the same system P_1 quite well; the *mean* residual for and after perihelion passage is zero. The maximum residual attains only $0^s\cdot6$ in right ascension.

6. The original work containing computations of the perturbations of the comet's motion during 1934–1942, as well as the elaboration of the comet's apparition in 1942, perished in the fire in 1944. However, previously to that we were able to carry out the main investigation, during our exodus from Warsaw. The results are given in the table below, which contains the sums Σ_6 of perturbations by Venus, the Earth, Mars, Jupiter, Saturn and Uranus.

Period	$\Sigma_6\delta M$	$\Sigma_6\delta\phi$	$\Sigma_6\delta\Omega$	$\Sigma_6\delta\pi$	$\Sigma_6\delta i$	$\Sigma_6\delta\mu$
1934 Apr. 16·5–1934 Dec. 29·0	+ 50·95	− 0·90	− 1·66	− 85·66	− 1·07	+0·0680
1934 Dec. 29·0–1942 June 10·0	+1558·39	+251·01	−242·71	+408·33	+144·05	+2·1159
1942 June 10·0–1942 Nov. 5·0	− 20·01	− 2·06	− 0·74	+ 50·77	− 1·10	−0·0048

Adding these perturbations to the system P_{16} for 1934 April 16·5 †, the author derived three new systems P_{17}, P_{18} and * for 1934 December 29·0, 1942 June 10·0 and 1942 November 5·0. The system P_{18} is as follows:

Epoch and osculation: 1942 June 10.0 U.T.

$$P_{18}\quad \left.\begin{array}{ll} M = 350^\circ\,22'\,54''\cdot10 & \Omega = 204^\circ\,20'\,33''\cdot21 \\ \phi = 23^\circ\,52'\,42''\cdot19 & \pi = 5^\circ\,18'\,28''\cdot70 \\ \mu = 428''\cdot1865 & i = 27^\circ\,18'\,06''\cdot70 \end{array}\right\} 1950\cdot0$$

$$\Delta M = -0''\cdot00000\ 021\,(t-t_0)^2$$

$$\Delta\mu = -0''\cdot00000\ 042\,(t-t_0).$$

When finally we take into consideration the further perturbations to 1942 November 5·0 and form the system * of elements for this date, we derive the following *computed* place of the comet on that date:

$$* \quad \left.\begin{array}{l} \alpha_{cal} = 2^h\,59^m\,38^s\cdot0 \\ \delta_{cal} = +1^\circ\,39'\,07'' \end{array}\right\} 1950\cdot0.$$

** Repr. astr. Obs. Univ. Warsaw*, No. 32, 1936.
†* *Repr. astr. Obs. Univ. Warsaw*, No. 36, 1937.

The comet was found by Dr Baade on a plate taken on 1942 November 5 with the 100-inch reflector at Mount Wilson.* It appeared like a minute grey spot of scarcely $19^{m}\cdot3$ photographic magnitude. Reducing this observation to the moment 1942 November 5·0 U.T., we obtain:

$$\left.\begin{aligned}\alpha_{obs} &= 2^{h}\,59^{m}\,43^{s}\cdot0\\ \delta_{obs} &= +1^{\circ}\,38'\,58''\end{aligned}\right\}\ 1950\cdot0.$$

Hence it follows that the theory of this comet represents its observation on 1942 November 5 as follows:

$$\Delta\alpha\cos\delta = +5^{s}\cdot0 \qquad \Delta\delta = -9''.$$

The author is much indebted to Sir Harold Spencer Jones, Astronomer Royal, for kindly supplying information of five observed positions of this comet in 1942.

The author studied also the observed brightness for the period 1884–1934, using Orloff's well-known formula

$$H = H_0 + 5\log\Delta + 2\cdot5k\log r; \qquad k = 4.$$

The absolute brightness $H_0 = 14^{m}\cdot0$ for 1942 October was *extrapolated* from a graph, representing the brightness of the comet for the above period. Hence the apparent brightness H for the time of observation ought to be:

$$H = 19^{m}\cdot2.$$

In reality, its photographic brightness was then $19^{m}\cdot3$.*

The systems P_{17}, P_{18} and * are extrapolated and not yet equalized over 24 years; they are attached to the already equalized system P_{10} for 1918 December 16·0.† Moreover, the change of the comet's orbit in 1922 was enormous. Having this in view, as well as the extreme faintness of the comet, we must conclude that the present theory of the motion of the Comet Wolf I represents its observation in 1942 with all the exactitude which may be required.

7. The further step to be done for the perfection of the theory of this comet, is the connection of *all* the 64 normal places during the period 1884–1942. It is to be expected that such a connection would diminish the above residuals for 1942. The author hopes that he will be successful in doing this before long.

It would be suitable to take into consideration perturbations due to Mercury and Neptune. They were already computed for the period 1884–1919, and the connection of the apparitions of the comet during this period with the Mercury and Neptune perturbations was done. But—alas—these calculations perished during the burning of the Warsaw Observatory and their reconstruction will take a considerable time. It is, however, evident that these perturbations are small enough and can hardly influence the general view of the connections of the several apparitions of the comet.

8. It has already been stated that the main fundamental system P_1 of the elements of the comet represent all its observations in 1884–1919 very well. Moreover, after taking into consideration the further perturbations as well as the

* *Circ. I.A.U.*, No. 933, 1943.
† *Publ. astr. Obs. Univ. Warsaw*, **7**, 1933.

secular retardation, this system represents comparatively well the next observations of the comet in 1925, 1933, 1934, 1942—i. e. during 58 years, although the comet approached very near to Jupiter in 1922.

With this in view, the author considered the system P_1 for 1884 September 24·0 as quite suitable and good for the possibility of performing with its help the computation of the perturbations in the retrograde motion of the comet till 1800. The aim of such computations was to investigate the problem of the origin of the Comet Wolf I as well as its relation to other comets, especially with that of Barnard 1892 V.

These researches resulted in a series of Memoirs entitled "Recherches sur l'origine de la comète Wolf I". Parts I, II, III, IV, V, VI. Of these, only Part I was published.* Unfortunately, all the store of the reprints perished by fire in 1944, as stated above. As to the manuscripts of the Parts II–VI, they were saved and are prepared for printing.

During the investigation of the cometary orbit for 1884–1800, the author took into consideration the *exact* perturbations due to Jupiter and Saturn only, since the minor perturbations from the other planets have no importance for explaining the *origin* of the comet.

9. The author paid much attention to the control of his computations or—where it was possible—to performing them by two independent methods; it took about 20–30 per cent. of the time used for the actual calculations. In such a way an absolute surety was given that the data, published by the author, do not contain errors, which could in any way influence the published results. Failures and divergencies in theories of the motion of some other periodic comets are undoubtedly due in the first place to the lack of proper control, which is well known to those scientists who specially work in the domain of investigation into the motions of comets.

Particularly, the close approaches of the comet to Jupiter in 1839, 1875, 1922 were computed by two methods—the heliocentric and the jovicentric. The results of the definitive computations of Jupiter's perturbations during the approach of the Comet Wolf I in 1875 to it are given below:

1875 Aug. 13·0–1875 Apr. 5·0

	Heliocentric method	Jovicentric method	Difference
	° ′ ″	° ′ ″	″
δM	+15 38 28·9	+15 36 32·7	+116·2
$\delta\phi$	−11 50 13·3	−11 50 31·4	+ 18·1
$\delta\Omega$	+ 0 46 50·4	+ 0 46 47·3	+ 3·1
$\delta\pi$	−13 11 37·9	−13 10 56·9	− 41·0
δi	+ 2 00 41·9	+ 2 00 41·2	+ 0·7
$\delta\mu$	−107″·430	−107″·412	−0″·018

As can be seen, the agreement is good enough, especially when we take into consideration the complicated calculations at the transition from the heliocentric orbit to the jovicentric and *vice versa*. Using 6-figure logarithmic tables, one could hardly get better results.

Similarly, when computing the perturbations by Venus and the Earth for the period 1884–1942, the two methods—the heliocentric and the barycentric—were applied. However, when deducing the systems of elements for the period

* *Bull. Acad. Pol. Cracow*, 1939; *Repr. astr. Obs. Univ. Warsaw*, No. 45, 1939.

1800–1942, the perturbations computed by the heliocentric method were definitely taken, because they should be more exact.

For the sake of uniformity, the method of variation of arbitrary constants was used throughout. The systems of elements were changed every $2\frac{1}{2}$, 5, 10, $12\frac{1}{2}$, 20, 25, 40, 50 days, and successive approximations were repeated, when it was necessary.

As a result of the retrograde computations, the following earliest system P_{-16} of the elements was found:

Epoch and osculation: 1800 January 4·5 U.T.

P_{-16}

$M = 288^\circ\,16'\,04''\cdot5$ $\quad$ $\Omega = 212^\circ\,54'\,18''\cdot6$

$\phi = 23^\circ\,42'\,04''\cdot2$ $\quad$ $\pi = 12^\circ\,37'\,16''\cdot7$ $\Big\}$ 1950·0.

$\mu = 421''\cdot3704$ $\quad$ $i = 26^\circ\,46'\,39''\cdot1$

10. On the basis of these researches and calculations, we can draw the following conclusions as to the *origin* of this comet and its *relation* to that of Barnard 1892 V:

A. The origin of the Comet Wolf I from matter ejected from Jupiter seems to be unfounded. In the very moment of the separation of these bodies, their mutual distance Δ ought to have been zero. However, the minimum distances of the comet from Jupiter in the period 1800–1942 were:

1816 Jan.	$7^d\cdot50$	$\Delta = 1\cdot9122$	1875 June	$8^d\cdot67$	$\Delta = 0\cdot1180$
1839 Nov.	$13^d\cdot12$	$\Delta = 0\cdot5382$	1922 Sept.	$27^d\cdot10$	$\Delta = 0\cdot1247$

Consequently, Proctor's (1881), A. Crommelin's (1910) and lately S. Vsessviatsky's (1933)* views, according to which the short period comets originate from matter ejected from the surface of planets, chiefly from Jupiter and even from the Sun, have not been found satisfactory, at least in respect of Comet Wolf I. Using the known circumstance of a rapid diminution of the brightness of the short period comets, S. Vsessviatsky extrapolates this brightness backwards to the moment when its absolute value H_0 was -1^m. The comet then should have been certainly discovered. However, as there was no comet with $H_0 = -1^m$ the *upper* limit A_e of its age is:

$$A_e = 50\,\frac{H_{1900} - H_0}{\Delta H},$$

where ΔH is the diminution of the brightness of a short periodic comet in 50 years. For the Comet Wolf I, S. Vsessviatsky admits $\Delta H = 3^m\cdot7$ and obtains in such a way $A_e = 120$ years.† If however we take into consideration a greater fall of its brightness during 1911, 1933, 1942, the upper limit of this comet's age should be reduced even to 97 years.

If we suppose however that its separation from Jupiter took place somewhere in the 18th century, its age would be considerably longer than follows from the Vsessviatsky's theory.

Finally, one of the greatest objections to the theory of the ejection of such comets from the surface of Jupiter is the computations of M. Axel Corlin‡,

* *Astr. J. U.S.S.R.*, **10**, 23, 1933.

† *Astr. J. U.S.S.R.*, **10**, 18–40, 1933.

‡ *Festskrift Tillägnad Östen Bergstrand den* 1 *September* 1938, Uppsala, 1938.

according to which the critical velocity of such an ejection should be 580 km./sec., and not 60 km./sec., as results from the computations of S. Vsessviatsky.

B. The statements of Schulhoff* and M. T. Coniel†, according to which comets Wolf I and Barnard 1892 V were once a single body and divided at the end of 1815 when they both were found near Jupiter, seem to be also entirely unfounded. The minimum distance Δ of the Comet Wolf I from Jupiter was then

$$1816 \text{ January } 7^{d}\cdot 50, \quad \Delta = 1\cdot 9122.$$

As to the position of Barnard's comet 1892 V for this time, it remains quite undetermined, for its elements, especially the mean daily motion, are very uncertain. These elements were determined from a very short period of observation (1892 October 13–1892 December 8). Tisserand's criterion cannot play an important part in this case.

C. The comet's orbit, after its close approach to Jupiter in 1922, returned nearly to the same shape, which existed before its previous approach to this planet in 1875. This is easily seen from a comparison of the perturbations which took place during the two approaches to Jupiter:

	δM	$\delta\phi$	$\delta\Omega$	$\delta\pi$	δi	$\delta\mu$
	° ′	° ′	° ′	° ′	° ′	″
1875 Aug. 13–Apr. 5	+15 38	−11 50	+0 47	−13 12	+2 01	−107·430
1922 July 8–Dec. 15	+20 06	− 9 55	−0 32	−13 25	+1 24	− 96·346

In consequence, the conditions of visibility of this comet become worse than they were before.

D. The motion of Comet Wolf I in the period 1884–1942 necessitates the introduction of some supplementary terms to the elements M and μ, which *formally* are expressed by the formulae:

$$M = M_0 + \mu_0(t-t_0) + \Sigma\delta M - 0''\cdot 00000\ 021(t-t_0)^2,$$
$$\mu = \mu_0 + \Sigma\delta\mu - 0''\cdot 00000\ 042(t-t_0).$$

The cause of the existence of such terms will probably appear by itself, after the completion of the supplementary computations to which reference is made above. At present the creating of any *ad hoc* hypothesis would not be advisable, especially when such an hypothesis is not founded on exact numerical computations. We have already seen how misleading were Schulhoff's and Coniel's statements, based on the system of the elements of the Comet Wolf I for the year 1875, extrapolated backwards without taking into consideration perturbations for the period 1875–1815.

Cracow:
1946 *January* 6.

* *A.N.*, **131**, 115, 1892 (No. 3127).
† *B.A.*, **12**, 245–261, 1895.

AN ABSTRACT ON THE SOLAR APEX

Rev. O. R. Walkey

(Received 1943 November 15 *)

Summary

Reference to early derivations of the Solar Apex is followed by a table of the more recent findings, stimulated by and based on either the Lick *Catalogue of Radial Velocities* or the Albany *General Catalogue* for Proper Motions. The occasionally unexplained divergence between the several positions found for the apex is commented on, and a simple numerical method is applied to the problem, based on these two catalogues. Independent of the actual sizes of the stellar motions, and therefore of any need to assign limits, the method by-passes the need for assumptions such as of distance, and so on. Further, the actual radial velocities—for which "natural" sampling limits appear—are used for an independent check on the numerically derived apical positions ; also to compute the solar velocity. The resultant positions are found to be in marked agreement, both between themselves and with the mean of those (more divergent) found by the more refined methods, using the same material. The present numerical study, involving 40,720 star motions in all, places the solar apex at (1900.0) R.A. $270°{\cdot}2 \pm 0°{\cdot}3$, Dec. $+28°{\cdot}7 \pm 0°{\cdot}5$, whereof the "true" galactic coordinates are l_g 22°·0, b_g +22°·2, whither the solar velocity of approach is found to be $20{\cdot}5 \pm 0{\cdot}6$ km./sec. ; its galactic planar component being 19·0 and the normal 7·75 km./sec.

Previous findings

It is generally recognized that the Sun is travelling † towards a point in Hercules. Summarizing the earliest positions found for the point of approach, Newcomb placed the apex at $18\frac{1}{2}°$ in R.A. and $+35°$ in Dec. Since when, as more and better radial velocities and proper motions became known, investigations by Campbell, Boss and others have ranged the apex from $268\frac{1}{2}°$ to $277\frac{1}{2}°$ in R.A., and from $+20°$ to 31° in Dec. Again, the position of the apex was found to vary slightly with the class of object referred to—predicating systematic motion for each class. Campbell, in summary (1911), adopted the "convenient" apex at R.A. 270°, Dec. +30°; whither the Sun was taken to travel at 19·0 km./sec., or just four astronomical units in a year.

Further research into the solar apex was stimulated by the appearance, full twenty years later, of two fundamental catalogues, one of which was J. H. Moore's catalogue ‡ of radial velocities for 6739 stars, including virtually all those down to magnitude 5·50, together with many fainter stars of peculiar interest. The

* Received in final form 1946 November 18.

† Compare incidentally the distinction between the "path" and the diurnal "circuit" in the Hebrew of Psalm xix, 5–6.

‡ *Publ. Lick. Obs.*, **18**, 1932.

other was B. Boss's * *General Catalogue* giving 33342 proper motions, covering all stars down to magnitude 7·0, with as many more fainter stars of particular note. Besides these lists, others, such as the Cape Catalogue of stars of about 10th magnitude and lists of still fainter stars, have been used to derive the solar apex. These foregoing later apices (all for 1900·0) are summarized in Table I, while a figure illustrates their several positions, in both terrestrial and galactic coordinates. The mean of the three positions derived for the bright stars down to the 6th magnitude is R.A. 271°·2 (ranging 5°·0), Dec. +29°·0 (ranging 3°·7), while that of the three apices for the 10th magnitude stars—the most concordant of the faint stars—is at R.A. 267°·5 (ranging 5°·1), Dec. +26°·8 (ranging 2°·3); the combined simple mean position for these two sets is at R.A. 269°·5, Dec. +27°·9. The frequent wide divergences—despite the mathematical refinements used—raises the question, apart from possible systematic error, whether rotation in a probable Local Cluster leavens the allowance made for galactic rotation. The increasing declination with magnitude † found by Wilson and Raymond—who remark it as "surprising"—may, if real, be due to some such cause; though the consistently lower declination noted for the 10th magnitude stars tells against this.

TABLE I

Year	Author and Data	Mag.	No. of stars	Apex 1900·0 R.A.	Apex 1900·0 Dec.	Entry No.
	By Radial Motions					
1933	Edmondson (possibly representing Gould's Belt)	1–4	711	271°·4	+ 26°·3	1
	Edmondson (combined)	1–6	3583	273·1	30·4	2
1936	Nordstrom, combined spectral types *	1–6	3238	272·3	26·7	3
1941	Ali, types O–B7 in Galactic belt	1–8±	788	272·7	34·3	4
	By Proper Motions					
1927	Bruggencate and Smart	11–14 *p*	4245	272·6	31·1	5
1928	Smart	11·5 *p*	3029	273·2	43·6	6
1934	Knox-Shaw and Barrett	13·7 *p*	24911	272	41	7
1936	Jackson, Cape Zone Catalogue	10±	18349	266·9	28·3	8
1937	Van de Kamp and Vyssotsky	11 *p*	18000	285	36	9
1938	Wilson and Raymond	1–6	4606	268·1	30·0	10
	,, ,,	1–7	14501	269·8	33·2	11
	,, ,,	1–9½	32096	270·2	37·0	12
1939	Smart and Tannahill (Cape Zone Cat. (Ellipsoidal hypothesis))	10±	18323	265·1	26·1	13
1941	Brown (Cape Zone Cat. (Ellipsoidal hypothesis))	10±	18349	270·6	26·0	14

p denotes photographic magnitude.

* Spectral range in R.A., from 263°·8 (A) to 280°·8 (G); in Dec., from +21°·2 (F) to 36°·8 (M).

* *Carnegie Publication* No. 468, 1937.

† The apex represented empirically as at: $\alpha = 270° + 2(m-6)°$, $\delta = +32° + 4(m-6)°$, roughly parallel to the galactic plane, where m is magnitude.

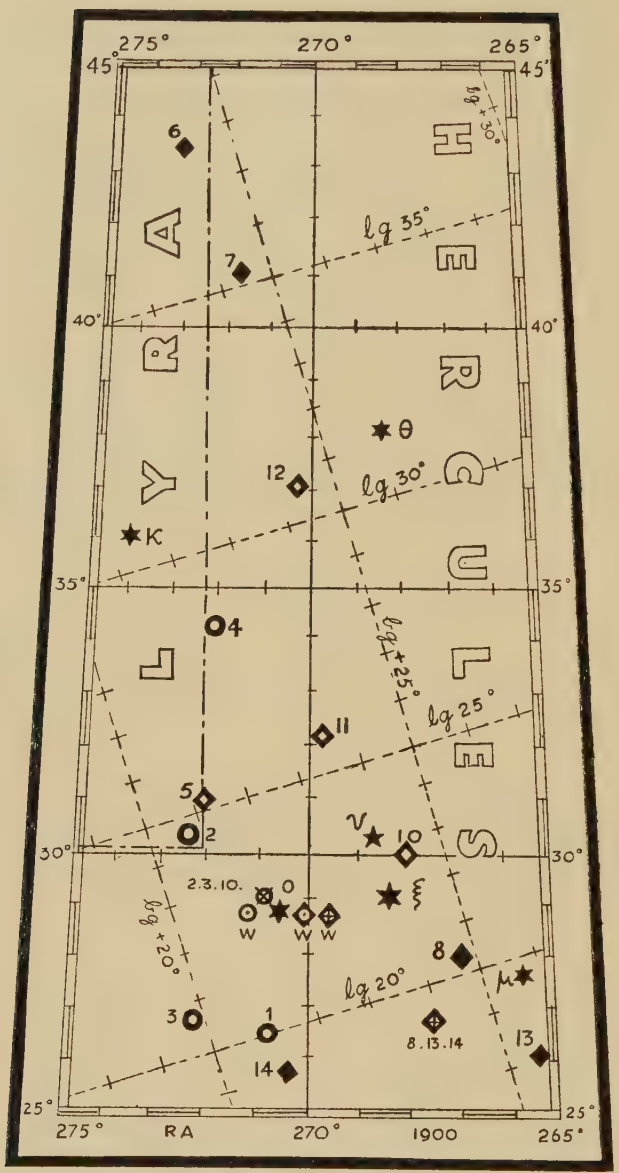

Conical Projection

Solar Apices.

The panel illustrates the various apices, previously found—numbered as entered in Table I—for the solar motion, except the far outlying No. 9. The circular dots are those based on radial velocities, and the diamonds those on proper motions. The solid dots of either form mark apices from single-magnitude stars ; the open ones those from combined magnitudes, as tabulated. The crossed circle (2, 3, 10) *marks the mean of the three apices for the* 1–6 *magnitude stars, corresponding to the basis of the present study—whereof the radial velocity and proper motion apices with their weighted mean (central dotted) are linked " W ". The quartered diamond* (8, 13, 14) *marks the mean of the three apices for the* 10*th magnitude stars. All stars brighter than* 5*th magnitude are plotted, in order to locate the sky. The chain line defines the I.A.U. boundary* (1900·0) *between Lyra and Hercules. The broken lines trace the galactic coordinates from their N. pole at* α 192° δ +27°. *The terrestrial coordinates are for epoch* 1900·0.

The general question therefore arises whether our ignorance of the actual peculiar motions of the stars, and the consequent assumptions needed to fill this gap in our knowledge, do not undermine the refined mathematical edifice built thereon. The mathematical barrel-organ, in fact, simply grinds out inexorably the tune resultant from the particular assumptions wherewith it has been primed—an air more tuneful, maybe, than true. Perhaps, under the present circumstances of the problem, simplicity is the soul of truth; and the fewer our assumptions, the nearer we get to reality.

Present investigation

Taking the two above-named standard catalogues, the *sense* alone of their respective motions is here considered, whether reflecting—"pro"—solar motion, or the reverse—"con".* In this way are by-passed assumptions, such as for distance (for the cross-motions) and so forth, as well as the general assignment of arbitrary limits for acceptable motions; thus we dodge the sampling-bogey—ever the determining factor in such problems as the present. This method—a development, actually, of that mentioned by Russell, Dugan and Stewart (*Astronomy* Vol. II)—is not concerned with the inequalities of stellar distribution. In order, therefore, to avoid consequent systematic error, the "pro" and "con" counts have been reduced to percentages of their totals. Though, strictly speaking, "pro" percentages of over fifty should alone be reckoned, it must be remembered that excessive peculiar motions have a unilateral effect, in that such "con" motions (swamping the solar effect) reverse the sense of otherwise "pro" motions, while large peculiar motions in the "pro" direction do not increase that count. This should explain why the "pro" motions do not reach 100 per cent. at the point of maximum reflex of solar motion. The several catalogue entries representing an obviously common star system have been treated as one in the counts; so too the known star groups and clusters, as the Perseus, Pleiades, Hyades, Orion and the Ursa Major, each as one. Zero motions have been shared half-and-half between "pro" and "con".†

Right Ascension.—For the R.A. of the solar apex, the sky was divided into meridional gores or lunes 5° wide in R.A. from pole to pole (as serving well enough) ‡ for both the radial and proper motion counts, with the antipodal lunes combined in the percentages. Owing to the indeterminate nature of the motions near the meridians of zero solar effect, the counts end with the meridians centred 15° on either side of these meridians of contraflexure, viz. the equinoctial in the radial, and the solstitial in the proper motions. As a check in each case, more detailed counts have been taken down each of the four colural meridians.

* Whence "pro" radial velocities recede at 6^h R.A. and approach at 18^h; while "pro" proper motions are positive in R.A. at 0^h, and negative at 12^h; "con" motions being the reverse in each case.

† Miss Jenkins's list (*A. J.*, **50**, 142, 1943) of corrections to the *G.C.*, has none affecting the present counts.

‡ It is realized, in the case of radial motions, that the tips of the lunes lying within the parts of the polar caps away from the solar apex and antapex reverse their "pro" and "con" sense, since these polar tips of such lunes fall within the other hemisphere of reflected solar motion. The combined area of these contrary areas (of polar radius 29°, as the approximate Dec. of the apices) is only a sixteenth of their lunes. Also, they lie near the belt of indeterminate motions. Hence any contrary effect scarcely justified the weeding out of motions above Decs. $\pm$ 61° on these far sides.

Declination.—To find the declination of the apex, spherical panels were taken, centred approximately round the solar apex and antapex, and ranging 60° from the equator—southward at 6^h R.A. and northward at 18^h, the panels being 15° wide in R.A. for the radial motions and 10° wide for the proper motions in Dec. The panels were divided into zonal belts 5° deep for the radial and 2° deep for the proper motion counts; these narrower divisions for the pattern adopted in view of the richer fields offered in the *GC*. Both yielded the same declination for the apex.

Probable Errors.—In deriving the probable errors, the percentage counts were plotted round their directions, and their divergences noted from the theoretical curve for solar reflexes. From these, the probable errors followed in the usual way:

$$\text{p.e.} = 0{\cdot}6745 \sqrt{\frac{d_1^2 + \ldots + d_n^2}{n(n-1)}}.$$

Velocities.—Though a departure from the precedent of ignoring the sizes of the motions, yet, as an independent check on the foregoing derivations, both in R.A. and Dec. the actual radial velocities were treated. On the policy of avoiding arbitrary assignments, all velocities up to 60 km./sec., to and from, were plotted, so to find the limits within which they naturally aggregate—according to both sense and position in the sky.* Opposed areas were chosen in the three cardinal directions *X*, *Y*, *Z*—equatorial along the solstitial (*X*) and the equinoctial (*Y*) directions, with the polar axis (*Z*); the equatorial pairs being spherical squares of 36° a side, the polar pair as caps extending from each pole down to its 70° declination, so approximating in area to each of the equatorial patches. The velocity plots showed the "con" frequencies to tail off at about two-fifths of the speeds whereat the "pro" frequencies fade along the *X* and *Z*-axes (at 21 and 51 respectively along *X*, with 20 and 48 km./sec. along *Z*). Crosswise, along the neutral *Y*-axis, the balance, as would be expected, was equal (at 27 km./sec.). It might be remarked incidentally that these seem to predicate peculiar velocities approximating to those of the velocity ellipsoid along these axes. Resolution of the three axial counts yielded a position for the apex in good agreement with the other findings.

The sundry resultant positions appear in Table II, and give a combined mean position, by the present method, at (1900·0) R.A. 270°·2 ± 0°·3, Dec. +28°·7 ± 0°·5 as the solar apex. This point lies 0°·6 west of the slightly variable fourth magnitude star *o* Herculis, near the S.W. corner of Lyra. The "true" galactic coordinates † of this apex are galongitude l_g 22°·0, galatitude b_g 22°·2. This point, again, lies some 13° north of the accepted plane of the Local Cluster, and 7° north of the line of Gould's bright-star belt.

Solar Velocity.—The apex found, a check was applied for solar velocity direct, from spherical panels centred at the apex and antapex. These were taken 25° wide in R. A., centred along the solstitial meridians, and ranging from 18° to 40° in Dec. past the apices (so adjoining the *X*-axial equatorial squares). The "pro" and "con" velocities were found to tail off at (50 and 20 km./sec.) virtually the same speeds as in the adjacent equatorial squares, as the natural limits for sampling. The solar velocity so found from the 156 stars involved was 20·75 ± 0·8 km./sec.,

* The relatively few stars moving at over 60 km./sec., as evidently a class by themselves, should be irrelevant to the present issue.

† *Observatory*, **64**, 126, 1943.

TABLE II

Positions of Solar Apex

Methods by Counting	Right Ascension			Declination		
	No.	Area sq. deg.	Position 1900·0	No.	Area sq. deg.	Position 1900·0
(*a*) Radial Motions						
Velocities round sphere	5370	35523	$272°.7 \pm 0°.6$	262	1488	$+28°.7 \pm 0°.5$
,, at colures	1050	6876	$269°.8 \pm 1°.0$	...	...	...
,, *X*, *Y*, *Z*	716	5100	$271°.6 \pm 2°.4$	981	7588	$+28°.6 \pm 2°.7$
Totals and means	7136	47499	$271°.9 \pm 0°.5$	1243	9076	$+28°.7 \pm 0°.5$
(*b*) Proper Motions						
μ_α and μ_δ round sphere	27762	35523	$269°.4 + 0°.4$	841	992	$+28°.7 \pm 1°.3$
μ_α at colures	3738	4584	$269°.5 \pm 0°.6$	...	...	...
Totals and means	31500	40107	$269°.4 \pm 0°.3$	841	992	$+28°.7 \pm 1°.3$
Combined Total and Means	38636	87607	$270°.2 \pm 0°.3$	2084	10068	$+28°.7 \pm 0°.5$

compared with $20{\cdot}2 \pm 0{\cdot}8$ km./sec. found by resolution of the 981 stars along the *X*, *Y*, *Z* axes; whence the combined weighted mean velocity derived from the 1137 stars concerned becomes $20{\cdot}5 \pm 0{\cdot}6$ km./sec. At this speed ($12\frac{3}{4}$ miles a second), the solar system traverses 4·32 astronomical units in a year.

Apical positions derived from subdivided magnitudes were found to agree substantially with the given final for solar motion relative to the bright stars.

It is a pleasure to acknowledge and to thank Professor H. H. Plaskett and Professor W. M. Smart for their helpful suggestions.

Sennen, Cornwall:
1946 *November* 16.

OBSERVATIONS OF NOVAE, 1945–1946

W. H. Steavenson

(Received 1946 May 3)

The observations which follow were, unless otherwise stated, made with the 30-inch Hindle reflector at Cambridge. They are in continuation of the series made at West Norwood with the 20-inch reflector and other telescopes up to the year 1939 and already published in the *Monthly Notices*.

Nova Aquilae (1918)

Observed on 1945 September 22, when the magnitude was estimated at 11·1. The colour was white and the image sensibly stellar.

Nova Aquilae (1925)

This nova was looked for on 1945 October 1 and 9 but not seen. The magnitude must then have been below 16.

Nova Aquilae (1945)

Magnitudes of the comparison stars down to 9·8 were taken from the Draper Catalogue. Those of the fainter stars are based on my own estimates which, I believe, conform closely to the McCormick photovisual system. A few seconds of arc north-following the nova there is a star whose magnitude I estimate at 15·8. This is probably the object which is faintly shown on the Franklin-Adams and Wolf-Palisa charts, Nos. 111 and 77 respectively. It seems improbable that the nova itself would be recorded on any photograph with a limiting magnitude above 18. In the list below the estimates down to and including September 18 were made with the 2-inch finder.

Date	Mag.	Date	Mag.	Date	Mag.
1945 Aug. 31	7·9	1945 Sep. 24	9·6	1945 Oct. 22	10·7
Sep. 2	8·1	29	9·7	25	10·8
5	8·2	Oct. 1	9·9	30	10·8
12	8·9	3	9·8	Nov. 3	10·8
13	9·1	5	9·9	27	10·9
16	9·5	9	10·0	Dec. 2	11·0
17	9·1	10	10·1	3	11·2
18	9·4	13	10·3	5	11·0
20	9·5	15	10·5	9	11·0
22	9·6	19	10·7	19	11·2

Nova Aurigae (1891)

Observed on 1945 November 27, when the magnitude was estimated to be 14·9. There has been little change in the brightness of this nova for many years.

T Coronae (1866)

Down to and including March 9 the estimates were made with the 3-inch Merz refractor.

Date	Mag.	Date	Mag.
1946 Feb. 10	3·7±	1946 Mar. 16	9·9
17	<6	22	9·9
19	7·7	28	9·8
20	8·1	Apr. 1	9·8
21	8·4	6	9·8
Mar. 9	9·6	9	9·8

The magnitude to which the nova had fallen by the middle of March is close to the average value observed over a number of years before the recent outburst. On the other hand, the former strongly yellowish tint of the nova had not returned at the date of the last observation, when the star was sensibly white in colour.

Nova Cygni (1876)

This nova has exhibited a small range of variability for a number of years. The magnitude was estimated at 14·86 on 1945 September 22 and 14·71 on October 9. The image is white and stellar.

Nova Cygni (1920)

Observed on 1945 September 22, when the magnitude was estimated to be 15·6. This represents a drop of only $0^{m}\cdot1$ since 1938 June and it seems probable that the nova has now reached a stationary condition.

Nova Cygni (1942)

On 1945 October 1 the magnitude was estimated at 14·6.

Nova Geminorum (1912)

Observed on 1946 January 27, magnitude 14·7. There has been no significant change in the brightness of this nova for many years.

Nova Herculis (1934)

Observed on 1946 April 30, magnitude 13·2. The image was not truly stellar, the appearance being that of a minute planetary nebula with a diameter between 2 and 3 seconds of arc. A greenish tint was suspected. Through a direct-vision prism a single bright image was visible, flanked by some very faint separate radiations, with suspicions of a continuous spectrum.

Nova Lacertae (1910)

Observed on 1945 September 22, when the magnitude was 14·4, as it has been for a great many years.

Nova Lacertae (1936)

This object is still fading slowly.

Date	Mag.
1945 Sep. 22	14·7
Oct. 5	14·7
10	14·8
15	14·8

Nova Persei (1901)

This nova continues its irregular fluctuations, as recorded both before and since its outburst. The small wisp of nebulosity on its south-preceding side has been steadily fading since its first detection in 1916 September, and is now so faint as to be invisible except on the most transparent nights.

Date	Mag.	Date	Mag.	Date	Mag.
1945 Aug. 10	12·97	1945 Nov. 26	13·47	1946 Jan. 19	13·05
Sep. 13	12·99	27	13·16	27	13·00
22	13·20	30	13·10	Feb. 1	12·69
Oct. 9	12·43	Dec. 2	12·95	4	12·84
10	12·48	3	12·90	5	12·90
15	12·69	5	12·84	9	12·79
16	12·32	9	13·20	20	12·53
19	12·48	10	13·20	Mar. 20	12·90
22	13·05	11	13·00	29	12·90
25	12·95	19	13·20	30	12·74
30	12·84	30	13·20	Apr. 1	12·79
Nov. 3	13·05	1946 Jan. 3	13·10	2	12·84
10	13·42	13	13·25	18	13·15
15	12·90	15	13·10		
17	13·26	17	13·00		

Cambridge :
1946 *May* 2.

ON THE DEEP MINIMUM IN THE LIGHT CURVE OF SLOW NOVAE

D. ter Haar

(Communicated by F. J. M. Stratton)

(Received 1946 July 15)

Summary

The deep minimum of some slow novae can probably be explained by the fact that the region between the outermost and the next shell becomes at a certain moment a *H* I region so that molecular formation is possible. A molecular cloud will then be formed and will produce the observed obscuration.

The hypothesis that the final state of a slow nova is a planetary nebula seems to be strengthened if this process is indeed taking place.

In some cases of slow novae (e.g. Nova Aurigae 1891, Nova Herculis 1934, Nova Cygni 1942) there has been observed a deep minimum in the light curve starting after the magnitude had dropped about $3^{m}\cdot5$ from maximum brightness. In some cases of fast novae (e.g. Nova Persei 1901) there has been observed an oscillating brightness. It has been suggested by Chandrasekhar and Stratton * that these obscurations might have been produced by the formation of a cloud of molecules between the nova and the innermost shells on the one hand and the outermost shell on the other hand, thus accounting for the fact that the spectrum of the outermost shell remains visible.

We will show in the following that this solution is indeed rather probable and that it seems possible to explain qualitatively the phenomena of both the deep minimum and the oscillating brightness. We suggest here that this molecular cloud will be formed at the moment when the distance from the nova to the space directly behind the outermost shell corresponds to the radius of the *H* II region (that in which the hydrogen atoms are predominantly ionized) as introduced by Strömgren.† If that should be the case the much smaller radiation density and the presence of neutral hydrogen will make the formation of molecules possible. It may be remarked here, that, up till now, interstellar molecular lines have only been observed in *H* I regions (those in which the hydrogen atoms are predominantly neutral).‡

It has often been suggested that planetary nebulae should be the final state of slow novae.§ It is therefore perhaps not irrelevant to remark that the dimensions of these nebulae (between 0·1 and 5 light years‖) are of the same order of magnitude

* *M.N.*, **105**, 275, 1946.

† *Ap. J.*, **89**, 526, 1939.

‡ See e.g. H. C. v. d. Hulst, *Ned. Tijdschr. Natuurk.*, **10**, 244, 1943 ; *Cf.* also H. A. Kramers, D. ter Haar, *B.A.N.*, **10**, 137, 1946 (No. 371).

§ See e.g. C. Payne-Gaposchkin, S. Gaposchkin, *Variable stars*, Harvard Observatory Monographs No. 5, p. 253, 1938.

‖ See e.g. *Handb. Astroph.*, **V**, **Part 2**, 806 *et seq.*, Berlin, 1933.

as the Strömgren radius which for densities of 10^3 to 10^4 cm.$^{-3}$ and a temperature of the central star of 100,000° is equal to 1 to 2 light-years.

In order to arrive at an estimate of the approximate molecular densities in the region concerned we have to make first an estimate of the atomic and radiation density in that region. The data at hand are, however, few and not very accurate but we still think that it is possible to arrive at a fairly trustworthy estimate of the above quantities.

For the atomic density we can use in the first place the data of Tai.* From the properties of the observed spectra he arrives at values for the electron pressure in the different shells between 10^{-5} and 10^{-3} atm., which, assuming with him a temperature of about 10,000°, corresponds to atomic densities between 10^{13} and 10^{15} cm.$^{-3}$. These densities have to be regarded as upper limits since regions where these densities are attained will be followed by regions where the density is lower.

We get an estimate of the overall density by dividing the total mass ejected by the nova by the total volume of the shells at the time of the deep minimum. From the velocities of the shells we get for the distance of the outermost shell to the nova a value of about 4×10^{14} cm. If we also accept the value of 10^{-5} solar masses for the total mass ejected as has been estimated by Ambarzumian and Kosirev †, we get an overall density of about 3×10^8 cm.$^{-3}$.

If we accept this overall density of 3×10^8 cm.$^{-3}$, a temperature of the nova of 100,000° and a radius of the nova of about one third of the solar radius, we get for the Strömgren radius s_0 a value of 2 to 3×10^{14} cm. which is in good agreement with our basic assumption since the radius of the outermost shell is of the order of 4×10^{14} cm.

Finally, accepting the hypothesis that the final state of a slow nova will be a planetary nebula and assuming, moreover, that the planetary nebula will be formed simply by the increase of the dimensions of the shells we can estimate the density in the shells of the nova from the dimensions and densities of planetary nebulae. In that way we find for the density values between 10^{10} and 10^{16} cm.$^{-3}$.

Altogether, we find a rather good agreement between the different estimates of the atomic density. When we bear in mind the fact that in the region concerned different shells are mixing ‡ and that moreover the formation of molecules will take place in regions just where the density is rather high, since the formation is very sensitive to a change in density, it seems safe to assume for the region under consideration an atomic density between 10^{12} and 10^{14} cm.$^{-3}$.

To get an upper limit for the dilution factor of the radiation we can take the square of the ratio of the radius of the nova to the radius of the outermost shell which gives, using the same numerical values as above, $g \sim 3 \times 10^{-9}$. Since we are in a H I region it is probable that g is still smaller, especially in the ultraviolet. We shall assume $g = 10^{-10}$ for $h\nu = 10$ eV.

To estimate now the density of the molecules we shall assume a density of hydrogen of 10^{12} cm.$^{-3}$, a density of the other elements corresponding to their density ratio in interstellar space, a dilution factor of 10^{-10} and a temperature of the nova of 100,000°. We can use now the same equations as have been used by

* *M.N.*, **100**, 435, 1940.
† *Z. Astrophys.*, **7**, 320, 1933.
‡ *Cf.* Tai, *loc. cit.*

Kramers and the present writer.* We will not enter here into the details of the calculations which can be found in their paper. If we use the same numerical values for the probability of radiation capture (Q_{rad}) and the transition probability (A), we get for the density of CH and CH^+ respectively 10^7 and 10^6 cm.$^{-3}$ and for the densities of CH_2 and CH_3 10^4 and 10^2 cm.$^{-3}$ respectively. For γ_2 and γ_3 we we have used $10\gamma_1$ and $100\gamma_1$.†

The time necessary to reach the above molecular densities is of the order of one hour or less.

We must remark here that the above values of molecular densities are certainly lower limits since apart from the fact that the assumed atomic density may well be much too small, three body collisions can also play a part in the formation of molecules at these densities so that the probability of the formation of a molecule may well be much larger than assumed in the above estimate. It may even amount to a factor 10 or 100.

Since apart from CH, CH^+, CH_2, CH_3 there will also be present CN, CO^+, HCN, etc. and since collisions are so frequent that a large part of the molecules may be in excited states it seems quite possible that the observed obscuration will be produced by the molecular cloud.

The fact that as the shells are expanding the density decreases may well account for the subsequent rebrightening, since the whole formation of molecules is extremely sensitive to a variation of the atomic density. Moreover, this same fact may also account for the oscillating brightness of fast novae, since the degree of ionization may not be constant either.

It should be very interesting to search for molecular lines in the spectra of the novae especially at the beginning or the end of the obscuration since it could be imagined that there would be a stage when the molecular density was high enough to produce some lines but not yet high enough to produce the complete obscuration. It is perhaps not irrelevant to remark that there is evidence that the observed molecular lines are possibly circumstellar rather than interstellar.‡

I want to express my sincere thanks to Professor F. J. M. Stratton and to Professor B. Strömgren for discussions on the subject of this paper and to the Rask-Ørsted-foundation for a grant which has enabled me to stay in Copenhagen.

Institute for Theoretical Physics,
University of Copenhagen,
Denmark:
1946 *June* 27.

* *B.A.N.*, **10**, 137, 1946 (No. 371).
† Cf. *loc. cit.*
‡ *Observatory*, **66**, 248, 1946.

ON THE USE OF ROTATING SECTORS IN ASTRONOMICAL PHOTOMETRY

A. W. J. Cousins and R. H. Stoy

(Communicated by H.M. Astronomer)

(Received 1946 June 24)

Summary

Tests made at the Cape Observatory indicate that with Ilford Special Rapid plates (H & D 270) and sectors giving 100 and more interruptions per second, the sector constant does not differ sensibly from that calculated from geometrical measurements on the assumption that the rotating sector cuts down the intensity of the incident light without affecting the exposure time.

Introduction.—The rotating sector has long been accepted in photo-electric photometry as a convenient method of reducing the intensity of a light source by a calculable amount without altering the spectral composition. Its use for the same purpose in photographic photometry has rarely been regarded as completely satisfactory because of the well-known reciprocity failure of most photographic emulsions and the uncertainty as to whether the rotating sector is to be regarded as cutting down the intensity of the incident light or as cutting down the exposure time. Webb *, who went into the subject with great care, came to the conclusion that at sufficiently high speeds, intermittent exposures are wholly equivalent to continuous ones. On the other hand, Sawyer and Vincent † maintain that Webb's conclusions are true for certain emulsions only. Any astronomer who wishes to use the rotating sector is therefore well advised to test the behaviour of his plates in the laboratory under conditions as similar as possible to those that will obtain at the telescope. This is the more desirable as the intensity of light encountered in astronomical photometry is quite different from that used in normal laboratory tests.

At the Cape we are interested in the photometric behaviour of rotating sectors in connection with an observing programme which has recently been started and which aims at providing accurate photographic magnitudes for all stars in the Southern Hemisphere whose HR visual magnitude is brighter than 5·0. These stars are being observed with a Fabry-photometer attached to the Astrographic Telescope. A series of sectors have been constructed and can be mounted in front of the Fabry lens. By proper selection of a sector the effective magnitude of a bright star can be cut down to about 5·8. The star images on any one plate are therefore of comparable density and the deduced relative magnitudes depend mostly on the assumed reduction constants of the rotating sectors. The small differences of magnitude, amounting at most to a few tenths, are measured with

* *J. opt. Soc. Amer.*, **23**, 157 and 316, 1933.
† *J. opt. Soc. Amer.*, **33**, 247, 1943.

the aid of calibration spots impressed on the plate with a tube sensitometer. During a short visit to the Cape last year, Cousins carried out laboratory tests of the observing equipment. The results of these tests, which were somewhat cramped by shortage of time, are given below.

Procedure.—To reproduce the conditions in the telescope the Fabry unit, consisting of the plate carrier, Fabry lens, diaphragm and filter, was mounted at one end of a tube in which was fixed an opal glass screen diaphragmed to approximately the aperture-ratio (F/11) of the Astrographic Telescope. The rotating sector with its electric driving-motor was mounted immediately in front of the Fabry unit. Three sectors were available. They are about 9 cms. in diameter and are made from No. 20 S.W.G. aluminium sheet. They were designed to reduce the light by 1, 2 and 3 magnitudes respectively. The 3-magnitude sector has two openings, the others four, which, with the motor used, gave 100 and 200 interruptions per second, respectively.

The light source consisted of a 6-volt coiled filament lamp operated from a storage battery and enclosed in a blackened metal enclosure with a diaphragm, of sufficient size to avoid vignetting, immediately in front of the lamp. The lamp assembly could be moved along the axis normal to the opal screen between 18 inches and 10 feet from the screen, permitting a change of intensity of 4 magnitudes. It was maintained approximately parallel to itself to reduce the effects of any variation of intensity with solid angle.

The square tube which supported the Fabry unit and opal screen extended some six feet beyond the latter so that the light source was usually within the tube. This was blackened internally with diaphragms at intervals to cut down scattered light. Battens were attached so that the light-source could be readily placed in a series of positions giving one-magnitude differences of illumination of the screen. This ensured that all images given the same exposure, whether obtained with a sector or not, would either match or differ by an integral number of magnitudes from one another.

All exposures were made through the same blue glass filters and with the same kind of plate (Ilford Special Rapid H & D 270—Backed) as is used for the ordinary stellar programme. The plates were developed in fresh I.D.2 developer and were neither brushed nor rocked during development. They were calibrated in a tube sensitometer, two of the calibration exposures being given before the Fabry exposures and two afterwards. The Fabry images are arranged in a rectangular array in the centre of the 8×8 cm. plate with the calibration images forming a ring round them. The Fabry images were obtained both with and without sectors, the exposure time and light intensity being changed from image to image and the sector from row to row, with the first and last rows and at least every third row without a sector in use.

The images were measured in the modified Schilt photometer. Characteristic curves were derived by plotting the galvanometer readings for the tube sensitometer spots against a scale of magnitudes calculated from the geometrical measurement of the sensitometer openings. The results from the four calibration exposures were combined to give a mean curve for each plate. All measures of Fabry images were reduced to the tabular magnitudes defined by this mean curve.

For evaluating the sector constants only matched images were selected for comparison, i. e. the reduction of the photographic effect by a sector was compared

TABLE I

Differences between Matched Images

(Reduction by Sector)—(Reduction by Distance)

Units $0^m.01$

Plate	Lamp Position \ Exposure (secs.)	1^m Sector 15	1^m Sector 30	1^m Sector 60	2^m Sector 15	2^m Sector 30	2^m Sector 60	3^m Sector 15	3^m Sector 30	3^m Sector 60
3	0	+3	−3							
	1	−1	0	−3						
	2		0	−3						
	3			−2 :						
4	0	+2	+1		+2 −2	+5	+5		+2 +5	+2 +2
	1	+2	+2	+1			+2 +6			−6 :
	2		+6	−3 :			−3 :			
	3			+1 :						
6	0	−1	0 :					+4 :		
	1	−8 :	0	+1	+4 +2			−1	−1	+1 :
	2		−2 :	0	+1 −1	−1	0			
	3			+3 :						
7	0				+2	+2				
	1	+1	−1		+2	+5	+3			
	2	0 +1	+2	+2		+3	+2			
	3		+3 :	+1						
	0				+2			+1 : +1 :	−1 :	+2
	1				+4 : +5 :	+1 :	+5		+2 :	+1
	2					+9 :	+5			
Means		+0·4	+0·7	−0·2	+1·7	+3·2	+3·1	+0·8	+1·6	+0·9
Sector Constants		$1^m.003$			$2^m.025$			3 ·011		

with the effect of increased distance of the light source. The actual differences between these images are only a few hundredths of a tabular magnitude so that even serious errors in the calibration will have little effect on the derived values of the sector constants. It will be shown later that there are, in fact, no such serious errors in the calibration.

A slight drift in the intensity of the light source occurred during the tests. To allow for this drift and also for possible photographic effects, exposures with the sectors were sandwiched between exposures without them.

Results.—Table I gives the individual differences from sets of matched images in the sense (reduction by sector)—(reduction by distance). Values marked with a colon are of low weight owing to under- or over-exposure or other causes. The column headed "Lamp Position" refers to the position of the light source when the sector was in use. To find its position for the corresponding comparison images obtained without the sector, the nominal sector constant must be added to the number shown. Grouping the residuals from the final means according to the duration of the exposure gives the following results (in magnitudes):

Exposure :	15 secs.	30 secs.	60 secs.
Average difference :	0·000	+0·003	−0·002
Average deviation :	0·016	0·020	0·019

There is no evidence in these figures of any effect depending on the length of the exposure and the error in timing is apparently small.

TABLE II

Sector Constants from Individual Plates

Plate	1^m Sector	2^m Sector	3^m Sector
3	0·989	...	...
4	1·019	2·025	3·018
6	0·994	2·008	3·003
7	1·010	2·034	3·011
Mean	1·003	2·022	3·011
Weighted Mean (Table I)	1·003	2·025	3·011
Computed (Geometrically)	1·002	2·018	2·989

Table II gives the sector constants obtained from individual plates and the unweighted mean of these. There is no significant difference from the weighted means in Table I. The last line of Table II gives the values of the sector constants calculated from geometrical measurements of the sector openings on the assumption that the sector cuts down the intensity of the incident light without affecting the exposure time. It will be noticed that there is a good agreement between the geometrically and photometrically determined sector constants, which is well within the probable error of the determinations except possibly for the 3-magnitude sector. It is difficult to know what the probable error to be attached to the geometrical determinations should be. From the interagreement of results obtained from several independent measurements with the long screw measuring machine, the probable error might appear to be as small as $0^m{\cdot}002$, but the question is complicated by the fact that the sector constant varies from centre to edge by over $0^m{\cdot}01$. The values given in Table II correspond as nearly as possible to that portion of the sectors which was used during the tests and in normal observing, i.e. at 32 mm. from the centre.

The differences in tabular magnitude between the images taken with the lamp in the same position and with the same sector but with different exposures suggest that had the effect of the sectors been equivalent to a reduction of exposure time, the sector constants found would have been about 0·9, 1·8 and 2·7 magnitudes.

The scale of the sensitometer.—The sector constants could, in theory, have been obtained from a direct comparison between the Fabry images and the calibration curves, i.e. in terms of tabular magnitudes. Certain defects in the tube sensitometer (since remedied) rendered this method somewhat unreliable. Moreover differences of three magnitudes cannot be dealt with effectively with a tube sensitometer on account of the range of densities involved. The determinations would therefore have to be made differentially by comparison of the sectors.

Working in the reverse direction, it is possible to test the scale of the tube sensitometer in terms of the inverse-square scale as standard. The results are given in Table III, where they are grouped plate by plate according to the exposure given to the Fabry images. Plate 4 could not be used for this purpose as the calibration images are too weak.

TABLE III

Sensitometer Magnitude Difference corresponding to 1 *Inverse-Square Magnitude*

Unit $0^m{\cdot}01$

	Plate 3			Plate 6			Plate 7		
Exposure (secs.)	15	30	60	15	30	60	15	30	60
No Sector	97	98	103	100	99	101	97	98	100
With Sector	93:	99	103:	95	100	99	97	99	99
Mean	96	98	103	98	99	100	97	98	100

There appears to be no significant difference between the values obtained with and without a sector. The calibration should therefore be equally valid for both groups of images. Grouping the values given in Table III according to the duration of the exposure gives:

15 secs. $0^m{\cdot}97$ 30 secs. $0^m{\cdot}98$ 60 secs. $1^m{\cdot}00$

The slight run in these values suggests an effect of exposure time on the magnitude scale of the Fabry images, the contrast being least for the shortest exposures. The calibration curves apply strictly to exposures of 50, 30 and 30 seconds for plates 3, 6 and 7 respectively. After allowing for this there appears to be no difference between the scale of the sensitometer and that derived from the inverse-square law in the case of plate 3, but there are still differences amounting to $0^m{\cdot}01$ or $0^m{\cdot}02$ in plates 6 and 7. This may be due to reflections off the smooth, though blackened, walls of the sensitometer tubes as the diaphragm usually placed about midway along them was omitted during these later tests. The sensitometer has since been completely rebuilt and Redman's * plan of drilling the tubes through a solid block of wood and then threading the tubes throughout their entire length has been followed.

In the foregoing it has been assumed that the scale based on the inverse-square law is accurate. The possibility of systematic errors due to various causes has

* *M.N.*, **105**, 217, 1945.

been examined. Of these, only one seems likely to have reached $0^m.01$, viz. the effect of uneven refraction or absorption in the glass of the lamp. The glass appeared uniform on inspection, but no quantitative measures were made so that it can not definitely be said that no unevenness was present. With the precautions taken, we believe that the total systematic error in the inverse-square scale does not exceed $0^m.01$ per magnitude. As a partial check on this, the magnitude differences between the different lamp positions were deduced on the assumption that the sector constants in the last line of Table II are correct. The differences from the assumed values that were thus found did not exceed $\pm 0^m.01$. By modifying the equipment and taking additional precautions, it should be possible to ensure that no error of this magnitude is present. Further work in this direction, however, could be done more effectively by using a rotating sector in combination with a tube sensitometer rather than with a Fabry photometer.

Note added 1946 *May* 27.—Dr Redman, who was kind enough to read through a rough draft of this paper, permits us to quote the results of some tests he made recently on Ilford HP3 plates, using sectors giving more than 10,000 flashes per minute and an exposure time of one minute. The sector steps were measured geometrically and against the inverse-square law with the following results, expressed in magnitudes:

Geometry	0·49	0·985	1·505	2·005	2·465	3·00	3·60
Inverse square	0·495	0·985	1·50	1·98	2·46	2·985	3·615

The two sets of measures are in as close agreement as the probable errors of the measures will allow. Redman points out that, while simple in theory, accurate measures by the inverse-square law demand extraordinarily great care in practice, owing to the difficulty (*a*) of getting a source with a perfectly uniform distribution of light in solid angle, (*b*) of completely eliminating all false light, particularly reflections from bench, walls, sector motor casing, etc.

Royal Observatory,
Cape of Good Hope:
1946 *May* 16.

Durban,
Natal.

PHOTO ELECTRIC OBSERVATIONS OF V PUPPIS

A. R. Hogg

(Communicated by the Commonwealth Astronomer)

(Received 1946 September 23)

Summary

A photo-electric light curve has been obtained for the eclipsing binary V Puppis, using χ Carinae as a comparison star. The photometric results have been combined with Harvard-Arequipa spectroscopic data to derive dimensions, masses, densities etc. for the V Puppis system. The results (see Tables V and VI) are generally intermediate between those obtained earlier by Shapley and by van Gent who used visual and photovisual light curves respectively. The present observations however give rather less ellipticity to the stars than do the earlier ones. There is an apparent decrease in the period amounting to $0^{s}\cdot1$ over 40 years, but this decrease is not regular nor is it so great as to be quite unaccountable for by experimental error. The existence of any appreciable apsidal rotation is considered to be improbable. The orbit is indeterminate from photometric data alone and further spectroscopic work would be of value.

---

1. *Introductory.*—The variation of light from the eclipsing binary V Puppis ($\alpha = 07^{h}\,55^{m}\cdot3$, $\delta = -48^{\circ}\,58$. (1900), B1 + B3, $4^{m}\cdot14$) was reported by A. S. Williams.* A visual light curve was determined by A. W. Roberts † at Lovedale and was found by him to be in agreement with a curve calculated for two spherical stars of equal diameter having uniformly illuminated disks and revolving, in contact with each other, in a circular orbit with a period of $1^{d}\cdot454476$. H. Shapley ‡ showed that the observations of Roberts were explicable by assuming a partially eclipsing system of two elliptical stars of nearly equal size revolving in a circular orbit and having surfaces separated by one-eighth of an orbital radius. To determine the nature of the eclipse Shapley made use of the Harvard-Arequipa spectroscopic data, which was later discussed by Miss A. C. Maury.§ More recently a light curve, derived from photovisual observations at Johannesburg, has been discussed by H. van Gent.‖ This showed that the dimensions of the stars are slightly smaller than the figures given by Shapley; also it was suggested that there existed in the system an apsidal rotation of about 10° per annum. It appeared that a photo-electric light curve would give interesting results and perhaps clarify the position regarding the apsidal rotation.

2. *Instrumental.*—Light intensities were measured by a gas-filled sodium photo-electric cell (Osram Type UNG7) attached to the Reynolds 30-inch reflector at the Commonwealth Observatory. The cell, according to the manufacturers'

* *M.N.*, **47**, 101, 1886.
† *Ap. J.*, **13**, 181, 1903.
‡ *Contr. Princeton Univ. Obs.*, No. 3, 82, 1915.
§ *Ann. Harv. Coll. Obs.*, **84**, 157, 1920.
‖ *B.A.N.*, **8**, 319, 1939 (No. 317).

data, is most sensitive in the blue and ultra-violet portion of the spectrum. An earthed guard-ring prevented the anode potential (usually 120 volts.) from leaking to the Lindemann electrometer system which was used in a null circuit to measure the photo-current (see Fig. 1). The observation consisted in determining, with a stop-watch, the time taken for the photo-current to neutralize a constant induced charge on the electrometer system. The anode potential was adjusted so that this time usually lay between 20^s and 60^s. The dark current was measured periodically and found to be about 10^{-15} amp. As the photo-current was of the order of 10^{-13} amp., the dark current had a practically negligible effect on the measured magnitude difference between the comparison and variable stars. The electrical system

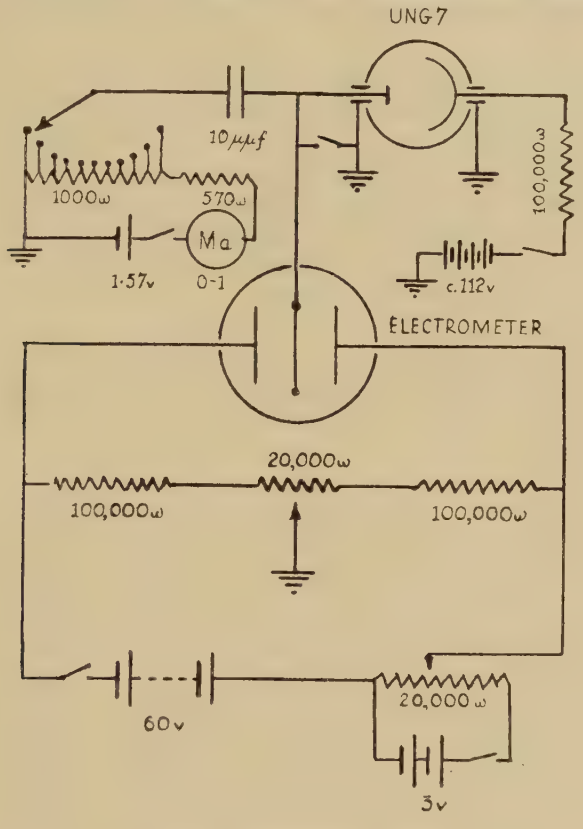

FIG. 1.—*Photometric circuit.*

proved extremely stable and it was possible to commence measurements immediately after switching on the plate potentials, without being troubled by drift. A slight drift of zero occurred owing to the change of position of the electrometer with the motion of the telescope but as this was regular it could readily be allowed for. With the telescope stationary the drift was quite negligible. The cell, mounted in a protecting brass case with a quartz window, was placed about 10 cm. behind the Cassegrain focus of the Reynolds reflector. A diaphragm strip with holes of various apertures could be moved in the focal plane of the telescope and served to define the effective field falling on the cell cathode. With the aid of a movable prism the apertures could be viewed in a finding eyepiece; when the star was properly located the prism was withdrawn and starlight was thereby

admitted to the cell cathode. The cell cathode was placed outside the focal plane in order to give an image of a size sufficient to minimise difficulties due to local variations of the sensitivity of the cathode. Similar arrangements were used by W. M. Smart * for measurements of Algol and other variables.

3. *Observations.*—Between 1946 April 3 and 1946 July 25 some 114 observations were made on 21 nights of the magnitude difference between V Puppis and the comparison star χ Carinae ($\alpha = 7^h\,54^m{\cdot}2$, $\delta = -52^\circ\,43'$ (1900·0), $3^m{\cdot}6$, B3). The previous observers had employed the star Lacaille 3069 ($\alpha = 7^h\,50^m{\cdot}2$, $\delta = -49^\circ\,21'$, B3, $4^m{\cdot}8$) as a standard. Each observation consisted usually of five readings of the light intensity of the variable star, interposed between two sets of five readings for the comparison star. To allow for extinction corrections the electrometer times for the comparison star were plotted, on semi-logarithmic paper, against the corresponding values of $\sec z'$. (z' = zenith distance of star at time of observation.) For good nights it was possible to represent the points by a straight line, the extinction curve. Owing to more or less obvious meteorological irregularities this relation did not hold for every night. The slope of this curve gave the extinction factor which varied from about $0^m{\cdot}25$ to $0^m{\cdot}4$ per unit of $\sec z'$. Only the observations taken on those nights when it was possible to obtain a satisfactory extinction curve were used to define the light curve. The extinction curve was used directly to obtain the corrected comparison times appropriate to the zenith distance of the variable.

Normals for the observations are set out in Table I which includes the phase (heliocentric) for an adopted period of $1^d{\cdot}4544$, Δm the magnitude difference (V Puppis–χ Carinae), and the number of observations used to define the normal.

TABLE I

Normal Magnitudes Δm = (V Puppis–χ Carinae)

Phase	Δm	Obs.	Phase	Δm	Obs.
d	m		d	m	
0·016	1·290	2	0·840	0·932	3
0·036	1·220	4	0·886	0·843	3
0·080	1·025	2	0·917	0·780	3
0·121	0·908	4	0·960	0·735	2
0·173	0·828	3	1·000	0·732	5
0·204	0·765	1	1·032	0·735	4
0·243	0·740	3	1·077	0·735	4
0·285	0·742	3	1·113	0·728	5
0·314	0·738	6	1·163	0·728	2
0·353	0·738	2	1·192	0·760	2
0·406	0·731	1	1·245	0·748	4
0·478	0·748	2	1·276	0·805	4
0·516	0·765	2	1·307	0·815	1
0·566	0·805	2	1·332	0·908	5
0·650	0·978	1	1·373	0·995	6
0·692	1·108	3	1·403	1·151	3
0·709	1·153	3	1·425	1·261	4
0·739	1·182	2	1·445	1·311	2
0·769	1·134	3	1·452	1·325	1
0·806	1·068	2			

Epoch of primary minimum = J.D. (heliocentric) 2431,965·952.

* *Observatory*, **56**, 75, 1933.

Normals were obtained by averaging the observations in phase intervals, in most cases of $0^d.04$, but near the minima smaller intervals were used to preserve the character of the curve. Some idea of the consistency of the observations could be obtained by noting the scatter of the observations outside of the eclipses. Thus the average deviation for 32 such observations rectified for the ellipticity of the stars in a manner described below, amounted to $0^m.012$. This figure refers to the average deviation of a non-eclipse observation (not a normal) from the mean of all non-eclipse observations. It was considered that a good deal of this variation was due to variations in extinction. The observed amplitudes of the light variation were as follows:—primary minimum $0^m.56$, secondary minimum $0^m.45$. The corresponding figures obtained by Roberts were $0^m.64$ and $0^m.53$, whilst van Gent gives $0^m.60$ and $0^m.47$.

4. *Period.*—For constructing the light curve a period of $1^d.4544$ was adopted, this being based on the observation of two primary minima at Julian dates (heliocentric) of 2431000 + 965·952 and + 917·957. This sufficed to calculate phases for the present observations; a more accurate value was obtained by comparison with the epochs of primary minima published by earlier workers. Thus, Table II shows that by assuming appropriate numbers of intervening cycles, the

TABLE II

Estimated Periods of V Puppis

Observations	Epoch J.D.	Period		Cycles	$\Delta P/\Delta E$
a. Harvard-Arequipa	2412,778·394	b–a	$1^d.454491$	1542	7×10^{-6}
b. Lovedale	2415,021·219	c–b	87	9369	1×10^{-6}
c. Johannesburg	2428,648·305	d–c	75	2248	5×10^{-6}
d. Canberra	2431,917·957	d–a	82	13,159	$0{\cdot}8\times10^{-6}$

results of four widely spaced sets of observations may be accounted for by a period close to $1^d.45448$. The actual figures show an irregular decrease of period with increasing epoch, but this decrease might be due, at least in part, to observational error. Thus the last column of the table shows $\Delta P/\Delta E$, the variation in period due to an uncertainty of $0^d.01$ (14·4 min.) in one of the adopted epochs. The variations in periods b–a and c–b could be accounted for by relatively minor errors in epochs a, b or c. but the difference in the period c–d from either b–a or c–b is unlikely to be due to this cause, for the present observations show a primary minimum about 30 minutes earlier than that predicted from Johannesburg observations. This discrepancy might be explained in terms of the "Tikhoff-Nordmann" effect.* These observers have shown, for about 20 stars, that the epoch of primary minimum varies with the wave-length of the measurements, being generally, but not invariably, earlier for yellow light than for blue. If this effect is operative in the present instance then the determination of the period by combining the earlier (yellow) observations with the photo-electric (blue) is open to question. It is noted however that the c–d period ($1^d.454475$) agrees almost exactly with that given by Roberts ($1^d.454476$).

5. *Light Curve.*—The results, grouped into the normals shown in Table I, were treated according to the methods given by Russell and Shapley.† A freehand curve drawn through the normals showed that the present observations agreed

* Payne-Gapsochkin and Gaposchkin, *Variable Stars*, p. 64, 1938.

† *Ap. J.*, **36**, 385, 1912.

qualitatively with those of earlier workers in indicating that the light variation is of the type arising from partial eclipses of ellipsoidal stars in a slightly eccentric orbit. The constant z, which defines the ellipticity of the equatorial section of the stars, was determined by averaging the ratio $(1-l^2)/\cos^2\theta$ for normals outside the eclipse limits. As l = light from systems for a given longitude θ, $1-l$ represents a light loss from maximum light. Maximum light in this instance was taken as $\Delta m = 0^{m}\cdot730$. Two normals were rejected (their residuals being more than 10 times the standard deviation) and the figure of $z = 0\cdot163 \pm 0\cdot014$ (s. d.) was obtained from 15 normals. This value was used to rectify the observations for the ellipticity of the stars, thus allowing for the increased light due to the increase of projected area which occurs as the stars approach their position of maximum light. The rectified normals are shown plotted in Fig. 2. The curve in this figure is computed from the "darkened" solution obtained below.

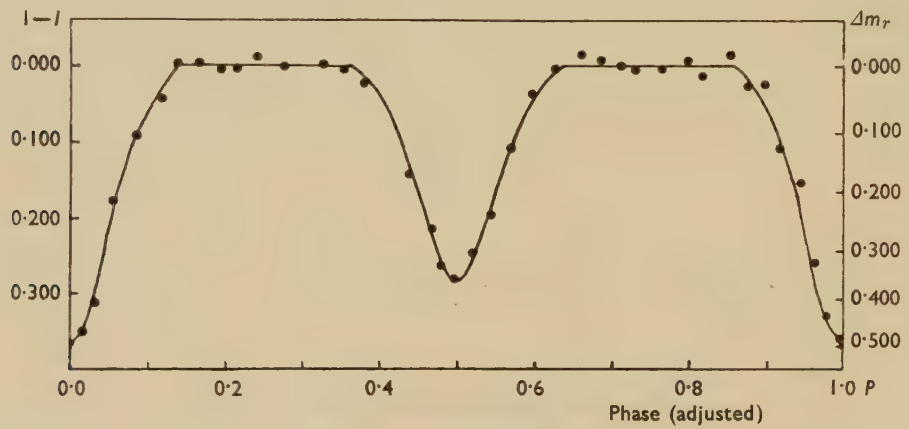

FIG. 2.—*Rectified light curve.*

A comparison of the depths of the minima in the rectified light intensity curve gives a measure of the relative surface brightness of the two stars, viz. $\mathcal{J}_1/\mathcal{J}_2 = 0\cdot367/0\cdot283 = 1\cdot29$.* A knowledge of the effective wave-length in which the measurements were made, combined with the Planck radiation formula would yield figures for the temperatures T_b and T_f of the components. This wave-length is not known with certainty but if, as is probable, it lies between 3500 and 4500A it can be shown that $1\cdot10 < T_b/T_f < 1\cdot16$. The effective temperatures given by Kuiper † for B1 and B3 stars are 23,000 and 18,000° C., their ratio being 1·28. Corresponding temperatures interpolated from a table given by Russell, Dugan and Stewart ‡ are 21,409° and 18,200°, of ratio 1·17. For comparison, values of the relative surface brightness at different values of T_b and T_f are set out in Table III which shows, assuming reasonable values for λ, that all the observational values of $\mathcal{J}_1/\mathcal{J}_2$ correspond to smaller values of T_b/T_f than would be expected from Kuiper's estimates.

6. *Orbital Elements.*—In a solution assuming a uniform distribution of brightness over the disk, the permissible values of the ratio k of the semi-major axes of the

* *Cf.* Roberts-Shapley 1·27 ; van Gent 1·36.
† *Ap. J.*, **88**, 446, 1938.
‡ Russell, Dugan and Stewart, *Astronomy*, **2**, p. 732, 1927.

two stars and the maximum fraction α_0 of the star hidden during an eclipse, are defined by the depths of the minima according to Russell's equation (j) (*loc. cit.*). Two sets of values of k and α_0 may be calculated, dependent on whether the primary eclipse is regarded as an "occultation" (i.e. large star front) or as a "transit" (small star in front). Two such sets of results are shown in Table IV and from the associated limiting values of α_0 and k it can be shown, by Russell's equation (k) that with the "occultation" hypothesis, the brightness of the larger front star is $0{\cdot}44 < L_1 < 0{\cdot}64$ and with the "transit" hypothesis the brightness of the smaller front star is $0{\cdot}28 < L_2 < 0{\cdot}44$. Shapley * assembles Harvard spectroscopic data

TABLE III

Ratio of Surface Brightness ($\mathcal{J}_1/\mathcal{J}_2$) *for values of* $T_b = 23{,}000$ *and* $21{,}400°$ *C.*

T_b	T_f	T_b/T_f	$\mathcal{J}_1/\mathcal{J}_2$				
			λ=3500 A	4000 A	4500 A	5000 A	5500 A
21,400	18,000	1·19	1·52	1·45	1·41	1·39	1·36
	18·500	1·15	1·41	1·36	1·34	1·32	1·28
	19,000	1·13	1·33	1·29	1·26	1·25	1·23
	19,500	1·10	1·25	1·22	1·20	1·19	1·18
23,000	18,000	1·28	1·76	1·68	1·63	1·58	1·55
	18,500	1·24	1·64	1·58	1·54	1·50	1·47
	19,000	1·21	1·54	1·49	1·45	1·42	1·40
	19,000	1·18	1·45	1·41	1·38	1·36	1·34

TABLE IV

Transit and Occultation Hypotheses for Primary Eclipse—(Uniform Disks)

Axial ratio	k	1·00	0·95	0·90	0·80	0·75	0·72	0·67
Occultation	α_0	0·651	0·683	0·718	0·812	0·872	0·916	0·999
Transit	α_0	0·651	0·691	0·738	0·857	0·935	0·992	...
$\chi(k, \alpha_0, \frac{1}{4})$		1·921	1·920	1·923	1·921	1·921	1·877	...

showing that the fainter B3 star is in front at primary minimum and has a brightness $L_2 = 0{\cdot}4$. Thus the "occultation" hypothesis which always assigns to the front star a relative brightness $> 0{\cdot}4$ is untenable, but the "transit" hypothesis which requires a range of brightness for the front star including 0·4 is applicable. Attention should be drawn to the derivation of these figures for the brightness of component stars. Miss Maury, in discussing the Harvard-Arequipa observations on which the figures depend, remarks "both components of this binary are visible and one is much fainter than the other, the relative intensity being about seven-tenths". Presumably the accepted values for L_1 and L_2, upon whose accuracy depend many derived values not only in this, but also in various other discussions, represent an approximate determination and probably could be improved by modern spectro-photometric technique. Furthermore there are variations in the intensity of the lines and it would seem that additional spectroscopic data would be valuable. However it is necessary to rely on the spectroscopic figures for the relative light, since as can be seen in Table IV, Russell's function $\chi(k, \alpha_0, \frac{1}{4})$ is practically constant over a large range of k and α_0, the photometric solution being in

* *Contr. Princeton Univ. Obs.*, No. 3, 73, 1915.

itself indeterminate. Adopting $L_b = 0{\cdot}60 = L_1$, and $L_f = 0{\cdot}40 = L_2$ the corresponding value of the function is 1·922 from which a "uniform" light curve can be constructed. The normal magnitudes of Table I, when rectified for ellipticity have a mean residual of $0^m{\cdot}009$ from this curve (not reproduced), provided a slight adjustment of the phase of secondary minimum is made to take account of a small orbital eccentricity.

7. *Orbital eccentricity and apsidal rotation.*—The uniform curve derived above, fitted the observations better if the secondary minimum was centred, not $0^P{\cdot}500$ later than the primary minimum, as would be the case for a truly circular orbit, but by $0^P{\cdot}508$. This indicates an eccentric orbit, but as the nature of the light curve was not such as would yield a satisfactory completely photometric determination of the eccentricity, Miss Maury's value of $e = 0{\cdot}08$ was combined with a value of $e\cos\omega$ obtained from the unequal spacing of the minima to calculate a new light curve. This curve differed only negligibly from the uniform solution with a displaced secondary minimum; e. g. in the eccentric solution the widths of primary and secondary minima were greater by about half a minute. Accordingly no further adjustment for eccentricity was made. The result is of interest however in giving a value for the longitude of periastron, viz. 87°. This agrees with the photometrically determined values quoted by van Gent, viz. $\omega = 88°$ (1900) and $\omega = 90°$ (1937). It seems improbable that there is any rapid rotation of the line of apsides. As can be seen in Fig. 2 the normals for the constant light portion of the curve are slightly higher around $0^P{\cdot}75$ than about $0^P{\cdot}25$, the average difference being about $0^m{\cdot}003$. This, taken in conjunction with the direction of displacement of the secondary minimum, suggests a periastron effect, but the observations are insufficient in number to make further discussion of the point of value.

8. "*Darkened*" *Solution.*—A solution was made by the Russell-Shapley method for stars completely darkened at the limb. The resultant computed curve differed mainly in having a slightly longer duration of eclipse than that for the "uniform" solution. The elements derived from the darkened solution, as may be seen in Table V, differed somewhat, but not greatly, from those of the uniform solution. The average residual for the darkened solution amounted to $0^m{\cdot}008$ as compared with $0^m{\cdot}009$ for the uniform solution.

9. *Absolute Dimensions.*—Various absolute dimensions calculated by combining results from the present darkened solution with other data are set out in Table VI. The orbital and stellar radii were obtained from Miss Maury's spectroscopic determination of $(a_1 + a_2)\sin i$ and the present value of i. The combined mass was also obtained from the spectroscopic value of $(m_1 + m_2)\sin^3 i$. The individual masses were obtained by two methods. Method (*a*) consisted in assigning trial parallaxes to the system until the resultant absolute magnitudes of the two components, converted by a mass-luminosity curve, yielded two masses whose sum equalled the total mass derived as above. Method (*b*) calculated the individual masses by the Gaposchkin formula * using the mass-luminosity relation, spectral type and effective temperature. The mass-luminosity data and effective temperatures given by Kuiper (*loc. cit.*) were employed for both methods (*a*) and (*b*). The values for the density (*a*) and (*b*) were calculated from the corresponding masses. The value for the parallax is in fair agreement with van Gent's figure of $0''{\cdot}0023$ and also with spectroscopic parallax of $0''{\cdot}003$ obtained by W. B. Rimmer.†

* *Proc. Amer. phil. Soc.*, **79**, 329, 1938.

† *Mem. Commonw. Solar Obs. Aust.*, No. 2, 31, 1930.

TABLE V

Solution for Ellipsoidal Stars

		Uniform	Darkened
Semi-major axis of relative orbit	a	1·00	1·00
Semi-major axis, equatorial, large star	c_1	0·40	0·42
Semi-minor axis, equatorial, large star	b_1	0·36	0·40
Semi-minor axis, meridional, large star	c_1	0·35	0·38
Semi-major axis, equatorial, small star	c_2	0·37	0·38
Semi-minor axis, equatorial, small star	b_2	0·35	0·36
Semi-minor axis, meridional, small star	c_2	0·34	0·35
Axial ratio $a_1/a_2 \times b_1/b_2 = c_1/c_2$	k	0·93	0·92
Light variation at primary minimum	$1-l_p$	$0^m·56$	$0^m·56$
Light variation at secondary minimum	$1-l_s$	$0^m·45$	$0^m·45$
Light of large star (adopted spectroscopic value)	L_1	0·60	0·60
Light of small star ($L_1+L_2=1·00$)	L_2	0·40	0·40
Greatest loss of light at primary minimum	a_0	0·71	0·64
Ratio of surface brightness	$\mathcal{J}_1 \mathcal{J}_2$	1·29	1·29
Equatorial ellipticity coefficient $\epsilon^2 \sin^2 i$	Z	0·16	0·10
Equatorial ellipticity	ϵ	0·42	0·33
Inclination of orbit (corrected for polar flattening)	i'	77°·9	74°·0
Eccentricity of orbit (adopted spectroscopic value)	e	0·08	0·08
Longitude of periastron	ω	87°	87°
Period of revolution	P	$1^d·4545$	$1^d·4545$

TABLE VI

Dimensions Masses etc. of Components (from " darkened " solution)

		$B1$	$B3$
Semi-major axis of relative orbit	$km \times 10^6$	12·5	12·5
Semi-major axis-equatorial	$km \times 10^6$	5·2	4·8
Mean radius $(abc)^{\frac{1}{3}}$	$km \times 10^6$	5·0	4·5
Mass (a)	$\odot = 1$	20·5	15·5
(b)	$\odot = 1$	19·1	13·0
Density (a)	$\odot = 1$	0·057	0·057
(b)	$\odot = 1$	0·053	0·048
Mean absolute magnitude		−4·28	−3·84
Parallax (from mass luminosity relation)	seconds	0·0016	0·0016

Commonwealth Observatory,
Canberra:
1946 *September* 16.

ELECTROMAGNETIC FORCES IN SOLAR PROMINENCES

David S. Evans

(Received 1946 April 9)

Summary

The paper considers the hypothesis that the forms of solar prominences and the motion of knots in them is to be accounted for as motion of ions in a magnetic field. In Section I the dispersion of systems of ions under their mutual electrostatic repulsion is considered, and the computed velocities compared with observations by McMath and his co-workers. Agreement with observation is obtained by assuming the existence of a background cloud of 10^{-11} or 10^{-12} elementary charges per c.c. In Section II the possible existence of a general electrostatic field above the solar surface is discussed. It is suggested that this may account for the support of prominences and of highly ionized atoms in the corona. Space tracks of moving knots are computed and found to be consistent with the observed forms of streamers. The forms of tornado and coronal prominences are also considered.

Introduction

The purpose of the present paper is to examine how far it is possible to account for the observed motions of the streamers of solar prominences on the hypothesis that these streamers consist of ions moving in a magnetic field. That electromagnetic forces must play a part in the economy of solar prominences can hardly be denied: sunspot regions, with which prominences are frequently associated, are often the seat of intense magnetic fields: the prominences themselves are regions of high excitation in which there must be a considerable degree of ionization. It is not suggested that the forces which determine the behaviour of prominence streamers are exclusively electromagnetic; but it is possible to give a general account of a rather surprising variety of prominence features on the basis of the hypothesis of the motion of charged particles in a magnetic field.

There is one objection which can immediately be made against the hypothesis, namely, that pure electromagnetic forces act always perpendicular to the direction of motion of the moving particle, so that it must follow that the linear speed of the particle remains constant. This is not in accord with the observed fact that prominence streamers and knots in them, while sometimes travelling with a constant velocity, do, on occasion, show accelerations. Evidence * has been advanced that such accelerations may take the form of instantaneous changes of velocity, and although doubt has been cast on the validity of this contention by Hulme †, there is no doubt that accelerations, whether of a continuous or discontinuous character do occur.

Equally there are some striking features in favour of the hypothesis. Ions of different charge moving in a magnetic field will follow different tracks just as they do in a mass spectrograph, so that the occurrence of streamers would find a ready explanation.

* Pettit, *Ap. J.*, **50**, 206, 1919 ; *Ap. J.*, **76**, 9, 1932 ; *Ap. J.*, **84**, 319, 1936 ; etc.
† *M.N.*, **99**, 634, 1939.

The variation of velocity would provide an insuperable stumbling-block in the case of a single ion, but it does not follow that all the members of a finite distribution of ions will suffer no acceleration in the direction of their motion. The whole of Section I is devoted to the consideration of this problem, and it is thought that sufficient evidence is advanced to remove the objection and to provide an explanation of the peculiar variations of the velocities of knots in streamers as observed by McMath and others. In Section II the hypothesis of the motion of ions in a magnetic field is developed. A preliminary discussion of the electrostatic field of the Sun provides a hint as to the mechanism of support of prominences, and of their association with sunspots. The electromagnetic hypothesis explains the forms of streamers in various types of prominence, and also suggests a mechanism for the existence and form of tornado prominences. Final paragraphs are devoted to a discussion of the combination of various effects (electromagnetic forces, gravity, electrostatic forces and velocity changes) which are, for convenience, initially discussed separately.

It must be emphasized that the present paper is exploratory. It is perhaps almost as valuable to have firm grounds for the rejection of a plausible astrophysical hypothesis as it is to establish a correct theory. The hypothesis discussed in this paper has therefore been pushed as far as possible in order to see whether any striking discrepancy would arise to disprove it. However, as far as can be judged, no such discrepancy has been found, and it is not impossible that the present hypothesis constitutes the true explanation of many prominence features. It is at least considered that the case made out is sufficiently sound to warrant the concentration of observational work on to the further investigation of its consequences.

Section I.—The Dispersal of a System of Ions

1. The purpose of this Section is to serve as a lemma, establishing certain propositions which will be applied subsequently. These applications will in the present instance be to the problem of solar prominences, but, in view of the fact that the analysis may have a wider astronomical interest, and perhaps even an interest for other branches of science, it is developed here in slightly greater detail than is strictly necessary for the present problem. Even so, some of these wider applications may have a value for the present discussion, as sketching out further possibilities which have not yet been followed up in detail.

2. *Dispersion of a spherical system*: *Non-overtaking case.*—It is convenient to begin by considering a mass of ions, each with a positive charge Ze, where e is the electronic charge, having a distribution both of position and velocity, which is spherically symmetrical. We suppose that at time t, there are, at distance r from the centre of the distribution, $N(r,t)$ particles per unit volume. We further suppose that the velocity of the particles at distance r at time t is $v(r,t)$. This apparently innocuous assumption has certain important consequences. It assumes that the velocity is a function of position and time, and, hence, that particles at a given distance from the centre are all moving with the same outward velocity. It follows from this that the character of the motion described is such that there is no overtaking—the order in which the particles find themselves at the initial moment is preserved throughout the motion. In a later paragraph we shall discuss the conditions for this state of affairs to obtain, and shall also consider

cases in which overtaking occurs. It will be found that this division into "non-overtaking" and "overtaking" motion is a very general one, and that it has a considerable importance for the subsequent development of the theory.

In the "non-overtaking" case with spherical symmetry, the force field in which each particle finds itself is due solely to the particles which are at distances from the centre less than the distance of the particle under consideration.

The acceleration of the particles at r is therefore given by

$$\frac{\partial v}{\partial t} = \frac{\kappa Z^2 e^2}{mr^2} 4\pi \int_0^r s^2 N(s,t) ds, \tag{I.1}$$

where the force between two particles is $\kappa Z^2 e^2/r$ and m is the mass of a particle. If we write

$$\lambda = \frac{4\pi\kappa Z^2 e^2}{m}, \tag{I.2}$$

then

$$\frac{\partial v}{\partial t} = \frac{\lambda}{r^2} \int_0^r s^2 N(s,t) ds. \tag{I.3}$$

In addition a continuity condition must be satisfied. The particles which, at time t, lie in the range r to $r+dr$ are $r^2 N(r,t) dr$ in number. All these have velocity v, and by the time $t+dt$ lie in the range $r+vdt$ to $r+dr+vdt+\partial v/\partial r\, dr\, dt$. The continuity condition is easily found to lead to the equation

$$\frac{\partial}{\partial r}(Nvr^2) + \frac{\partial}{\partial t}(Nr^2) = 0. \tag{I.4}$$

In order to solve equations I.3 and I.4 we write

$$P(r,t) = \int_0^r s^2 N(s,t) ds, \tag{I.5}$$

so that $P(r,t)$ is proportional to the total number of particles interior to r at time t. Then

$$\frac{\partial P}{\partial r} = r^2 N, \tag{I.6}$$

so that I.4 may be written as

$$\frac{\partial}{\partial r}\left(v \frac{\partial P}{\partial r}\right) + \frac{\partial^2 P}{\partial r \partial t} = 0 \tag{I.7}$$

and I.3 as

$$\frac{\partial v}{\partial t} = \frac{\lambda}{r^2} P(r,t). \tag{I.8}$$

The condition that there should be no overtaking can by integration of I.4 be expressed as

$$P(r+vdt, t+dt) = P(r,t), \tag{I.9}$$

which reduces to

$$v \frac{\partial P}{\partial r} + \frac{\partial P}{\partial t} = 0, \tag{I.10}$$

leading to the equation

$$vr^2 \frac{\partial^2 v}{\partial r \partial t} + 2vr \frac{\partial v}{\partial t} + r^2 \frac{\partial^2 v}{\partial t^2} = 0. \tag{I.11}$$

If we write

$$\chi = vr^2 \qquad \text{I.12}$$

equation I.11 reduces to

$$\frac{1}{r^2}\frac{\partial^2\chi}{\partial r\partial t} + \frac{1}{\chi}\frac{\partial^2\chi}{\partial t^2} = 0. \qquad \text{I.13}$$

This equation possesses no intermediate integral and is not integrable by the method of Ampère. One set of conditions does, however, give a finite solution, which is of physical interest. If we take as initial conditions $N = N_0$, $v = 0$ the function χ splits into two factors and, as can easily be verified, the solution is given by

$$\left.\begin{aligned} v &= \tfrac{1}{3} r\sqrt{2\lambda N_0}\tanh\sqrt{\frac{\lambda N_0}{2}}\,t, \\ N &= N_0\operatorname{sech}^2\sqrt{\frac{\lambda N_0}{2}}\,t. \end{aligned}\right\} \qquad \text{I.14}$$

Before considering a more general form of solution we must consider the general boundary conditions which have to be satisfied. By equation I.12 $v = \chi r^{-2}$ so that the initial distribution of velocities is given by

$$v(r, 0) = r^{-2}\chi(r, 0). \qquad \text{I.15}$$

Since, by I.8

$$P(r, 0) = \frac{r^2}{\lambda}\left(\frac{\partial v}{\partial t}\right)_0$$

we have, using I.6,

$$N(r, 0) = \frac{r^{-2}}{\lambda}\frac{\partial}{\partial r}\left\{r^2\left(\frac{\partial v}{\partial t}\right)\right\}_{t=0}. \qquad \text{I.16}$$

In cases of physical interest it will usually happen that the initial distribution of ions is spatially limited, whereas it appears from these equations that, unless the initial conditions are smoothed so as to produce partial derivatives where required, then the analysis so far considered will only apply to a distribution of infinite extent. However, in fact, there is no limitation of this kind: the analysis will apply as it stands, even to cases where the initial distribution of ions is sharply limited, and where $\partial v/\partial r$ is non existent at the boundary of the initial distribution. Since the force field acting on each particle is due to only those particles which are nearer to the centre, then, provided there is no overtaking, any problem in which the initial distribution has a sharp boundary has the same solution out as far as a certain distance from the centre as the problem in which the initial distribution is infinite, but where the initial distribution of space density and velocities is identical in the regions common to the two cases. Any limited initial distribution may be completed by continuing it to infinity with a distribution arbitrary as to its space density and velocity distribution, provided that this does not infringe the "non-overtaking" condition. Thus, for example, if the initial distribution were of radius a, and if, within this radius the initial space density were constant, then the problem might be solved by considering initially an infinite distribution with the same space density. The subsequent fate of the actual distribution would be the same as that of the particles initially inside a radius a in the second case, and the expansion of the actual surface could be found by tracing the expansion of the shell which, in the second case, had an initial radius a.

The method of solution proposed is in the form of a power series. Mathematically this is far less general than a complete integral in finite terms of I.13 would be, but practically it seems likely that this form of solution will be sufficient. If, for example, the initial distributions were given in graphical form, it would always be possible to approximate, arbitrarily closely to them, by a solution of this orm.

We therefore seek a solution in the form

$$\chi = f_0(r) + f_1(r) \cdot t + f_2(r) \cdot \frac{t^2}{2!} + \ldots = \sum_0^\infty f_s(r) \frac{t^s}{s!}, \qquad \text{I.17}$$

where $f_0(r)$, $f_1(r)$, $f_2(r)$ etc. are functions of r, all of which vanish when $r=0$. It should also be noted that singularities when $t=0$ are physically inadmissible.

Then

$$\frac{\partial \chi}{\partial t} = \sum_1^\infty f_s(r) \frac{t^{s-1}}{(s-1)!}; \quad \frac{\partial^2 \chi}{\partial t^2} = \sum_2^\infty f_s(r) \frac{t^{s-2}}{(s-2)!}; \quad \frac{\partial^2 \chi}{\partial r \partial t} = \sum_1^\infty f_s'(r) \frac{t^{s-1}}{(s-1)!}, \qquad \text{I.18}$$

When this is substituted in I.13 we obtain the general recurrence relation

$$f_{n+2}(r) = -\frac{1}{r^2} \sum_0^n {}^nC_s f_s(r) f'_{n+1-s}(r), \qquad \text{I.19}$$

the first few examples of which are

$$\left.\begin{aligned} &r^2 f_2(r) + f_0(r) f_1'(r) = 0, \\ &r^2 f_3(r) + f_0(r) f_2'(r) + f_1(r) f_1'(r) = 0, \\ &r^2 f_4(r) + f_0(r) f_3'(r) + 2 f_1(r) f_2'(r) + f_2(r) f_1'(r) = 0. \end{aligned}\right\} \qquad \text{I.20}$$

The initial conditions I.14 and I.16 then becomes

$$f_0(r) = r^2 v(r, 0); \quad f_1'(r) = \lambda r^2 N(r, 0) \qquad \text{I.21}$$

and it will easily be seen that the subsequent functions, $f_2(r), f_3(r)$ etc. may then be calculated in turn.

As an example, if the initial conditions for the solution I.14 are taken, then $f_0(r) = 0, f_1(r) = \lambda N_0 r^3/3$.

All the even functions are then zero, and we have

$$v = \frac{\lambda N_0}{3} r\left(t - \lambda N_0 \frac{t^3}{3!} + 4\lambda^2 N_0^2 \frac{t^5}{5!} + \ldots\right),$$

$$N = N_0\left(1 - \lambda N_0 \frac{t^2}{2!} + 4\lambda^2 N_0^2 \frac{t^4}{4!} + \ldots\right),$$

which are, in fact, the series expansions of the functions on the right of I.14.

This solution will be considered in more detail in a later paragraph.

The solution of the problem in power series, and the similar solution of the "overtaking" case proposed below, must be regarded as tentative, since it has, so far, not proved possible to give any kind of general discussion of their convergence. This problem is in fact likely to be very difficult and to involve considerations of a very advanced kind. It seems worthwhile however to include these formal solutions even without discussion of their convergence: the solutions themselves are in fact not used in this form in the present paper, but, in view of

suggestions made later on, if the present discussion meets with general acceptance, it seems likely that the formal solutions will acquire a certain importance, which may then justify the devotion of the necessary attention to the difficult convergence considerations which they involve.

The limitations which must be placed on $f_0(r)$ and $f_1(r)$ to ensure that the "non-overtaking" condition is satisfied, are, first, that the initial velocity must not decrease outwards (and this condition cannot be made more stringent), with the result that f_0, if not zero, must be of degree at least two in r. It cannot contain terms of lower degree without introducing a singularity in $v(r, 0)$ at the origin. $N(r, 0)$ must be of degree greater than -1, so that $f_1(r)$ must be of degree at least two, in r. If the degree actually is two, then $N(r, 0)$ has a singularity at the origin, but the total number of particles within a sphere of finite radius is finite.

3. *Spherical system*: "*Overtaking*" *case.*—When the analysis is extended to the "overtaking" case the velocity is no longer a function of the position at any given time. Physically we may sketch a picture of more rapidly expanding inner shells passing through the outer ones so that, at a position where, and at a time when, overtaking is in progress, particles of a number of velocities will have the same radial coordinate. Clearly, in any practical case this phase of motion will be a temporary one. After a limited time the sorting out of the higher speed particles to the larger distances will be complete, and the analysis of the preceding subsection can be applied.

We may put the problem into mathematical terms by postulating a function $N(v, r, t)$ which is such that $N(v, r, t)dv$ represents the number of particles per unit volume which, at distance r and at time t have velocities in the range v to $v+dv$. The acceleration of a particle at r at time t will then be

$$K = \frac{\lambda}{r^2} \int_0^r ds \int_0^\infty dv s^2 N(v, s, t), \qquad \text{I.22}$$

where λ is defined, as before, by equation I.2.

The continuity condition becomes

$$v \frac{\partial}{\partial r}(Nr^2) + \frac{\partial}{\partial t}(Nr^2) + Kr^2 \frac{\partial N}{\partial v} = 0 \qquad \text{I.23}$$

or, putting $\xi = r^2 N(v, r, t)$,

$$v \frac{\partial \xi}{\partial r} + \frac{\partial \xi}{\partial t} + K \frac{\partial \xi}{\partial v} = 0. \qquad \text{I.24}$$

Again, we attempt a solution in series, writing

$$\xi = \sum_0^\infty F_s(v, r) \frac{t^s}{s!}, \qquad \text{I.25}$$

from which we have

$$\frac{\partial \xi}{\partial r} = \sum_0^\infty \frac{\partial F_s}{\partial r} \frac{t^s}{s!}; \quad \frac{\partial \xi}{\partial v} = \sum_0^\infty \frac{\partial F_s}{\partial v} \frac{t^s}{s!}; \quad \frac{\partial \xi}{\partial t} = \sum_1^\infty \frac{\partial F_s}{\partial r} \frac{t^{s-1}}{(s-1)!}. \qquad \text{I.26}$$

If we put

$$G_s(r) = \int_0^\infty F_s(v, r) dv \qquad \text{I.27}$$

then

$$\int_0^\infty \xi(v, r, t) dv = \sum_0^\infty G_s(r) \frac{t^s}{s!}. \qquad \text{I.28}$$

If further, we write

$$H_s(r) = \int_0^r G_s(r)dr \qquad \text{I.29}$$

then

$$K = \frac{\lambda}{r^2}\sum_0^\infty H_s(r)\frac{t^s}{s!}. \qquad \text{I.30}$$

If all these are substituted in I.24 we obtain the general recurrence relation

$$\frac{\partial F_{n+1}(r)}{\partial r} = -v\frac{\partial F_n(r)}{\partial r} - \frac{\lambda}{r^2}\sum_{s=0}^{r} {}^nC_s \frac{\partial F_s(r)}{\partial v} H_{n-s}(r) \qquad \text{I.31}$$

of which the first few members are

$$\left.\begin{aligned} \frac{\partial F_1}{\partial r} &= -v\frac{\partial F_0}{\partial r} - \frac{\lambda}{r^2}\frac{\partial F_0}{\partial v}H_0, \\ \frac{\partial F_2}{\partial r} &= -v\frac{\partial F_1}{\partial r} - \frac{\lambda}{r^2}\left\{\frac{\partial F_0}{\partial v}H_1 + \frac{\partial F_1}{\partial v}H_0\right\} \text{etc.} \end{aligned}\right\} \qquad \text{I.32}$$

The initial condition is that $F_0(v,r)/r^2$ represents the initial spatial and velocity distribution of the system. From the first of I.32 $\partial F_1/\partial r$ may be found, and, since for all s, $F_s(v,r)$ must be zero for $r=0$, the additive constant in the integration is determined, and hence $F_1(v,r)$ found. In a similar way the successive members of the set of functions may be calculated. These problems provide an instructive example of a type which is becoming increasingly common in all branches of physical science, namely, problems in which the behaviour of a single element is conditioned by the aggregate behaviour of the whole, and which find mathematical expression in mixed integro-differential equations.

4. *Two dimensional system.*—It would clearly be possible to multiply indefinitely the problems falling under the general heading of the dispersion of systems of ions. One further example of immediate interest is, however, the two-dimensional case, in which the distribution consists of a series of infinite plane layers, dispersing along axes normal to all the layers. If we take as origin that plane such that the total number of particles on the two sides of it are initially equal, and if, at a distance x from this plane, there are $N(x,t)$ particles per unit volume, then the acceleration of a particle at x at time t is simply

$$\frac{\lambda}{r}\left\{\int_{-\infty}^{x} N(s,t)ds - \int_x^\infty N(s,t)ds\right\}, \qquad \text{I.33}$$

where λ has the same meaning as in I.2. If the motion is of the non-overtaking variety, then the acceleration of each particle is constant with time, and may be calculated directly from the initial conditions.

5. *Application to the motion of knots in prominence streamers.*—It is now necessary to relate this mathematical apparatus more closely to the problem of the motions of prominence streamers. In this section we are concerned solely with the accelerations observed, not with the shapes of the streamers, which will be considered in a later section. Nor shall we, for the moment, for reasons also explained below, attribute any part of the observed accelerations to the gravitational field of the Sun.

We shall first consider the case of knots in a prominence streamer, which have the appearance of areas of extra luminosity travelling along tracks already occupied by luminosity. We shall endeavour to account for the observed motions in two ways: we shall regard some knots as groups of ions passing through a dispersing system of ions: we shall regard other knots as portions of a dispersing system which take part in the motion of that system.

Consider a two-dimensional system of ions of the kind described in the preceding paragraph, all of whose members are initially at rest and suppose that the initial density of ions is constant, and equal to N_0. Then the acceleration of a particle at distance x from the median plane is $\lambda N_0 x$. This acceleration depends only on the distribution interior to x, and increases outwards. It will be easily seen that these two properties always hold, whatever the initial distribution of particles, and it therefore follows that, if initially all the particles are stationary, then the subsequent motion is always of the non-overtaking variety.

At time t the particle originally at x will have reached y, where

$$y = x(1 + \lambda N_0 t^2/2). \qquad \text{I.34}$$

TABLE I.I

T	$f(T)$	$g(T)$	$g'(T)$	T	$f(T)$	$g(T)$	$g'(T)$
0·0	1·00	0·0000	2·0000	1·5	3·25	4·6941	4·9484
0·1	1·01	0·2007	2·0200	1·6	3·56	5·2034	5·2390
0·2	1·04	0·4053	2·0790	1·7	3·89	5·7421	5·5330
0·3	1·09	0·6177	2·1750	1·8	4·24	6·3100	5·8294
0·4	1·16	0·8414	2·3044	1·9	4·61	6·9078	6·1280
0·5	1·25	1·0795	2·4636	2·0	5·00	7·5355	6·4284
0·6	1·36	1·3349	2·6484	3·0	10·00	15·4900	9·4940
0·7	1·49	1·6099	2·8550	4·0	17·00	26·5369	12·6056
0·8	1·64	1·9065	3·0796	5·0	26·00	40·7058	15·7330
0·9	1·81	2·2117	3·3190	6·0	37·00	57·9961	18·8636
1·0	2·00	2·5708	3·5708				
1·1	2·21	2·9409	3·8326				
1·2	2·44	3·3374	4·1024				
1·3	2·69	3·7616	4·3792				
1·4	2·96	4·2135	4·6614				

Since the acceleration of each particle of the system is constant, the acceleration of the particle at y will have the same value as it did initially when it started from x i. e.

$$\ddot{y} = \lambda N_0 x. \qquad \text{I.35}$$

If we now suppose that, superposed on the dispersing system, there is an additional particle projected so as to pass through the system, then, when the added particle is at y, it will have the acceleration of those particles of the dispersing system with which it is momentarily coincident, i. e. it will have the acceleration of particles of the system originally at x where y and $\ddot{y}$ are related to x through I.34 and I.35.

The additional particle will therefore have for its equation of motion

$$\frac{\ddot{y}}{y} = \frac{\lambda N_0}{1 + \lambda N_0 t^2/2} \qquad \text{I.36}$$

whose solution is

$$y = A(1+T^2) + B\{T + (1+T^2)\tan^{-1} T\}, \qquad \text{I.37}$$

where

$$T^2 = \lambda N_0 t^2/2. \qquad \text{I.38}$$

For convenience we write

$$f(T) = 1+T^2, \qquad g(T) = T + (1+T^2)\tan^{-1} T. \qquad \text{I.39}$$

If, when $T=0$, $y=0$, then $A=0$, and I.37 reduces to $y=Bg(T)$. Table I gives values of $f(T)$, $g(T)$ and $g'(T)=2(1+T\tan^{-1} T)$.

We now compare the solution of I.37 with observed motions of knots in prominences. For this we require observations of true space motions in all three

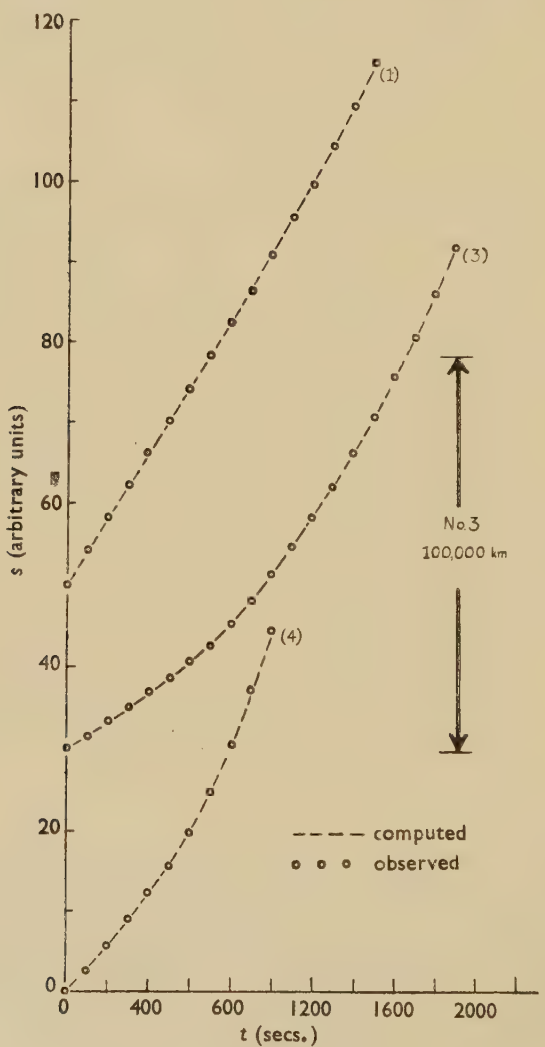

FIG. I.1.—(1) $s=6{\cdot}00g(t/3000)$.
(3) $s=6{\cdot}00g(t/800)$.
(4) $s=7{\cdot}90g(t/600)$.

coordinates, combined so as to give the distance travelled, s, as a function of time. McMath * and his collaborators have given observations of this kind which are graphed in Figs. I.1, 3 and 4. The results are taken from McMath's Fig. 4, where the curves are given on arbitrary scales, and illustrate the results of his Table I. It is clear that the time interval is 100 seconds, and also that curve No. 3 in his Fig. 4 is the same as that of his Fig. 2 where a scale in kilometres is given. In Fig. I.1 are given McMath's results for three knots (Nos. 1, 3 and 4) of his Fig. 4, together with the scale for No. 3. To these curves have been fitted curves of the form $Bg(T)$ where B and the scale factor of T in terms of t are at our disposal. The

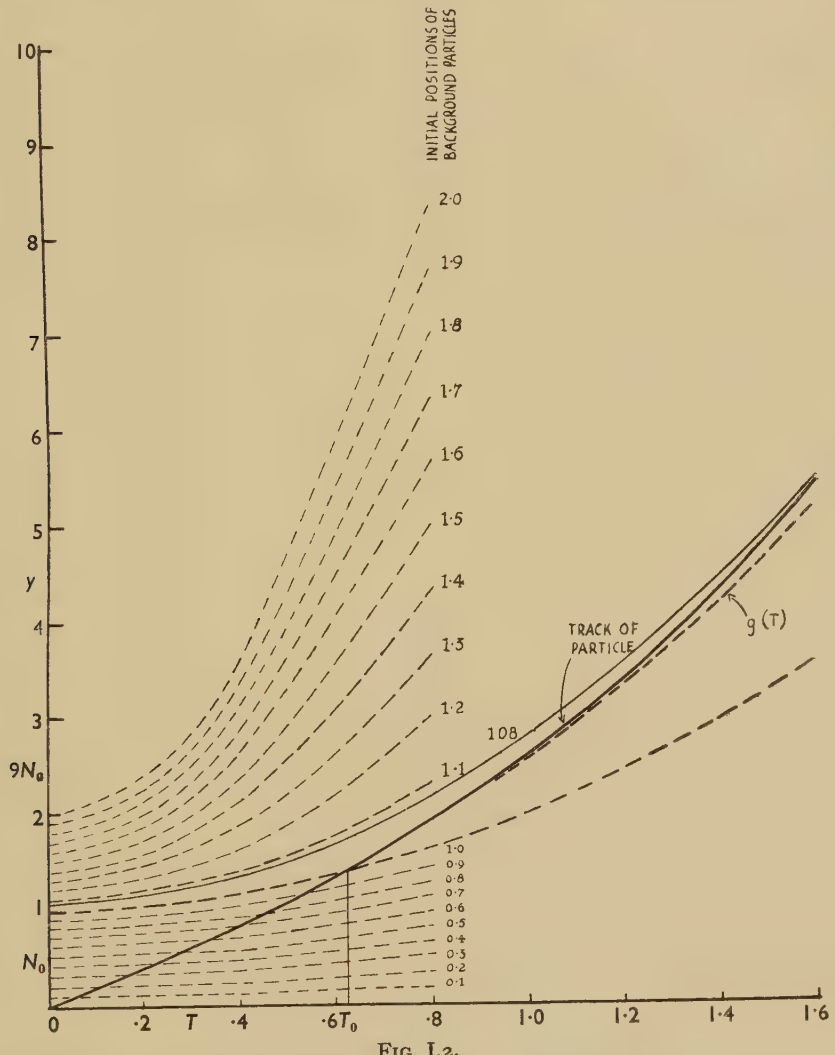

FIG. I.2.

three fitted curves are shown in the figure. Their scale factor gives, respectively

$$\frac{\lambda N_0}{2} = \frac{1}{(3000)^2}, \quad \frac{1}{(800)^2}, \quad \frac{1}{(600)^2} \qquad \text{I.40}$$

* *Loc. cit.*

and, substituting the value of λ given by I.2, and writing $m = Am_0$, where m_0 is the mass of a hydrogen atom, we obtain in general

$$\log\left(\frac{N_0 Z^2}{A}\right) = -2\log C - 5{\cdot}94, \qquad \text{I.41}$$

where C is the scale factor, giving in our three cases

$$\log\left(\frac{N_0 Z^2}{A}\right) = -12{\cdot}89,\ -11{\cdot}75,\ -11{\cdot}50. \qquad \text{I.42}$$

For hydrogen ions the values on the right are actual values of $\log N_0$. If it should be assumed that the "background" ions are different from the "knot" ions, then Z^2 must be replaced by $Z_1 Z_2$ and A refers to the "knot" ions.

McMath remarks on the general similarity of all these curves, but there are, in fact, in the present view of the matter, two distinct types, corresponding to different values of the arbitrary constants in equation I.37. So far we have only dealt with cases where the "knot" particle is projected from the centre of the distribution at time $T=0$. If now, we suppose that, when $T=0$, $dy/dT=0$, then we are dealing with a case (for which $B=0$) of a particle taking part in the general motion of dispersal. The observed curves must be divided into two classes: those giving zero velocity at $T=0$, and those with a non-zero velocity at $T=0$. It may be asked how we know when $T=0$: what assurance have we that there should be no shift in the zero of the time scale, corresponding to starting observation some time after the knot has already set out on its journey? It is essential that $T=0$ should correspond to the time at which the knot particle leaves the median plane of the background distribution, and the assurance that this is so lies in the fact that McMath's observations represent selections from long continuous records of prominences. When measuring a run of frames the measures will surely start from the moment that a knot is visible as such.

6. *Influence of density variations in ionic background.*—In Fig. I.3 are plotted curves Nos. 5 and 6 from McMath's Fig. 4. These are trajectories of the second kind, for which $B=0$, and we shall see how far they are explicable on the present hypothesis. It is convenient to couple this with a reference to a somewhat inconclusive incidental investigation which was concerned with the question of the reality or otherwise of Pettit's hypothesis of discontinuous changes of velocity. In order to test this it was an obvious step to investigate the effect of considering an initial "background" distribution of ions where sharp changes of density occurred, the idea being that, in crossing such a boundary a particle might suffer a sudden increase of velocity. It should be noted that, since, if we assume a zero velocity for all the ions of the "background" at $T=0$, and since the initial acceleration always increases outwards, then it follows that in the consequent "non-overtaking" motion, only sudden increases of velocity, and never sudden decreases, can occur. This is of course in general accord with Pettit's views.

Consider an ion distribution of uniform density N_0 as far as $x=a$, while thereafter the initial density is N_1. Then the initial accelerations are $N_0 x$ in the first region, and $\lambda\{(N_0 - N_1)a + N_1 x\}$ in the second. In the first region the motion is described by I.36 and I.37 and the solution holds until

$$y = af(T). \qquad \text{I.43}$$

Here the particle crosses the boundary and enters the second region where its equation of motion is easily found to be

$$\frac{d^2Y}{dT'^2} = \frac{2Y}{1+T'^2}, \qquad \text{I.44}$$

where

$$Y = y + \frac{N_0 - N_1}{N_1} \cdot a \qquad \text{I.45}$$

and

$$T'^2 = \frac{\lambda N_1}{2} t^2. \qquad \text{I.46}$$

If we write $K^2 = N_0/N_1$ then the continuity conditions at the boundary give

$$\begin{aligned} f(T_0) = Bg(T_0) &= A'f(T_0/K) + B'g(T_0/K) - (K^2 - 1), \\ KBg'(T_0) &= 2A'T_0/K + B'g'(T_0/K), \end{aligned} \qquad \text{I.47}$$

where in the first region $y = Bg(T)$ and in the second $y = A'f(T') + B'g(T') - (K^2 - 1)$, where $T = KT'$, where the crossing into the second region takes place at T_0, and where all the constants B, A' and B' have been expressed in terms of a as the unit.

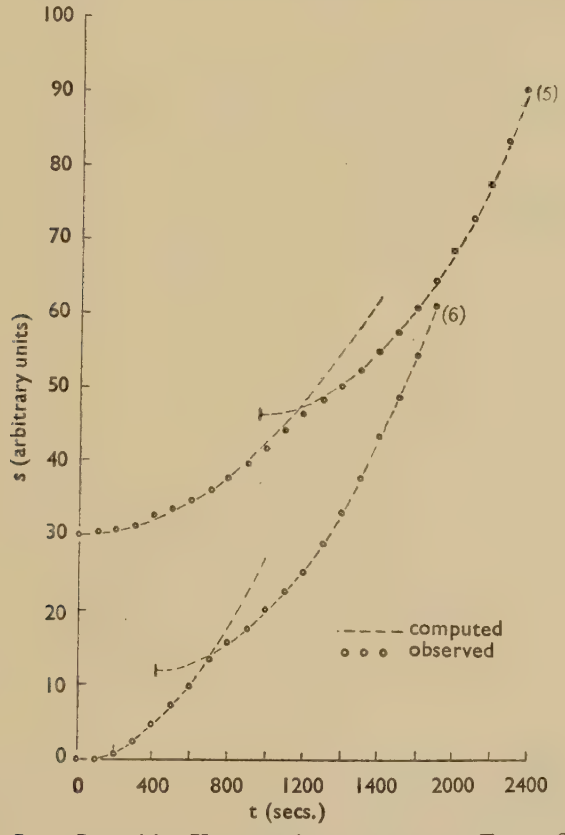

FIG. I.3.—*Curve* (5): *Upper portion* $s = 35{\cdot}25 - 3{\cdot}99T + 0{\cdot}208T^2$.
Lower portion $s = 0{\cdot}127T^2$.
Curve (6): *Upper portion* $s = 15{\cdot}58 - 1{\cdot}900T + 0{\cdot}226T^2$.
Lower portion $s = 0{\cdot}271T^2$.

$T = \frac{t}{100}$: *curve* (5) *displaced* 30 *units in* s.

An example of the working is provided by the case $K=1/3$, i.e. in the outer region the ion density has nine times the value in the inner, and $B=1$. T_0 therefore is 0·62 and we find $A'=-1{\cdot}292$, $B'=0{\cdot}945$. The resulting curve is plotted in Fig. I.2 where the dotted lines show the dispersal of the background system of ions. It will be seen that there is nothing which could be described as a discontinuous change of velocity. Physically, what happens is that the "knot" particle comes up to the boundary at $T_0=0{\cdot}620$ after crossing rapidly across the tracks showing the dispersal of the irons in the inner region. In the outer region the dispersal is more rapid, so that, by the time the "knot" particle enters the outer region the density ratio has fallen from 9 : 1 to about 2 : 1. The "knot" particle overtakes the background particles more and more slowly, although its velocity is continually increasing, and finally, in the given conditions just overtakes the particle which started from 1·08 and remains with it.

Analytically this arises from the fact that

$$g(t)\sim(1+t^2)\frac{\pi}{2}-\frac{2}{3t}+\frac{1}{3t^3},$$

so that

$$-1{\cdot}292f(3T)+0{\cdot}945g(3T)+0{\cdot}889\sim1{\cdot}081(1+9T^2)-8T^2-\frac{0{\cdot}21}{T}+\frac{0{\cdot}0117}{T^3}$$

which should be compared with the track of a particle in the outer region moving with the general dispersion and starting from x_0, namely, $y=x_0(1+9T^2)-8T^2$. It may be asked whether a steeper initial trajectory in the inner region, leading to a more rapid overtaking of background particles once the outer region was reached, would lead to apparent discontinuities. As far as a considerable number of experimental solutions entitle one to form a judgement, this is not the case. What we can conclude from this discussion is that, physically, what happens when a particle crosses a boundary of this kind is that it fairly soon falls in with the general background motion.

7. *Further comparison with observation.*—We may now return to the consideration of McMath's observational curves already referred to at the beginning of Section I.6. Clearly a simple solution of the form $f(T)$ will not serve, unless we are prepared to assume that the humps in these curves are due to observational error. Nor will passage through layers of different densities account for the observed shapes by what has just been said. In fact, no single background system of the type so far considered can account for the motion, since there is, in one region, a definite deceleration. In any single system, as we have seen, the acceleration must increase outwards. The hypothesis which will account for the observed motions is given below. It seems the simplest possible one which will account for the facts within the general framework of the present theory. It must be left to further observation to decide whether it savours too much of a "special creation" hypothesis.

It is clear the curves 5 and 6 can be fitted as to their lower portions by parabolas. We can also fit parabolas to their upper parts as is shown in the figure. We can attach a physical meaning to this by supposing that, initially, each knot forms a region, perhaps of rather higher density, in a dispersing system of the type we have been discussing. If now, during the motion, a second cloud of ions appears in the path of the knot, we may expect by the last section, that the knot will penetrate into the new ion-system, and then, after a lapse of time, will take part in

its motion of dispersal. This is the hypothesis advanced to cover the motions in curves 5 and 6. In curve 5 the initial parabolic curve persists until, at a point which roughly coincides with the vertex of the second parabola, a deviation takes place, and the actual track gradually merges with the new parabola. It is not desired to stress too much this coincidence in time, but if the hypothesis is true, we may expect the divergence to coincide with the vertex of the new parabola. This will happen because, until that moment there has been no retarding force on the knot, but, as soon as this mass of ions appears in its track and begins dispersing, a retardation will be experienced and the transition stage will begin. We cannot in either case estimate the ion density of the background, but we can, from the coefficients of the square terms in the two fitted curves deduce the necessary ratio of ion densities, since these coefficients are in the ratio K^2 given in I.47. In the first case $N_1/N_0 = 4{\cdot}05$, so that the retardation should be large and the transition time relatively long. In the second case, $N_1/N_0 = 0{\cdot}90$, so that here the retardation should be less noticeable, the transition period shorter, and the coincidence between the onset of the transition period and the vertex of the upper parabola less marked.

In discussing the likelihood of the correctness of this hypothesis it must be borne in mind that solar prominences are by no means static: new areas of excitation are continually appearing, and old ones changing their shape and position. It does not seem at all unlikely that the motions of knots may be deviated from the paths and velocities they would otherwise have followed, by changes in the general complexion of the prominence.

8. *Final comparison with McMath's Observations.*—We can now turn to the remaining observational curve (No. 2, Fig. I.4) given by McMath. In this there is

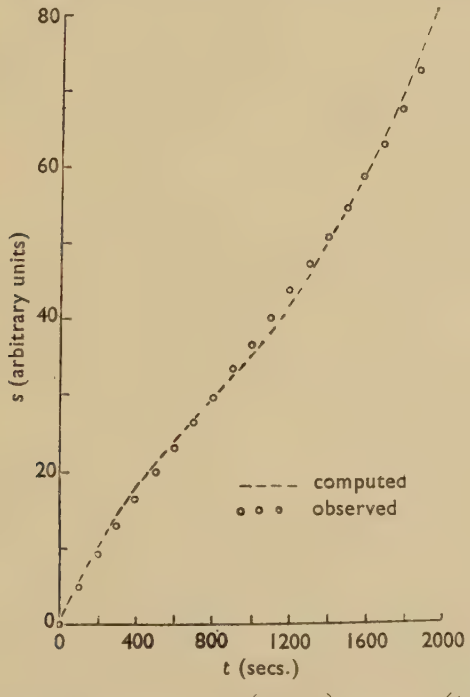

FIG. I.4.—*Curve* $s = 25{\cdot}0 - 10{\cdot}13f\left(\frac{t-300}{589}\right) + 10{\cdot}47g\left(\frac{t-300}{589}\right)$.

a point of inflection, and the form of the curve suggests that, in conformity with the foregoing discussion, it is possible that this may be explained as the track of a knot entering a dispersing system against the general motion of expansion, passing through the centre and out on the other side. We have at our disposal the parameter t_0 defining the epoch at which dispersal began, and the scale factor of the time, C. We seek to fit a solution of the form

$$s = s_0 + A \,.\, f\left(\frac{t-t_0}{C}\right) + B \,.\, g\left(\frac{t-t_0}{C}\right).$$

The dotted curve has the parameter values $s_0 = 25$, $t_0 = 300$, $C = 589$ ($= 1000/1{\cdot}7$). This corresponds to $\log(N_0Z^2/A) = -11{\cdot}48$. The fit is not first class, but is easily seen to be of the correct type of curve: doubtless by further processes of trial and error an improvement could be secured, but the fact that so many free parameters are at our disposal reduces the evidential value of an exact fit.

We may conclude that, within the limits of a single hypothesis it has proved possible to account, more or less satisfactorily, for all the curves given by McMath as typical of the motions of knots in prominence streamers.

9. *Inadequacy of hypothesis of elongation of streamers under it own electrostatic field.*—It was, at first, considered that there should be a differentiation in behaviour between knots moving in streamers and the ends of streamers themselves. The idea was that the lengthening of the streamer might be due to the repulsion of the ions of which it was combined. If we consider, for mathematical convenience, a long streamer of square section, the side of this square being $2a$, then a particle at the centre of one of the ends is subject to a force of acceleration of $7{\cdot}05\,N_0xaZ^2e^2$, while the corresponding force at the centre of one of the side faces is $6{\cdot}93\,N_0xaZ^2e^2$, i. e. there is some slight tendency for which a long mass of ions to stretch, rather than disperse sideways, and it was thought that, if initially, all the velocities were along the length of the mass, this tendency would be enhanced. In calculating the advance of the leading end of the streamer, account has to be taken of the sideways dispersion of the mass.

For the total number of ions to be constant

$$Nxy^2 = A \text{ (a constant)}, \qquad \text{I.48}$$

where x is the half length, y the half width of the streamer at time t. If the end and side accelerations are both taken as kNy, where $k = k'xZ^2e^2/m$ and k' has, by what has just been said, approximately the value $7{\cdot}0$, then we find by eliminating N

$$\ddot{x} = \ddot{y} = kNy = kA/xy. \qquad \text{I.49}$$

If the initial conditions are $x = x_0$, $y = y_0$, $\dot{x} = V$, $\dot{y} = 0$, then $x - y = Vt + c$ where $c = x_0 - y_0$. If we now write

$$X = \frac{1}{\beta}\left(x - \frac{Vt+c}{2}\right), \qquad S = \frac{Vt+c}{2\beta}, \qquad \beta = 4kA/V^2, \qquad \text{I.50}$$

the equation relating X and S is

$$(X^2 - S^2)\frac{d^2X}{dS^2} = 1. \qquad \text{I.51}$$

As far as is known, only numerical solutions of this equation are obtainable. The initial conditions are

$$X = \frac{x_0+y_0}{2\beta}, \qquad S = \frac{x_0-y_0}{2\beta}, \qquad \frac{dX}{dS} = 1. \qquad \text{I.52}$$

If the streamer is initially a long one X/S is initially just larger than 1·0. A few solutions of this equation are given in Figs. I.5 and 6, and it will be seen that, although there is some resemblance to the type of curve already considered the "toe" part is always too short. The streamer can only give itself a very short initial kick. In

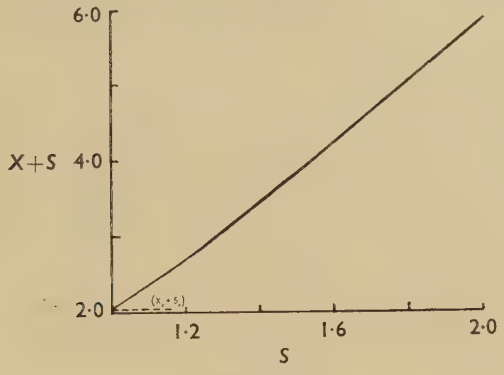

FIG. I.5.

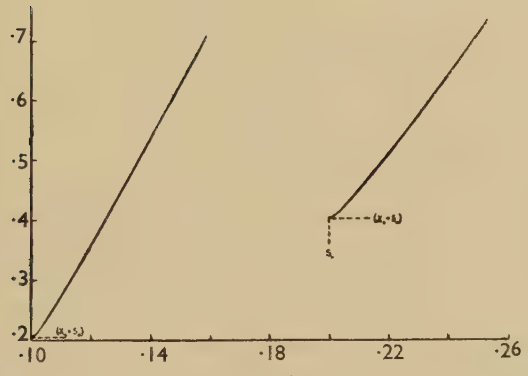

FIG. I.6.

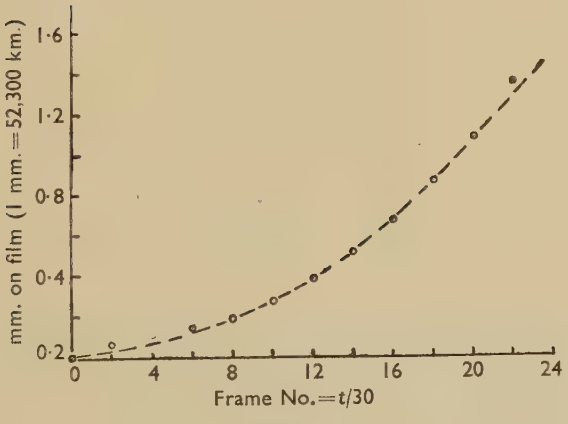

FIG. I.7.

the early stages when X/S is small d^2X/dS^2 is large but then falls rapidly to zero: we cannot get a fit with the observed curves in all of which d^2x/dt^2 falls off slowly however the scale is changed.

What is needed is a set of observations of the movement of the leading end of a streamer, which, as far as can be judged, is breaking a new path for itself and not following the track of an old one. The author has, with rather inaccurate means, measured what appears to be a streamer of this kind on the Lyot prominence film. The results are shown in Fig. I.7. There can be no doubt that this approximates to a parabola and not to a curve of the type of the solution of I.51. The acceleration is twice that of solar gravity.

If this is generally true it follows that we cannot think of the streamers themselves as providing the ion "background" required by the preceding discussion. It has always been a matter of controversy as to whether prominences as seen represent the true total extent of the matter above the solar surface, or whether what is seen is only the luminous part of some larger invisible cloud. If the "leaders" of streamers show the same behaviour as knots in streamers, then it seems likely that the latter view is correct, and that the ionic clouds which could produce the observed accelerations are considerably more extensive than the visible prominence.

10. *Comparison with spherical ionic background.*—Throughout the preceding discussion we have used, for our ionic background, a system of infinite layers. This has the marked advantage of mathematical simplicity, but it is open to some criticism. Such a system might well serve as a model of a very extensive ionic background where we have to deal with only a small part of a large distribution. In such a case it will be a matter of indifference whether the layers are really plane, or are really parts of very large curved surfaces.

However, it will no doubt render the picture more acceptable if it can be shown that the same kinds of velocity changes can be produced by distributions of other forms. It will certainly be anything but a recommendation for the present hypothesis if it requires a very highly specialised type of background distribution.

For this purpose we may consider once more the spherical distribution for which the solutions are given in equations I.14. Both for a "knot" particle and for a particle taking part in the general motion of dispersal whose individual fate we wish to follow, we must equate the acceleration $\ddot{r}$ to the field acceleration $\partial v/\partial t$. We then have, by equation I.3,using equation I.14,

$$\frac{\partial v}{\partial t} = \frac{\lambda N_0}{3} . r \operatorname{sech}^2 \sqrt{\frac{\lambda N_0}{2}} . t \qquad \text{I.53}$$

or, making the same transformation as in I.46, we readily obtain

$$\frac{d^2 r}{dT^2} = \frac{4r/3}{1 + \cosh 2T} . \qquad \text{I.54}$$

The solutions to I.54 are obtainable only numerically. The equation is linear, and hence we can reduce the solutions to two, which are the analogues of the two solutions of I.36 given in I.37. In the first, $r = 0$ when $T = 0$, and $\dot{r}$ is not zero: in the second, when $T = 0$, $\dot{r} = 0$ but r is not zero. It will also be seen that, since I.54 is linear in r, we have always a scale factor at our disposal. The two types of solution are graphed in Fig. I.8. It will be seen that they are of the same general type as those given by I.37 and it is possible to fit combinations of these two curves to the observations. The fits obtainable are not quite as good as those obtainable in the plane case, nor, since we now have an additional parameter available, is the

fact that fits are obtainable as striking as before. What we can say is the features of the observed curves do not restrict us to the model of the infinite plane background, although in that case the observed features do reveal themselves in the calculated curves in a rather pronounced way.

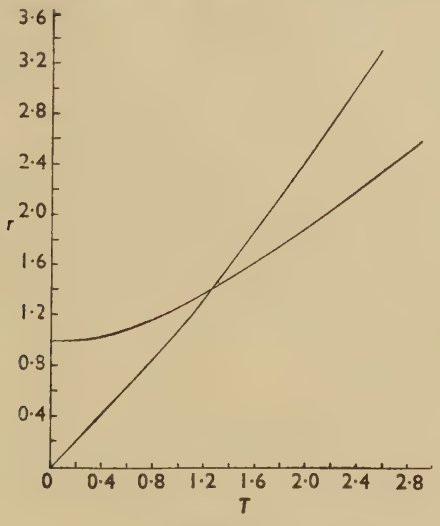

FIG. I.8.

11. *Discontinuous changes in velocity.*—In concluding this section it is desirable to review the possibilities of discontinuous changes of velocity in the light of our discussion. As we have seen, so far there is no place for true discontinuities. As Hulme pointed out, observational errors affecting a smooth curve, and a previous impression that the correct way to represent such a curve was by a series of straight lines, could produce Pettit's results. The question is, to some extent, more a matter of psychology than solar physics. For what it is worth, the opinion is given that some of the observed curves when drawn on suitable scales do strike the eye as resembling successive segments of straight lines. Even some of the computed curves give the same impression. For example, the upper curve of Fig. I.8 and the curves fitted to Nos. 3 and 4 in Fig. I.1 give this impression. The lower curve in Fig. I.8 also shows a sharp change in gradient of about 30 per cent. due to the fact that d^2r/dT^2 is initially small, then rises rapidly to a maximum, and rapidly falls again. The bend, though slight, is quite a good approximation to a sharp change of velocity. There is, of course, no question of real changes of velocity by small multiples of some standard as Pettit supposed, and, although this feature might be worked into our picture, it would require special hypotheses to do this.

On the other hand, the present discussion does not rule out the possibility of real discontinuities of velocity. Consider, for example, Fig. I.2. If a knot or streamer end were originally at 1·0 it would follow the heavy dotted curve. If, in this case, at the same moment, particles were projected from the origin along the full curve, then at $T = 0{\cdot}620$ the latter would burst out ahead of the former, and, since the observer would measure the leading end of a streamer, he might well regard his observations as showing a sudden acceleration of the same particles rather than their replacement by new, faster particles. This then, is the importance of the "overtaking" solution of the dispersal problem. It does leave open the way for the occurrence of true discontinuities of velocity.

Section II.—The Motion of Ions above the Solar Surface

1. When the cinematograph films of prominences made at the McMath-Hulbert Observatory and at the Pic du Midi were first shown in Britain there at once arose marked differences of opinion as to their interpretation. On the one hand it was contended that the appearance of the streamers was most consistent with the hypothesis of an advance through invisible material of a visible condition of excitation. On the other hand it was suggested that the observed motions were true movements of incandescent material. The "three-dimensional" observations of McMath * seem to suggest that the latter hypothesis is true.

We have considered in the previous section the electrostatic forces which must be associated with the movement of ions in a magnetic field, and have concluded that we must assume that there is a considerable cloud of invisible material present, in addition to the visible prominence itself, so that, in a sense, the present hypothesis represents a combination of these two, apparently incompatible, points of view.

In introducing the previous section we contented ourselves with remarking that electromagnetic forces must certainly play some rôle in the behaviour of regions of high excitation on the solar surface. It is now necessary to examine in more detail the various types of force which may be operative, and to assess their magnitudes.

The forces which are possible seem to be those of radiation pressure, of hydrodynamics, of electrostatics, of gravitation and of electromagnetism. The force exerted by radiation pressure has received extensive discussion and the general conclusion seems that, apart possibly from selective radiation pressure in the case of ionized calcium, radiation pressure at the solar surface is unlikely to play any very striking rôle. Certainly it does not seem possible that it can be of the same order as that of gravitation.

To assess the influence of hydrodynamic forces it seems simplest to compare the observed order of magnitude of velocities in prominence material with the velocity of sound in the medium. The observed velocities are of the order of $50\,\text{km./sec.} = 5 \times 10^6\,\text{cm./sec.}$ If this were also the velocity of sound in the medium then, even with the largest possible ratio of specific heats, we should have to have

$$P/\rho = 1{\cdot}5 \times 10^{13}.$$

Even taking P as high as 100 dynes/cm.^{2} we obtain a very small value for the density and, on the present view of solar conditions it seems probable that this is far too low. Tentatively therefore we must conclude that the observed velocities of prominence knots are far in excess of the velocity of sound in the material, and, rightly or wrongly, we have assumed that both the hydrodynamic forces and the force of radiation pressure can safely be neglected in our treatment.

2. *Electrostatic forces.*—We have so far been concerned only with local electrostatic forces in the prominences themselves. General electrostatic forces occurring within the interior of stars have received close consideration by many authors. Pannekoek † showed that, as a result of the tendency of the lighter

* McMath, Sawyer and Mohler, *Publ. Univ. Michigan*, **8**, 123, 1941.

† *B.A.N.*, No. 19, 1922. See also, *Internal Constitution of the Stars*, p. 272.

electrons to diffuse towards the surface against gravity, and to become separated from the heavier ions, there would be called into existence a polarization field tending to resist the separation. The same topic has been discussed by Milne * and by Rosseland † and the conclusions is that, within the stars there is no appreciable separation of the positive and negative constituents.

The electrostatic field $d\psi/dr$ is proportional to the gravitational field $d\phi/dr$ at each point and is given by

$$\frac{d\psi}{dr} = \alpha \frac{m}{e} \frac{d\phi}{dr}, \qquad \text{II.1}$$

where m is the mass of a proton, e the electronic charge, and α is the mean molecular weight of the ions and their associated electrons. An ion of charge Ze and mass Am will experience an upthrust due to the electrostatic force. The ratio of electrostatic upthrust to gravitational force on such an ion is then

$$\frac{Ze\, d\psi/dr}{Am\, d\phi/dr} = \alpha \,.\, Z/A. \qquad \text{II.1}(a)$$

In the interior of a star where hydrogen is abundant and dissociation complete α will have the value $\frac{1}{2}$, so that half the weight of the hydrogen ions will be supported by the electrostatic upthrust. As the surface is approached and the proportion of hydrogen ionized falls, the average molecular weight of the *ions* and their electrons will increase. Consequently the electrostatic upthrust on ions for which Z/A is larger than the average will increase. Physically what is happening is that the elements concerned in the potential separation of ions and electrons become heavier: the electrostatic field needed to keep the average ion thoroughly mixed with the electrons becomes greater: hence any of the lighter ions which may be present will experience a stronger upward force. If this tendency is continued to temperatures which are so low that the majority of the ions are metallic, then the coefficient α will approach a value corresponding to about half the atomic weight of the most abundant metal ions, i. e. in the Sun α may have a maximum value of about 12. This simple argument will not be strictly correct, since a result will be that the upthrust on the hydrogen and other light ions will exceed gravity, so that these ions will crowd towards the surface and will tend to reduce the average molecular weight. This type of phenomenon has been discussed by Rosseland ‡ mainly in connection with stellar interiors. In fact the present discussion of conditions near a stellar surface corresponds to his discussion of a star containing only a small proportion of hydrogen. We may therefore expect that, near a stellar surface, ions for which Z/A is larger than the average will have an abnormally great abundance. It should be noted that this effect may have some importance in discussions of the abnormally high abundance of hydrogen and helium in the chromosphere.

If we were to consider only the Pannekoek-Rosseland field, stars would have no resultant surface charge. Once the star surface had been reached, i. e. as soon as a level was reached at which good mixing of ions and electrons ceased, then the excess positive charge on the main body of the star would be balanced by a layer of electrons, simply because the whole effect is one of polarization of dissociated

* *Proc. Camb. phil. Soc.*, **22**, 493, 1924. † *M.N.*, **84**, 720, 1924 ; *M.N.*, **85**, 541, 1925.
‡ *Loc. cit.*

material. It is arguable that these contentions will be invalidated by the existence of convection layers near the surface, but this objection does not seem to be a valid one. Even though the ion drift is masked by the far more obvious phenomena of of convection, the field must persist in order to maintain good mixing throughout the star.

A further effect which tends to produce a positive charge on the surface of stars has been discussed by Milne * who considered the greater tendency of electrons to escape from stars as compared with positive ions. In the case of the Sun the limits of positive potential at the surface were 1900 and 30 volts, the former being sufficient to support hydrogen ions against gravity, the latter providing a support of less than 1 per cent. The important consequence of this discussion is that the surface electrons needed to balance the Pannekoek-Rosseland field will not remain on the surface, but will be spread out to great distances from the Sun. The result will be that as far as the extent of the Pannekoek-Rosseland field is concerned the surface of the star must be taken at the top of this electron cloud. Tentatively we shall identify these electrons with those of the corona. From a great distance the Sun will appear to have only the total surface charge as calculated by Milne. Near the visible surface there will be a resultant positive field whose minimum possible value will be sufficient to support about 1 per cent. of the weight of a hydrogen ion, while the maximum possible value will be that corresponding to $\alpha = 12$, providing an upward force on a hydrogen ion of 12 times that of gravity. It has been observed by Thackeray † and by Brück and Moss ‡ that, in prominences, hydrogen and helium are well mixed. If we attribute the force which supports prominences to the electrostatic field above the solar surface, then we can make some estimate of the value of α in equation II.1 (*a*) which is not otherwise obtainable by simple considerations.

For complete support of hydrogen ions α must have the value 1·0 : for complete support of single ionized helium the value must be 4·0. Let us, for the sake of argument, consider a value intermediate between these, say 3·0, which will have the effect of supporting almost completely the helium and ions of ejecting hydrogen ions from the Sun. The latter will tend to recombine with available electrons and will be visible as clouds of neutral hydrogen falling back towards the solar surface.

The choice of $\alpha = 3{\cdot}0$ is arbitrary but it is possible to advance other considerations which suggest that this is approximately correct. In regions of the solar surface where hydrogen ions are especially abundant, e. g. in the disturbed areas round sunspots, clouds of ions will accumulate until the field near the solar surface is neutralised. In Section I we estimated the ion density of the prominence backgrounds as $10^{-11} - 10^{-12}$ per c.c. We can readily calculate the diameter of a spherical cloud of ions above the solar surface which will just neutralise the excess over gravity of the electrostatic support provided by the surface field. For $\alpha = 3$ we find a diameter of 2 million km. for a space density of 10^{-12} and 200,000 km. for a space density of 10^{-11}. For smaller values of α the dimensions are reduced proportionately to $(\alpha - 1)$. A cloud of this density and dimensions will have a fairly permanent existence. As long as ions are supplied by the disturbed region of the solar surface they will be admitted to the cloud until the critical size has been

* *Trans. Camb. phil. Soc.*, **22**, 83, 1923.
† *Observatory*, **64**, 169, 1941.
‡ *M.N.*, **103**, 258, 1943 ; **105**, 17, 1945 ; **105**, 282, 1945.

reached, and this size will be maintained as long as the rate of production of ions from below equals the rate of diffusion of ions off the top and sides of the cloud.

A second fact of significance is that, below the main cloud of coronal electrons electrostatic upthrust will be capable of supporting any ion for which Z/A is sufficiently large. We have chosen $\alpha = 3$ so as to give support for hydrogen and helium. We can also calculate the ratio of electrostatic upthrust to gravitational force for the ions of the corona identified by Edlén. He found the following ions :

Fe X, XI, XIII, XIV, XV:	*Ni* XII, XIII, XV, XVI:
Ca XII, XIII, XV:	*A* X, XIV.

Using the chosen value of α the ratio of electrostatic upthrust to gravity for these has the following system of values:

Fe: 1·05; 1·13; 1·35; 1·5; 1·65	*Ca*: 1·65; 1·80; 2·10
Ni: 1·20; 1·28; 1·50; 1·65	*A*: 1·50; 2·13

At high levels, such that a considerable proportion of the coronal electrons lie below, these ratios will be reduced, but it seems of some significance that the assumption of an electrostatic field of the correct order to support the prominences is also correct for the order of size of prominences and suggests an association between prominences and spots and, in addition, suggests a mechanism for the support of the coronal ions.

It must be noted that it is not suggested that the ions either of the prominences or of the corona are produced *in situ*. If the present suggestion is correct, there still remains the problem of accounting for the original production of the coronal ions. This and many other problems remain for full consideration, but it is perhaps worthwhile mentioning some of the lines of explanation which this suggestion may open up. If the coronal ions are produced near the solar surface then the possibility of their reaching great heights depends on their avoidance of obstacles. A prominence relatively much more abundant in electrons would constitute such an obstacle, for the coronal ions would tend to pick up electrons at the expense of the prominence ions. It should follow that there should be gaps in the coronal structure above prominences and this feature has been noted by Lyot in his latest series of observations. An extension of the same argument would also suggest a connection between the frequency of occurrence of prominences, i. e. the sunspot cycle, and the form of the corona.

For the present purpose, in view of the great uncertainty as to the magnitude of α we shall simply assume that there is some force, possibly electrostatic, which acts so as to neutralise approximately the gravitational force on the prominence ions and, in later discussion we shall therefore, as a first approximation, neglect the effect of gravity in considering the paths followed by moving ions above the solar surface.

3. *Electromagnetic Forces.*—It now remains to compare the electromagnetic forces with the force of gravity. For a proton moving at a speed of 50 km./sec. across the lines of force of a field of 100 gauss, the transverse force is $7{\cdot}95 \times 10^{-12}$ dynes, as compared with a gravitational force of $4{\cdot}55 \times 10^{-20}$ dynes. Fields of 1000 gauss or more have been observed in sunspots, but, even at considerable distances from the spot itself, so large, for example, that the field has fallen to 1 gauss, the electromagnetic force will still be two million times as great as the gravitational.

We shall therefore consider the electromagnetic effects and, as a first approximation will consider the case in which this is the only force, with the result that the linear speed of the moving ion will be constant. We have already ascribed the accelerations of knots in the last section to the background electric field: for the moment these two effects will be considered separately, being combined later.

The electromagnetic forces will be regarded as producing the spatial curvature of the observed thin streams, but before proceeding to this topic it is necessary to consider why these forces, rather than, for example, those of gravitation should have to be invoked. Although a considerable number of the tracks bear a strong resemblance to parabolic curves, such as might be described under gravity alone, there are many examples (e. g. those of Fig. II.1 (Plate 7)) where this explanation would be insufficient. Any trajectory described under gravity alone is a parabola with axis radial to the Sun and any projection of such a trajectory is also a parabola. It follows then that gravity alone cannot account for any trajectory which intersects any normal to the Sun more than once. Fig. II.1 shows examples of such streams, and it follows that, certainly in this case, and possibly quite generally, other forces besides gravity must be at work. This is true also of course in the case of downward streams which have an acceleration greater than that of solar gravity, such as were noted in I.9 above.

For the moment we shall leave the exact specification of the magnetic field rather open. Two possibilities seem to present themselves. One is the case of a dipole with axis in the solar surface, serving perhaps as a model for the magnetic field of a bi-polar spot. The second possibility is a magnetic dipole with vertical axis which may serve as a model for a uni-polar spot. In view of a possible future discussion of other solar phenomena it is not desired to tie down this second possibility completely to the case of a uni-polar spot. It may be that magnetic fields with radial axis can arise in the solar surface by other mechanisms.

4. Let the dipole moment be denoted by M and take Cartesian axes with the z-axis along the axis of the dipole. The field at (x, y, z) is then

$$H=(3Mzx/r^5,\ 3Myz/r^5,\ 3Mz^2/r^5-M/r^3), \qquad \text{II.2}$$

where $r^2=x^2+y^2+z^2$. The lines of force are, of course, plane curves lying in planes through the z-axis.

The general equations of motion * are

$$\left.\begin{aligned} \ddot{x}&=\mu r^{-5}\{3z(\dot{y}z-y\dot{z})-r^2\dot{y}\},\\ \ddot{y}&=\mu r^{-5}\{3z(\dot{z}x-z\dot{x})+r^2\dot{x}\},\\ \ddot{z}&=\mu r^{-5}\{3z(\dot{x}y-x\dot{y})\}, \end{aligned}\right\} \qquad \text{II.3}$$

where

$$\mu=\frac{eMZ}{mA},$$

e being the electronic charge, m the mass of a proton, and Z and A are the degree of ionization and the atomic mass of the moving ion.

5. *Projection of ions in the median plane of a dipole.*—We shall consider first the motions of ions in the plane $z=0$. These are possible since there is then no

* See for example Störmer, *Z. Astrophys.*, **1**, 237, 1930.

acceleration in the z direction. H reduces to $-Mr^{-3}$ parallel to the z-axis and the curvature of the path ρ is then given by

$$\frac{mAv^2}{\rho} = \frac{ZevM}{r^3}. \qquad \text{II.4}$$

This gives

$$\rho = r^3/c^2, \qquad \text{II.5}$$

where

$$c^2 = \frac{ZeM}{mAv}. \qquad \text{II.6}$$

The most convenient form of the equation is the pedal form, specified (Fig. II.2) by the radius vector, r, and the perpendicular on the tangent, p. In this form

$$\rho = r\,dr/dp, \qquad \text{II.7}$$

so that the required trajectories are given by

$$p = p_0 + c^2/r_0 - c^2/r, \qquad \text{II.8}$$

r_0 and p_0 being the initial values of r and p.

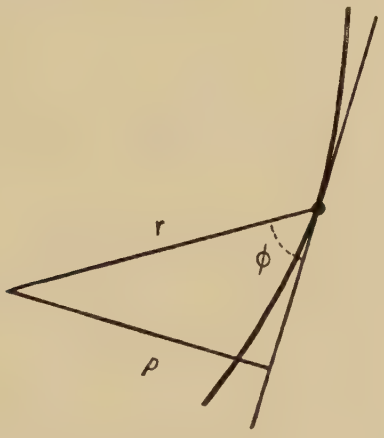

Fig. II.2.

In II.8 we must, clearly, have $|p| \leqslant r$. When $p = r$ the particle is moving perpendicular to the radius vector, while, when $p = 0$, the motion is radial. The relation is best discussed by plotting p against r giving a series of hyperbolas with horizontal and vertical asymptotes. The requirements $|p| \leqslant r$ means that real motions correspond to those parts of the curve which lie between the lines $p = \pm r$ (see Fig. II.3). Three cases can be distinguished as follows:

A there are no intersections with $p = r$. In this case there is a minimum distance given by $p = -r$, and the curve extends from this point to infinity. It is of course symmetrical about the radius from the origin through the point of minimum distance.

B there are two coincident intersections with $p = r$. Circular motion is possible, but is unstable, since, if a slight outward displacement occurs, the radius of curvature increases and the particle spirals outwards. If the displacement is inward the particle moves in to a certain minimum distance.

C there are two separate intersections with $p=r$. In this case, motion is possible between a distance corresponding to the larger value of r and infinity, or between the smaller value and the minimum distance given by $p=-r$. In this latter case the spatial curve is either a closed loop, or is so nearly re-entrant that it has the appearance of a slowly progressing loop.

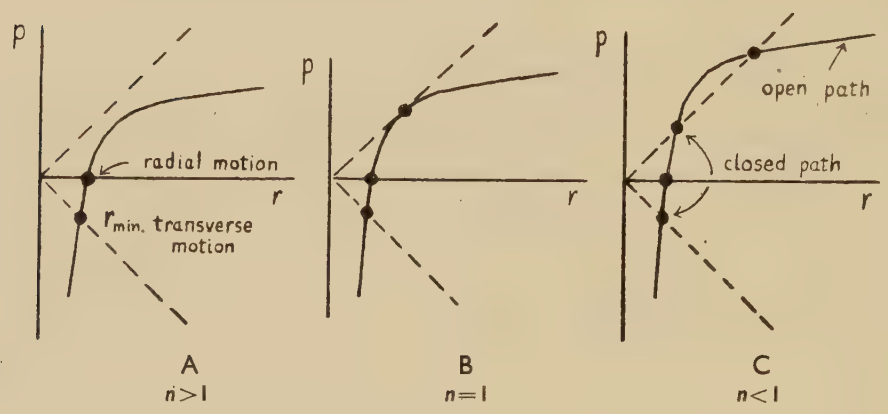

FIG. II.3.

Examples of these cases are plotted in Figs. II.4 A, B and C. For simplictiy we write

$$p_0+c^2/r_0=\chi \qquad \text{II.9}$$

and then express all the parameters in terms of χ by means of

$$r'=r/\chi; \qquad p'=p/\chi; \qquad c=n\chi/2, \qquad \text{II.10}$$

so that II.8 becomes

$$p'=1-n^2/4r'. \qquad \text{II.11}$$

The various points on these curves singled out for special discussion can be readily identified. Motion is radial when $p'=0$, i.e. when $r'=n^2/4$. The minimum distance (given by $p'=-r'$) is $\frac{1}{2}(\sqrt{1+n^2}-1)$. The motion is transverse at this distance and also at the radii for which $p'=r'$, i.e. when $r'=\frac{1}{2}(1\pm\sqrt{1-n^2})$.

Thus the three cases discussed correspond to the following conditions:

$$\left.\begin{array}{ll} \text{A } n>1 & r'\geqslant\tfrac{1}{2}(\sqrt{1+n^2}-1) \\ \text{B } n=1 & \\ \text{C } n<1 & \tfrac{1}{2}(\sqrt{1+n^2}-1)\leqslant r'\leqslant\tfrac{1}{2}(1-\sqrt{1-n^2}) \\ & \text{or } \tfrac{1}{2}(1+\sqrt{1-n^2})\leqslant r'. \end{array}\right\} \qquad \text{II.12}$$

We shall first consider case A and compare the calculated curves with the observed shapes of prominence streamers.

To plot the curves, graphs of ϕ where $\sin\phi=p/r$ were first drawn for various values of n. The actual curves were then drawn on polar coordinate paper, starting from the value of r for which the motion was radial. Thereafter the curve was plotted as a series of short segments inclined to the radius vector at the calculated values of ϕ.

6. *Analysis of Prominences.*—The resulting curves are very similar in shape to the observed prominence streamers, but a complication arises in fitting the calculated curves to them. We have to determine both a scale factor and the value of n. Now it is found that, on different scales the various curves given by different values of n are superposable upon each other through a considerable part of their length. Further, each curve is, when its scale is altered, similarly superposable on itself. In neither case is the superposition exact, but it is sufficiently

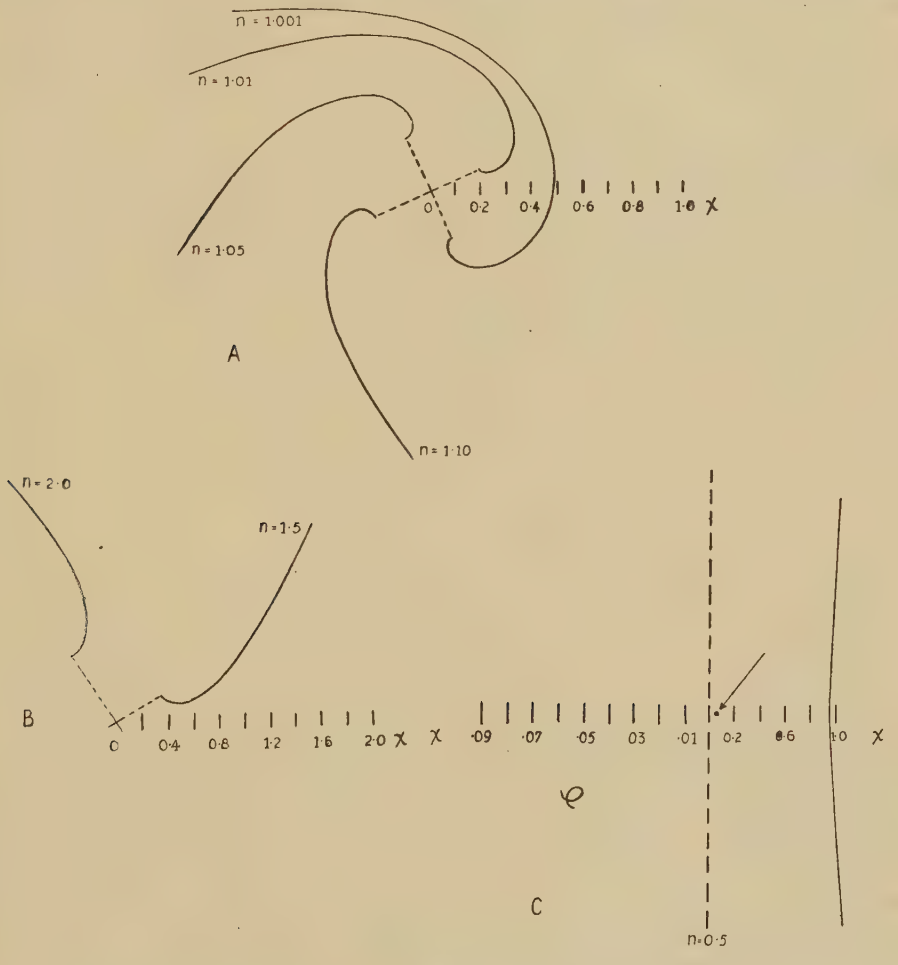

FIG. II.4.

close to make the determination of the parameters uncertain when the observed streamer covers only a small part of the curve to which a fit is sought. This similarity is to be expected: all the curves have the property that the radius of curvature is inversely proportional to the cube of the distance from a fixed point.

The method adopted was, therefore, to draw each curve on transparent paper, and to project it by means of an enlarger on to a print of the prominence under consideration. For different degrees of enlargement the positions of best fit defined a locus on the print along which the position of the hypothetical dipole moved. It was found that, in general for values of n considerably above 1·0 this

locus never intersected the solar surface, and, in order to bring the position of the hypothetical dipole down to the solar surface values of n close to 1·0 had to be used. For example, if we were considering streamer B in Fig. II.5 A (Plate 8) we should, by fitting the curves for 1·1, 1·05, 1·01, 1·001 at different enlargements obtain a series of curves representing possible positions of the dipole. Some of these are well above the solar surface, while others intersect it. For $n = 1{\cdot}001$ for streamer A (Fig. II.5 A) we obtain the curve marked A 1·001. The process is repeated for the other streamers and a whole series of curves obtained. It is found possible to select particular values of n for the various streamers such that all these curves pass very nearly through the same point on the solar surface. This point is adopted for the position of the dipole, and then, using for each streamer the curve appropriate to the selected value of n, that degree of enlargement is chosen to give the best fit on the assumption that the pole of the curve is at the adopted position of the dipole. In addition, curves to fit other, less well-defined, streamers may then be drawn using the same adopted dipole position. For example, in Fig. II.6 (Plate 9) the dipole was located by means of the streamers A, B, C, D, E and F and then curves to fit G, H, J, K, L and M were added.

If the scale of the print is known * it is then possible to find χ for each curve in kilometres, and using equation II.10 to derive c for each curve. If in addition the velocity of material in the streamer is known then we can use II.6 to obtain ZM/A. It is readily found that if the speed is v' km./sec., and if the magnetic moment measured in electromagnetic units is M', then

$$ZM'/Av' = 1{\cdot}16\,c^2. \qquad \text{II.13}$$

The films were measured with the aid of a microfilm reader, which projected the original positive of the Lyot film on a convenient scale. It was found that estimation of the velocities with any accuracy was exceedingly difficult. This is a little surprising in view of the consistency obtained by the McMath-Hulbert observers, but there are important points of difference. A minor difficulty is that Lyot exposed only two frames per minute, which is considerably slower than the rates used by the American workers. More significant is the fact that the McMath-Hulbert results for the motions of knots refer to specially selected well-defined knots of long life. In our case we need information about the velocity of material in all the well-defined streamers on a given still photograph. This is a far more severe requirement. In particular, if a streamer is well-defined then it very often has no knots in it which might be used for measurement. Knot measurement is most easy in streamers which are broken up, and which are beginning to be slightly difficult to recognise as continuous curves. In addition, knots in streamers very often change shape considerably during their movement, so that it becomes difficult to fix a satisfactory reference point in a moving knot. In other cases knots simply disappear after being followed for a frame or two, while very often the best defined knots are not in motion at all. It will, in passing, be noticed that these features are not inconsistent with the hypothesis under discussion.

These difficulties unfortunately reduce the further analysis of these prominences to the level of an order of magnitude discussion, but the results are included

* In the Lyot film from which Figs. II. 1, 5 and 6 are taken, the height of the frame is approximately 400,000 km.

for what they are worth. More than usually uncertain figures are given in brackets:

TABLE II.1

Prominence (1) : *Eastern limb* : 1937 *June* 10 *and* 11. *Fig.* II.5

Streamer	n	$1{\cdot}16c^2\times10^{-20}$	v'	$ZM'/A\times10^{-20}$	r'(1 = 100,00 km.)
A	1·001	4·85	(351)	(1700)	2·66
B	1·01	2·88	(212)	(610)	1·60
C	1·01	4·13	(306)	(1260)	2·30
D	1·01	0·82	271	222	1·24
E	1·05	2·31	265	611	1·72
F	1·01	2·75	(296)	(813)	1·97

For ions of fairly low ionization potential the lowest value of Z/A is 1·0 for hydrogen, so that, if we were to say that streamer A consisted of hydrogen ions then M' would be of the order of 2×10^{23} e.m.u. This is the minimum value of M' deducible from Table II.1 taking it at its face value. The figure is perhaps a trifle low: the curves of $|H|$ in gauss as seen from above the solar surface for $M'=10^{24}$ are sketched in Fig. II.7. Perhaps the most that can be said is that this might be mistaken for a sunspot magnetic field.

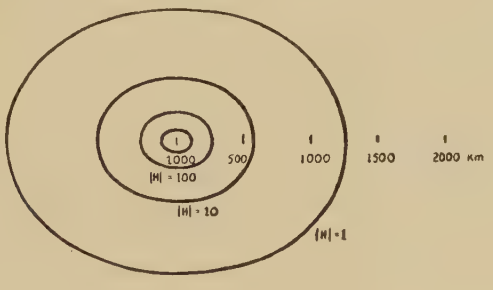

FIG. II.7.

Any attempt to identify the different ions in the streamers A–F of Table II.1 would be pushing the data a good deal too far. We note, however, that in our hypothesis the various ions should follow different tracks, and that we could fit the ratios of ZM'/A, within the very considerable limits allowed by the uncertainty of the velocities, by the following identifications, assuming streamer A to consist of hydrogen ions:

A: *H* II B: *He* II C: *He* III D: *O* III E: *He* II F: *He* III

None of these identifications is to be taken seriously, but the fact that more accurate and extensive observations might enable a serious attempt at identification to be made, immediately raises a problem. Lyot's films * are taken in $H\alpha$ light defined by filters which transmitted a band some 300 A. wide. Should we expect to see streams of ions in light of this range of wave-length: in particular, should we expect to see *H* II and *He* III at all?

There seem to be grounds for believing that such streams would be visible. In the present picture the ionic background is kept up by electrostatic repulsion and all that has been demanded is that the electron defect should be of the order of 10^{-12} per c.c. It is hardly to be supposed that there will be a complete separation

* *M.N.*, **99**, 580, 1939.

of ions and electrons: rather it may be expected that the electron defect will be handed round in turn, so that any particular hydrogen atom will spend part of its time falling into the Sun as a neutral atom, and part of its time being thrown upwards as an ion. If there is a certain amount of neutral hydrogen mixed with the ionic cloud then this will be excited by collisions as the ions pass through marking the track with Balmer emission. A similar argument may be advanced for *He* III the tracks of which may be marked by *He* I and *He* II spectra.

In addition there is a special mechanism which may apply to the case of *H* I and *He* II which is peculiar to this case.

The frequencies for the line series of these two elements are of course given by

$$\text{H:} \quad \nu = 109677{\cdot}759\left(\frac{1}{n_1^2} - \frac{1}{n_2^2}\right),$$

$$\textit{He}\,\text{II:} \quad \nu = 4 \times 109722{\cdot}403\left(\frac{1}{n_1^2} - \frac{1}{n_2^2}\right).$$

A Doppler shift corresponding to a velocity of 122 km./sec. is sufficient to superpose the two series. A stream of *He* II ions will thus be capable of exciting the complete neutral hydrogen spectrum as soon as its relative velocity exceeds 122 km./sec. For velocities in excess of this figure hydrogen atoms some distance off the track will be excited when the resolved part of the velocity of approach reaches the critical value. We must therefore expect streams of *He* II ions to produce tracks showing a relatively strong Balmer spectrum.

Finally there is the question posed by the relatively high ionization potentials of *He* III and *O* III. It must be remembered that we have nowhere required that these ions shall be produced *in situ* by thermal ionization, any more, for example, than it is expected that the coronal ions are actually produced at high levels by thermal ionization. Any attempt to ascribe particular streams to particular ions should be made with great reserve, but the suggestion of the presence of an ion of a high order is not an objection in itself, since in fact the higher the charge the easier it will be for the ion to remain above the solar surface.

The results for Prominence (2) corresponding to those of Table II.1 are given below. M' will clearly be of the same order as before. Any attempt to identify the ions in the streamers is even less justifiable than in the previous case.

TABLE II.2

Prominence (2): *Eastern limb*: 1937 *June* 12: $8^h\ 30^m$–$13^h\ 10^m$. *Fig.* II.6

NOTE:—This is apparently not to be identified with Prominence (1)

Streamer	n	$1{\cdot}16c^2 \times 10^{-20}$	v'	$ZM'/A' \times 10^{-20}$
A	1·01	4·45	(69)	(306)
B	1·05	3·17	(81)	(256)
C	1·10	2·50	(40)	(100)
D	1·001	7·97	107	852
E	1·10	3·75	95	355
F	1·05	3·32	138	458
K	1·01	1·95	...	..
H	1·001	9·08	...	. .

It has therefore proved possible, on the assumption that the streamers are tracks of ions moving under electromagnetic forces alone to determine the position and order of magnitude of the dipole responsible.

To adopt the position of devil's advocate, the most suspicious feature of this result is the fact that all the parameters n are so very slightly above 1·0. As n approaches 1·0 the total curvature of the curve increases (see Fig. II.4) and, in this sense, the range of values just above $n=1{\cdot}0$ is that which offers most scope in the introduction of almost as much curvature into the calculated curves as we please. There is the uncomfortable feeling that, in reality, we might, by exploiting this region, be able to fit almost any system of curves whose curvatures were in the correct sense. On the other hand, there is the safeguard that we must fit all the streamers of a complex prominence to the same dipole position, and that this dipole position must lie approximately in the solar surface. Clearly a deduction based on only two or three streamers would be of little very value. The fact that all the streamers can be fitted into the same picture entitles us to view the result with a little more confidence.

There is the further difficulty presented by the question "what is a streamer?". Curve fitting has to be done on still prints, but there is no doubt that in watching the running of the film the eye performs a synthesis which reveals far more than a close study of still prints can elicit. The first impression is that streamers follow definite tracks, but a closer study suggests that this is not quite true. The material wavers and each part follows one of a series of tracks covering a small angle of projection. In fitting curves on prints we may deceive ourselves by involuntarily lining up, as members of one streamer, knots which are all following slightly different paths. Again there is the question of the point of origin of a streamer. Is it to be counted as starting from the thin tip of the cone-shaped clouds which form a striking feature of prominences, or are we to count only the thin streaks of matter definitely in apparent motion? If we see a series of knots which seem to be stationary and which lie along a line (such a case occurs on the right of Fig. II.6, streamer D), are we to count this line as part of the streamer or not?

In view of these uncertainties, perhaps the most that can be said for the present hypothesis is that it is self-consistent. Assuming that it is correct we must explain why the parameter n should always be so close to 1·0. We defer this discussion until after we have considered the trajectories for which n is less than 1·0.

Before proceeding to this it is necessary to add a remark on the subject of projection. We have so far not allowed ourselves to introduce the additional possibility that the plane of the sky may not be the plane of motion of our hypothetical ions. The two prominences which have been analysed have been considered on the assumption that the prominences are seen "full-face" and that the streamers are not moving in the line of sight at all. There is nothing which can be done at the moment to improve this situation except to note the suggestive appearance of the projections of our computed curves into planes at 45° to the line of sight, having intersections with the sky plane inclined at various angles to the general run of the curves (Fig. II.8).

7. *Tornado Prominences.*—In the case $n<1{\cdot}0$ greatest interest attaches to the possibility of the motion of ions in very small, effectively closed, orbits. For $n=\frac{1}{2}$ the diameter of such an orbit is $0{\cdot}08\chi$ while for $n=0{\cdot}1$ the diameter is only $0{\cdot}0000125\chi$. It is natural to enquire whether there are any observed solar phenomena with which these small orbits could be identified. The proposed identification is with the tornado type prominences of Pettit.* In this case it

* *Ap. J.*, **98**, 6, 1943.

must be assumed that the magnetic dipole has a vertical axis. The closed orbital motion will then be in the plane of the solar surface, or slightly above it, so that a short spinning column of ions will be formed which remains fixed or moves only very slowly over the solar surface. In Fig. II.9 (Plate 10) is reproduced a series of frames from a sequence discussed by McMath and Pettit.* The authors describe this type of prominence as extremely small and as being very slow moving. The figure of 10 km./sec. is quoted for the velocity of the tornado type prominence illustrated, which was observed on 1936 August 10. Further details of the motion to be expected in a prominence of this type are considered in Section II.8.

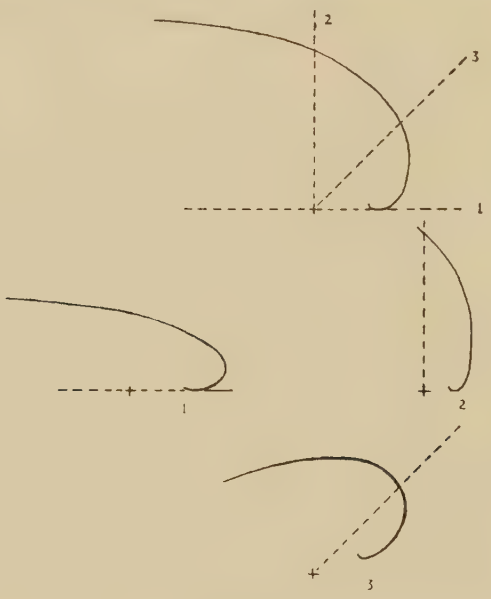

FIG. II.8.

It seems likely that there will be motion along the axis of the prominence as well as in spirals round the axis. When a certain height has been attained the spreading of the magnetic lines of force will begin to permit the spirals to open out and the closed orbital motion will give place to a dispersive one. This would be consistent with McMath and Pettit's description *: "A feature of this prominence which is typical of those already examined is the formation of a smoke-like column at the top of the vortex. This seemed always to be present, reaching a height of 90,000 km. above the chromosphere, fading and brightening now and again, finally becoming as brilliant as the vortex itself. It then inclined strongly, bent, and detached itself, and, in the last stage observed, floated as an isolated cloud set at an angle of 45° to the vertical, expanded to several times its original volume".

A more detailed discussion of the relations between these "closed" orbits and the tornado prominences is as follows:

Consider a number of ions of different degrees of ionization which are projected radially in the median plane of a dipole, all of them having the same initial velocity.

* *Ap. J.*, **85**, 279, 1937.
† *Loc. cit.*

Let us replace II.6 by the equation

$$c_Z^2 = \frac{ZeM}{mAv}. \qquad \text{II.14}$$

Then in II.9 $p_0 = 0$ and we may write

$$\chi_1 = c_1^2/r_0. \qquad \text{II.15}$$

If we express p and r in terms of χ_1 we find, in place of II.11,

$$p' = Z(1 - n_1^2/4r'), \qquad \text{II.16}$$

where n_1 is the parameter as defined in II.10 which applies to the loci of the singly ionized atoms. If we were to apply equations II.9, 10, 11 to the other ions we should get values of χ and n given by

$$\chi_Z = Z\chi_1; \qquad n_Z = n_1/\sqrt{Z}, \qquad \text{II.17}$$

so that, as Z increases we shall eventually arrive at a value of n_Z which is less than unity. For successive values of Z the hyperbolic $p - r$ curves (see Fig. II.3) are pushed up by a constant amount (and their shapes changed) until, eventually, intersections with the line $p = r$ occur.

If, as an example, we take $n_1 = 1{\cdot}1$, then, for various values of Z the possible ranges of r are given in the table below, being calculated from the readily derivable formulae:

$$r_{\min} = \frac{\sqrt{Z}}{2}(\sqrt{n^2+Z} - \sqrt{Z}): \qquad r_{\max}(n<1) = \frac{\sqrt{Z}}{2}(\sqrt{Z} - \sqrt{Z-n^2}). \qquad \text{II.18}$$

Z	$r_{\min}$	$r_{\max}$	$r_{\text{radial motion}}$
1	0·244	...	
2	0·267	0·372	0·303
3	0·277	0·346	
4	0·283	0·330	

Thus, in this case, all the once ionized atoms will get away to infinity, while the higher ions will be held in closed orbits close to their original position. It is easy to see that this type of condition holds generally.

If our interpretation of the tornado prominences is correct they will represent regions which can retain the higher order ions, while rejecting the lower ones. They will be regions where energy, extracted from the magnetic field, can be retained, and this feature may go some way towards explaining how this particular type of prominence can remain as a superficially static region of a degree of excitation far higher than its surroundings.

We can also apply the same argument in a tentative way to explain the deduction that, if the streamers in prominences such as those of Figs. II.5 and 6 do consist of ions moving in a magnetic field, then all the parameters n must have values only slightly exceeding 1·0. If we suppose that the ionic clouds are in turbulent motion then a large part of each prominence must consist of vortices of particles moving in spiral orbits. Those ions for which n is much greater than 1·0 will be thrown out at once.

If owing to a random disturbance or due to electrostatic forces in the prominence an ion for which n is less than 1·0 has its parameter pushed over the critical value, then, provided it is sufficiently near the edge of the prominence it will be

able to escape and become part of a streamer. This suggestion must be regarded with a good deal of caution, but, if the previous arguments are correct, an explanation roughly on these lines is the natural one to choose.

8. *Axial projection of ions.*—So far we have been concerned with particles projected in the median plane of the dipole. We now turn our attention to particles projected parallel to its axis.

We shall simplify equation II.3 by assuming that x and y are small in comparison with z, and we shall therefore neglect $\dot{x}$ and $\dot{y}$. This gives $\ddot{z}=0$ or $z=z_0+vt$, $\dot{z}=v$. The other two equations reduce to

$$\ddot{x}=-y\frac{3\mu v z}{r^5}: \qquad \ddot{y}=x\frac{3\mu v z}{r^5}, \tag{II.19}$$

while, if we replace r by z, these further reduce to

$$\ddot{x}=-y\frac{3\mu v}{z^4}: \qquad \ddot{y}=x\frac{3\mu v}{z^4}. \tag{II.20}$$

One way of treating these is to approximate still further and take

$$p^2=\frac{3\mu v}{z^4}$$

as a constant, in which case the solution for projection parallel to the dipole axis is

$$x=x_0\cos pt\cosh pt-y_0\sin pt\sinh pt,$$
$$y=y_0\cos pt\cosh pt+x_0\sin pt\sinh pt,$$

but, although this still preserves the general character of the solutions the approximation is rather a bad one. Apparently only numerical solutions of II.20 are possible. However, the work can be reduced, first by making the equations non-dimensional. If we take z as independent variable, and express x, y and z in terms of $\sqrt{3}\,.\,c$, where c is defined in II.6, then equations II.20 reduce to

$$\frac{d^2X}{dZ^2}=-\frac{Y}{Z^4}: \qquad \frac{d^2Y}{dZ^2}=\frac{X}{Z^4}. \tag{II.21}$$

If c is of the same order, namely $10^{10}-10^{11}$ as in Section II.6, then the unit in which these distances are measured is of the order of 100,000 to 1 million kilometres. Equations II.21 are also linear in X and Y so that any multiples of any solutions obtained will also satisfy the equations. We may therefore lay out a computing schedule in which the variable parameter is Z_0. We shall cover all the solutions if we take as initial conditions $X=X_0$ (an arbitrary quantity), $Y_0=0$ and, since projection is parallel to the dipole axis $X_0'=Y_0'=0$. The values of Z_0 which are of interest are, naturally, small compared with unity, since we wish to consider the fate of particles projected from points approximately in the the solar surface.

The solutions for $Z_0=0{\cdot}1$ and $0{\cdot}2$ are graphed in Figs. II.10 A and B. These represent the X- and Y-elevations of the curve, and so, in addition the curves corresponding to projection into the planes $X=Y$ and $X=-Y$ are given. One further point is that the curves for smaller values of Z_0 will be included in those already given, since, if a particle is projected from a very small value of Z_0 sufficiently close to the dipole axis so that it is still effectively travelling parallel to it when it reaches, say $Z=0{\cdot}1$, then it will follow one of the curves calculated for

FIG. II.1.—Prominence of 1937 June 11 (see also Sawyer and Brodie, *Publications of the University of Michigan*, **7**, No. 3, 79, 1938).

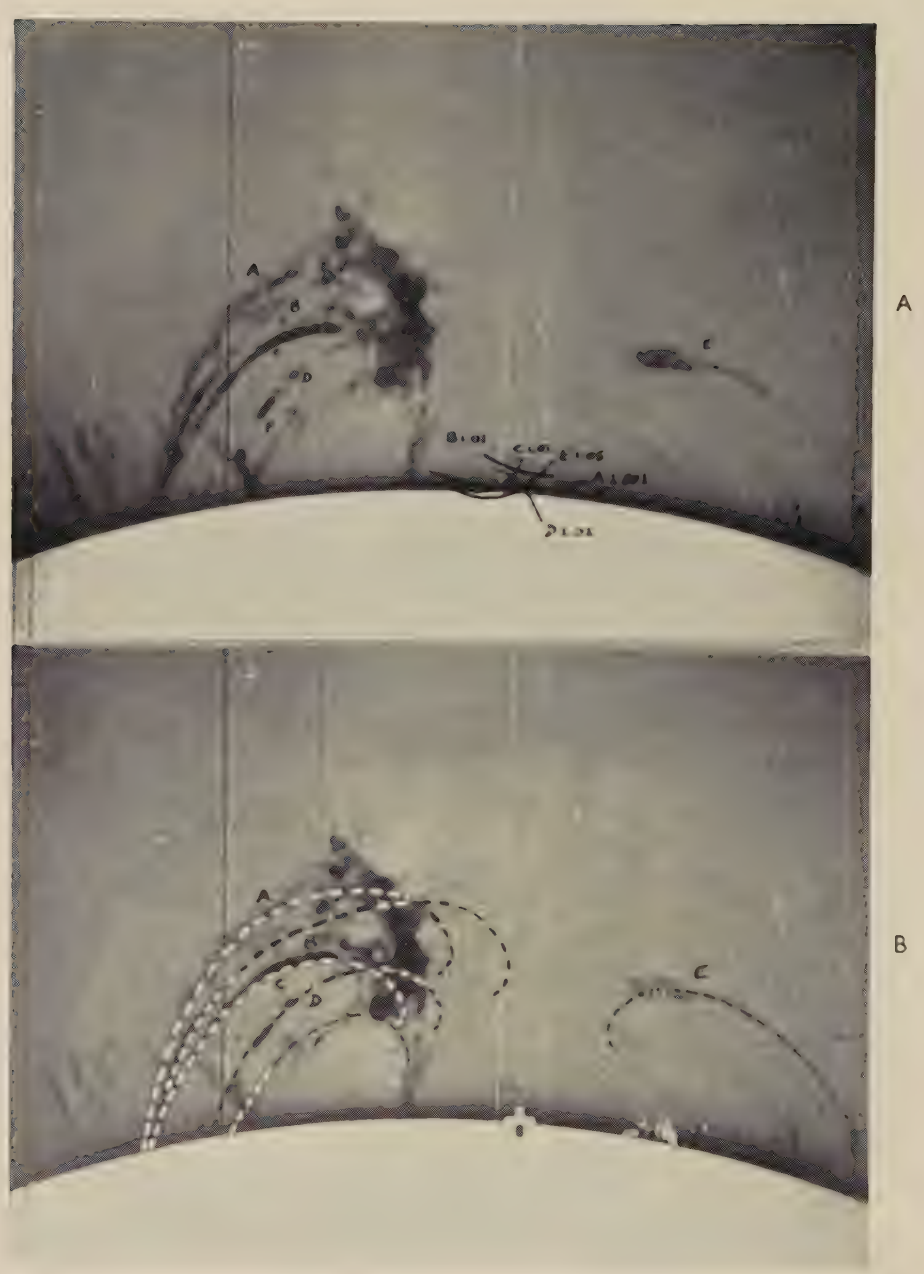

FIG. 11.5.—Height of frame ~ 400,000 km.

Fig. 11.6.—Height of frame ~400,000 km.

FIG. 11 9.—Active and tornado prominences at 20 minute intervals, 1936 August 10.

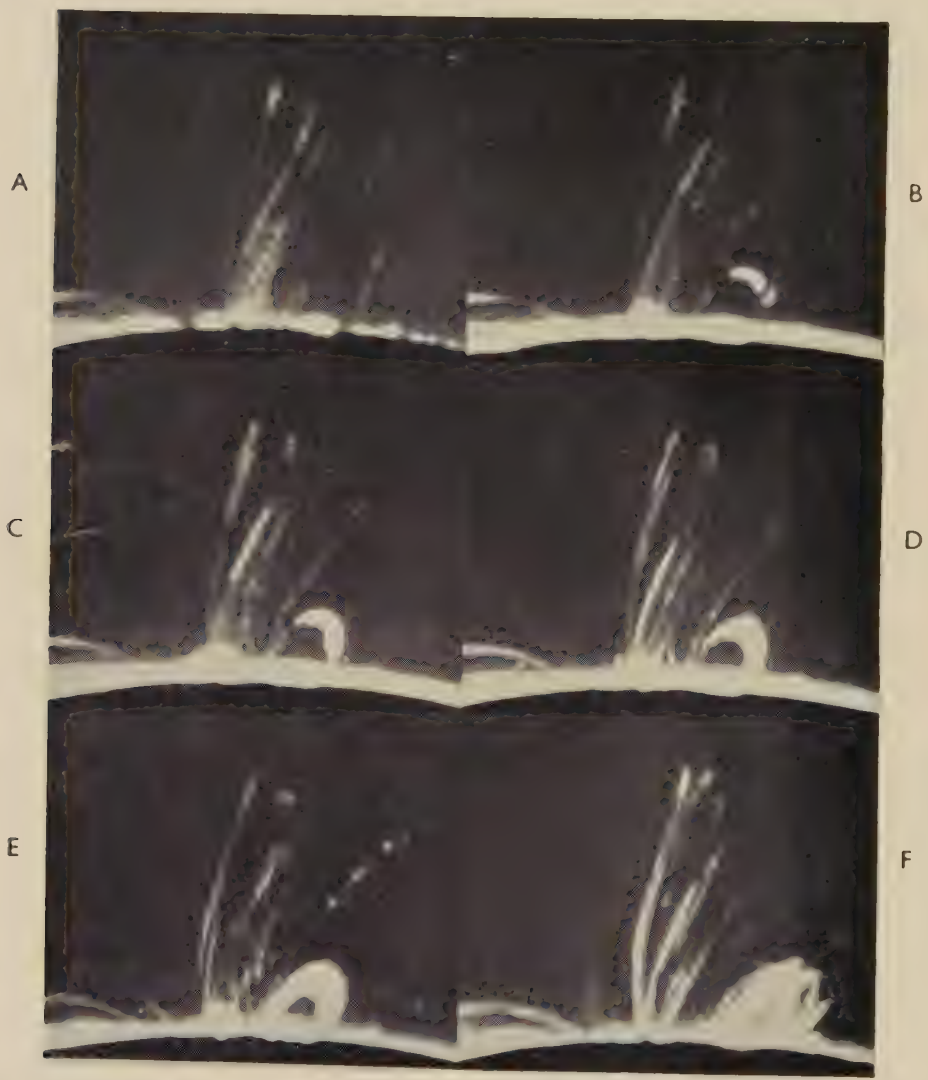

FIG. 11.13.—Formation of prominence loop, 1939 September 7. H_α Spectroheliograms.

A	$16^h\ 20^m{\cdot}16$ GCT	B	$16^h\ 23^m{\cdot}28$ GCT
C	$16^h\ 30^m{\cdot}66$ GCT	D	$16^h\ 32^m{\cdot}87$ GCT
E	$16^h\ 38^m{\cdot}43$ GCT	F	$17^h\ 45^m{\cdot}52$ GCT

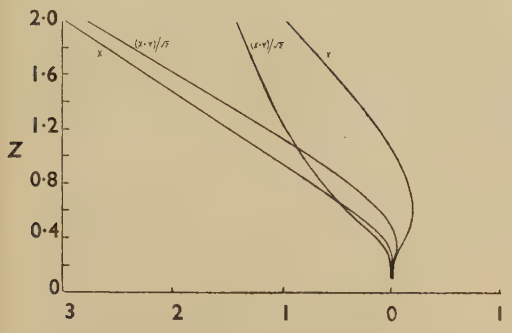

FIG. II.10A.—$Z_0=0{\cdot}1$.

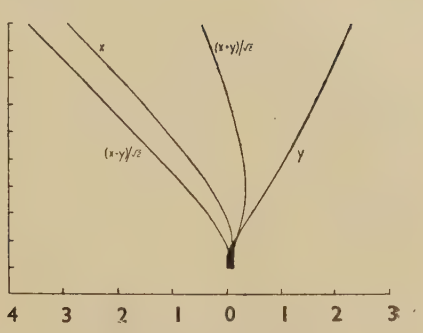

FIG. II.10B.—$Z_0=0{\cdot}2$.

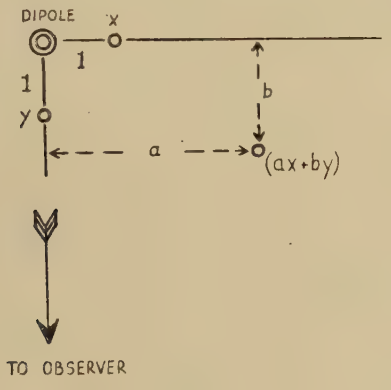

FIG. II.11

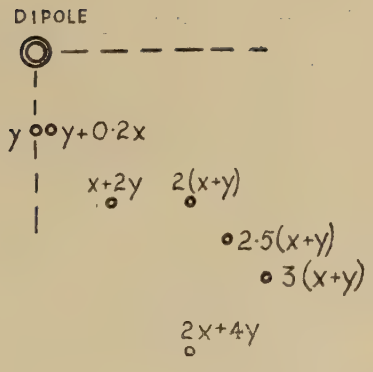

FIG. II.12A.

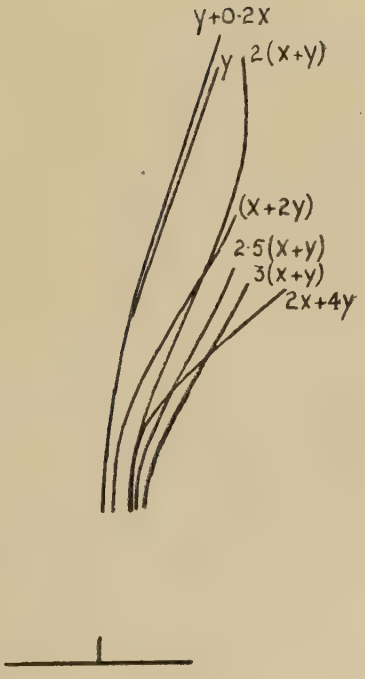

FIG. II.12B.

$Z_0 = 0{\cdot}1$. In order to explore the solutions of II.21, it is therefore sufficient to consider one reasonably small value of Z_0 as we have done.

In comparing these results with the observed prominence forms it must first be noted that they have an application to the case of the tornado prominences discussed in Section II.7 above. There it was shown that, in the median plane of the dipole, motion in small closed orbits was possible. These orbits lie close to the dipole axis, and, if we superpose on the whirling motion a motion of translation parallel to the dipole axis, then this whirling motion will be drawn out into a vertical column. The conditions for this latter motion will be practically the same as for the projections parallel to the dipole axis which we have just been considering. Fig. II.10 shows that as the whirling motion breaks up with the gain in height of the moving particle, the track will change to an inclined linear motion. We can refer once more to McMath's and Pettit's words already quoted: "It then inclined strongly, bent, and detached itself, and, in the last stage observed, floated as an isolated cloud set at an angle of 45° to the vertical, expanded to several times its original volume". It is noteworthy that if the region where the tracks are densest is shaded a remarkable similarity to the tornado prominences is found. If the height of the top in Fig. II.10 B is taken as 100,000 km. we find $c^2 \sim 2{\cdot}3 \times 10^{20}$ which should be compared with Table II.1.

However, in general we shall seek to identify this solution of the problem of ionic motion with that type of prominence (Pettit's Class III *b*) which consists of a series of fine streamers emerging almost radially from the solar surface. Unfortunately it does not seem possible to evolve any simple technique of curve fitting applicable to this case. The number of parameters involved is too large, since we can vary, not only the location of the dipole, but also, within small limits, its axial direction, while, for the streamers themselves we can dispose Z_0, the scale perpendicular to the dipole axis, and the plane of projection on to the sky. Thus, for example, no useful criterion can be derived from fixing the position of the maximum transverse coordinate of a streamer, since, by varying the plane of projection of our computed curves we can push the maximum up or down almost to any level we choose. The best that we can do is to see whether we can, from the materials at our disposal create something which looks like a prominence of this type. Suppose, for example, we consider the ejection of a number of particles all parallel to the dipole axis, from the points laid out in plan view in Fig. II.11. It is easy to show that if the two projections of the curve are denoted by X and Y, then the track originating at the point (a, b) on the plan will be seen projected on the sky as the track $aX + bY$. By selecting the points of origin as shown in Fig. II.12 (A), we produce a series of streamers of the form shown in Fig. II.12 B which bears a strong resemblance to the McMath-Hulbert prominence of Fig. II.13. In the latter the height of each picture appears to be of the order of 100,000–200,000 km. and, since our "model" has been carried up to $Z = 1$, this means that c is of the order of $10^{10} - 10^{11}$. This conclusion is rather uncertain, but at present there seems no way to improve upon it, and we can only remark that values of c of the order found for the prominences of Figs. II.5, 6 and 9 would also be consistent with the form of the prominence of Fig. II.13 (Plate 10).

9. *Variations of ion velocity.*—So far we have proceeded on the assumption that the velocities of the moving ions are constant. We must now enquire whether the velocity changes of the kind considered in Section I would produce

any serious change in the shapes of the trajectories. We consider the case when $z=0$ so that II.3 reduce to

$$\ddot{x}=-\mu\dot{y}/r^3: \qquad \ddot{y}=\mu\dot{x}/r^3. \qquad \text{II.22}$$

For convenience in computation it is desirable to put these equations into a form which eliminates the constant. Suppose we write

$$\mu=\kappa^3\sigma, \qquad \text{II.23}$$

where κ is a length and σ^{-1} a time. The transformation

$$X=x/\kappa: \qquad Y=y/\kappa: \qquad R=r/\kappa: \qquad T=\sigma t \qquad \text{II.24}$$

will do this satisfactorily. Further, we must choose the initial velocity of such a magnitude that the parameter n will be just over 1·0. If we take M as 10^{14} e.s.u. and $Z/A=\frac{1}{4}$ then μ is of the order of 10^{28}. We can choose κ and σ in any way we please provided that the value of the product $\kappa^3\sigma$ is correct. Taking $\kappa=10^{11}$ and $\sigma=10^{-5}$ we have the following system of units:

Distances: unit 1 million km.
Times: unit 10,000 seconds.
Velocities: unit 10 km./sec.

In our example we take $v=70$ km./sec. and compute the space track numerically as far as $T=0{\cdot}20$, corresponding to 2000 seconds. Then, at $T=0{\cdot}06$ we multiply the values of X' and Y' there by $\sqrt{2}$ and compute the new curve from this point onwards. The space tracks are shown as curves (1) and (2) of Fig. II.14 A, while the distance-time graphs are numbered correspondingly in Fig. II.14 B. We obtain curves (3) and (4) by making the same type of change, as indicated by Fig. II.14 B at $T=0{\cdot}10$. What we have done in fact is to use Pettit's approximation to the type of velocity changes observed as a convenient representation for mathematical calculation. The changes produced are surprisingly small: even the change from curve (1) to curve (2) would probably make very little difference to the results of curve fitting on a still print. We have, of course, made the velocity changes at points on the curve where the curvature is not very great, but this can be defended on the ground that most prominence streamers do in fact refer to these parts of the hypothetical curves to which we fitted them. The differences in spatial tracks would be much greater if we placed the velocity change at a point such as P in Fig. II.14 A, where the curvature is much greater. However, a moment's reflection will show what the consequences of this would be. We should obtain a new curve differing considerably from (1) appropriate to the new value of the velocity taken. If we sought to fit to this curve one of our computed curves, we should fit one which was satisfactory over the greater part of the length, i. e. we should fit the one which was best for the part above P which would have a value of c appropriate to the changed velocity. The lack of conformity would be in the part of the curve preceding P and would be negligible because of the short length of this part of the curve. In fact, in fitting curves to streamers we have not so far (see Figs. II.5 and 6) had to make use of the sharply curved parts of them near their minimum values of r. The important question from our point of view is the following: "If we consider those parts of the streamers and of our computed

curves where the curvature is moderate, and if, in this region we suppose a discontinuous change of velocity to take place, will there be any significant difference between the curves fitted to this trajectory and to the trajectory calculated on the assumption that the velocity is constant?" Figs. II.14 A and B suggest that the answer to this question is that the error involved is not greater than the uncertainty of picking out a streamer track on a still print.

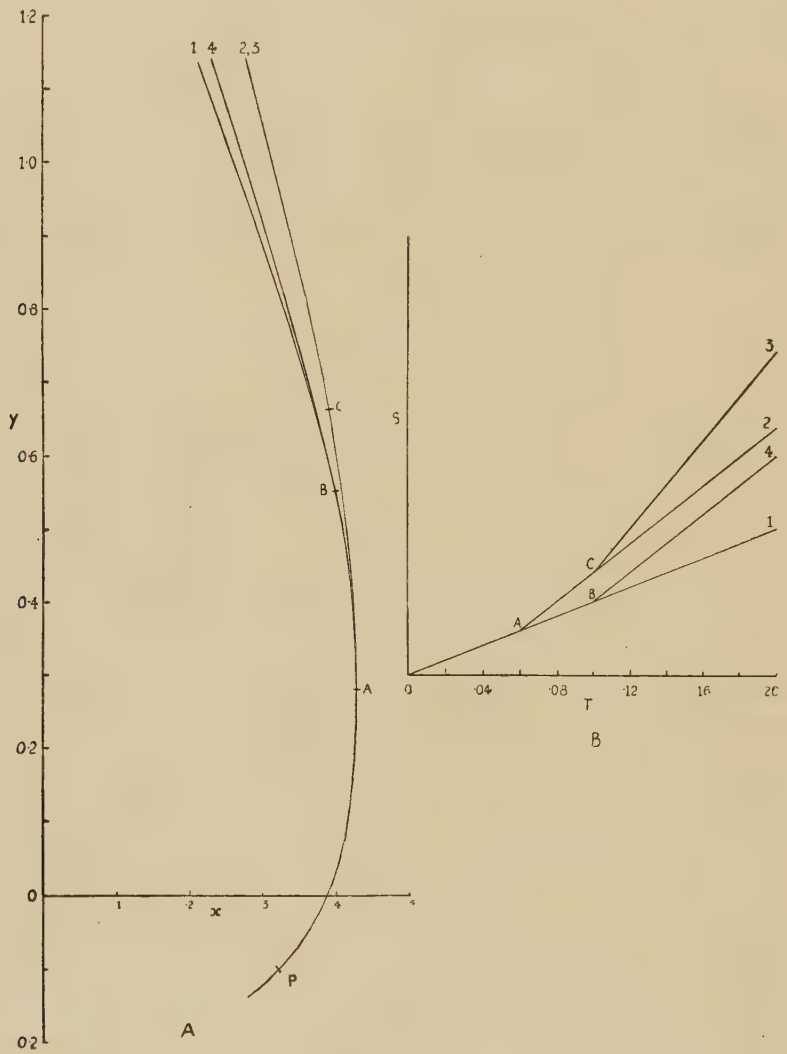

Fig. II.14.

10. *Effect of Gravitational Force.*—Finally we can now give more precision to the question of the gravitational force. There will be a certain distance from the dipole at which, for a given type of particle moving with a given velocity, the electromagnetic force will be equal to the gravitational force. At smaller distances, because of the rapid variation of the dipole field, it will be a reasonable approximation to neglect the gravitational force in comparison with the electromagnetic

force. At larger distances the reverse will be true. The acceleration in the orbit is

$$\frac{v^2}{\rho} = \frac{v^2c^2}{r^3}$$

and, if we equate this to the solar gravitational acceleration, $2{\cdot}736 \times 10^4$ we find $r = 10^{-2}\sqrt[3]{36{\cdot}5v^2c^2}$, or, if r is expressed in units of 100,000 km. and v in km. per sec.

$$r' = 10^{-9}\sqrt[3]{365v'^2c^2}. \qquad \text{II.25}$$

This gives a basis for comparison which does not depend on the particular value of M which is chosen, but only on the curvature of the observed track. For streamer A of prominence (1), r' comes out as 2·66, a radius which is sufficient to include the whole prominence. The values of r' for the other streamers are given in Table II.1. We find that, even if we include the full value of the gravitational force (neglecting for the moment any question of electrostatic support) then the whole of streamers A and B lie within the calculated value of r': the greater part of E lies inside, B lies on the borderline and D outside. It also follows of course that these trajectories cannot be described under gravity alone because their radii of curvature are too small. If in addition to gravity we suppose that there is an electrostatic upthrust, then the radius of action of the dipole is correspondingly increased.

We may conclude that, as far as the initial parts of the streamers are concerned, we must invoke some force other than gravity, and it is a self-consistent hypothesis to attribute this force to an electromagnetic origin. It is however, possible for a streamer at the end of its trajectory to pass outside the radius of action of the dipole, and then the force of gravity will be dominant. Since this is directed normal to the solar surface it will modify the end of the trajectory by bringing this nearer to the normal to the solar surface than would otherwise be the case. This is in fact what has been noticed in studying the curves. There seems to be a definite tendency as the end of the track is reached for the streamers to turn towards the normal.

11. In this discussion we have also neglected any sensible general solar magnetic field at great heights. If such a field existed it would alter considerably the form deduced for the tracks.* It is however in accordance with observation that the intensity of the Sun's general magnetic field is limited sharply in height and is of a sensible magnitude only at chromospheric levels.

12. The present paper was written after the appointment of the author as second assistant at the Radcliffe Observatory, Pretoria, and he wishes to express his thanks to the Radcliffe Trustees. It is a pleasure to acknowledge the help and encouragement given by Professor H. H. Plaskett and Miss M. G. Adam of the University Observatory, Oxford. The author also wishes particularly to express his thanks to Professor E. A. Milne for his criticisms, particularly of the original presentation of the discussion of electrostatic forces, and for his most valuable suggestions.

University Observatory,
Oxford:
1946 *April.*

* See S. Chapman, *M.N.*, **89**, 57, 1928 ; T. G. Cowling, *M.N.*, **90**, 140, 1929.

OCCULTATIONS OF STARS AND PLANETS BY THE MOON OBSERVED AT THE NIZAMIAH OBSERVATORY, HYDERABAD, DURING THE YEAR 1945

(Communicated by the Director)

(Received 1946 April 16)

TABLE I

No.	Star	Mag.	Phase	Date 1945	U.T. h	m	s	Remarks
1	BD−16° 5998	7·1	D	Jan. 16	13	17	13·2	
2	BD+10° 352	6·8	D	,, 21	16	47	06·3	
3	BD+ 9° 353	6·7	D	,, 21	18	06	03·2	
4	85 Ceti	6·3	D	,, 21	18	22	32·7	
5	68 Tauri	4·2	D	,, 23	13	22	56·3	
6	BD+20° 948	6·8	D	,, 24	15	34	33·0	
7	δ Gemini	3·5	D	,, 26	15	16	43·3	
8	δ Gemini	3·5	R	,, 26	16	24	49·9	
9	ν Virginis	4·2	D	,, 31	23	48	15·7	
10	ν Virginis	4·2	R	Feb. 1	00	36	16·3	Seen through clouds
11	14B Gemini	6·0	D	,, 21	16	49	09·9	
12	BD+21° 1146	var.	D	,, 21	18	15	04·5	
13	68B Ophiuchi	5·9	R	Mar. 6	23	03	34·6	
14	58 Ophiuchi	4·9	R	,, 7	20	41	20·6	
15	BD+16° 527	6·9	D	,, 18	14	39	28·2	
16	BD+20° 2185	7·0	D	,, 23	17	18	51·8	
17	BD+18° 2207	7·5	D	,, 24	13	43	13·8	
18	4 Capricorni	6·0	R	Apr. 6	22	38	25·0	
19	Saturn	0·3	D	,, 17	13	04	37·6	Sky hazy ; time uncertain
20	BD+4° 2583	6·8	D	May 21	14	25	47·6	
21	BD−0° 2632	6·6	D	,, 22	15	41	58·8	
22	336B Aquarii	6·5	R	June 3	23	17	24·4	
23	9 Cancri	6·2	R	Nov. 23	18	57	28·8	
24	BD−8° 6166	7·1	D	Dec. 12	14	15	32·6	

Numbers 1 to 12, 15, 16 and 19 were observed by M. V. V. Sastry and the rest by A. Ramanathan. The instrument used throughout was the 15-inch visual refractor. The corrections to the standard clock were determined from observations with the transit instrument.

The reductions were carried out by M. V. V. Sastry, assisted by S. Aravamudan. No correction was added to the observed time.

TABLE II

No.	$\sigma'-\sigma$	$\cos(\rho-\chi)$	$\sin(\rho-\chi)$	No.	$\sigma'-\sigma$	$\cos(\rho-\chi)$	$\sin(\rho-\chi)$
	"				"		
1	−0·1	+0·94	+0·34	13	+0·2	−0·76	−0·65
2	0·0	+0·69	+0·73	14	+3·9	−0·83	+0·55
3	−0·1	+0·85	−0·52	15	−0·3	+0·98	−0·21
4	−0·7	+1·00	+0·04	16	+0·2	+0·43	−0·90
5	+0·1	+0·95	−0·32	17	−0·6	+0·80	−0·61
6	+0·3	+0·47	−0·88	18	+0·8	−1·00	+0·04
7	−0·9	+0·79	−0·61	19	(−4·0)	+0·99	+0·12
8	+1·7	−0·67	−0·75	20	−1·1	+0·96	−0·27
9	−0·6	+0·73	+0·68	21	+3·6	+0·54	−0·84
10	+2·4	−0·35	+0·94	22	+1·2	−1·00	+0·07
11	−1·5	+0·85	+0·53	23	+3·4	−0·73	−0·68
12	−0·7	+0·81	−0·59	24	−1·6	+0·85	+0·53

Nizamiah Observatory,
Hyderabad, Deccan, India :
1946 *February* 27.